635

HIGH ENERGY HADRONIC INTERACTIONS

by

Hilary Nowell Thompson

A thesis presented for the degree of
Doctor of Philosophy
of the University of London

Department of Mathematics,
Royal Holloway College.

September 1978

ABSTRACT

This thesis is presented in two distinct parts.

In part one, the single lepton yield due to internal conversion of soft virtual photons in high energy proton-proton collisions is calculated using soft photon techniques. Photons originating in bremsstrahlung of charged hardons, directly produced photons and interference effects are considered. The result is compared with the experimental e/π ratio as a function of transverse momentum.

In part two, a Mueller-Regge model for the process $\pi^- + p \rightarrow p + X$ is constructed and compared with newly available inclusive cross section data. Cut corrections are required for baryon exchange by the Carlitz-Kislinger prescription for removing unobserved parity partners and accordingly absorption effects are calculated. The conventional Δ_δ baryon trajectory is found to be satisfactory, contrary to other reports.

PREFACE

The work described in this thesis was carried out under the supervision of Dr. K.J.M. Moriarty in the Department of Mathematics, Royal Holloway College, University of London, between October, 1975 and September, 1978. Except where stated, the work described is original and has not been submitted to this or any other university for any degree.

My supervisor and I wish to acknowledge the assistance of Professor G. Kramer (in communicating to us the work of Dr. R. Tegen) and Professor H. Six and Dr. H. Yoshida (for providing us with their data and for valuable discussions).

I am indebted to Dr. N.S. Craigie of the Department of Theoretical Physics, Imperial College, London for instigating the topic of part one of this thesis and for his direction and collaboration during the course of that work.

I am grateful to J. Anderson for his help with computing, to Dr. J.H. Tabor for numerous useful discussions, to the Science Research Council for a Research Studentship and to Mrs. Rutherford for her fast and efficient typing of the manuscript.

My greatest obligation is to by supervisor, Dr. Moriarty. His advice and encouragement have been essential to me throughout my postgraduate career.

CONTENTS

PART ONE

Calculation of single lepton yield at small transverse momentum from soft virtual photons in high energy proton-proton collisions.

CHAPTER I

The experimental search for leptons created in collisions of strongly interacting particles was initially ($\sim$ 1964) motivated by the study of weak interactions. Attempts were made to find the mediating particles of weak interactions, the W vector meson, by its proposed leptonic decay ($W^+ \rightarrow \mu^+ + \nu_\mu$ etc.). An obvious difficulty arose with the overwhelming background from the decay of pions (e.g. $\pi^+ \rightarrow \mu^+ + \nu_\mu$) and kaons. It was at this stage that the advantages of looking for leptons with high transverse momentum and large production angles were first utilised. In this situation, the kinematics no longer favour the production of light hadrons compared with heavier particles. Furthermore, the heavier particles will decay promptly into leptons whereas the lighter hadrons, such as pions and kaons, decay more slowly at high energies so that they can sometimes be detected before they decay. A useful additional property of large p_T physics is the way in which the single lepton spectrum reflects both the shape and the normalization of the parent spectrum, (widely discussed as "parent-child kinematics", we shall meet this result again in Chapter III).

The failure of the first searches to find the W, from the detection of single leptons, stimulated an experiment to detect lepton (muon) pairs - to look for the W^o and for other interesting theoretical proposals in the literature of the time (e.g. B^o "heavy photon"). At the same time, deep inelastic scattering data prompted consituent models of hadronic matter and the quark-parton

model was born (quarks had been previously proposed theoretically). The now famous dimuon data (which gave the first hint of the ψ/J) gave support for quark-parton theories and particularly the Drell-Yan (scaling) mechanism, which was widely quoted. In this picture, the emerging end of a virtual photon dissolves into a lepton pair while the other end arises from quark-antiquark annihilation (with one quark or antiquark coming from each incident hadron). This process is related [1] to the processes involving the decay of vector mesons and hence also related to the coupling of massive virtual photons to multi-hadron final states (see fig. 1.1),

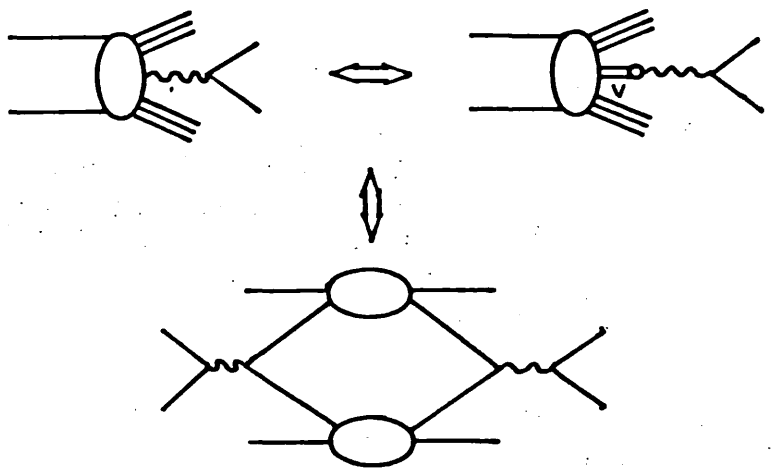

Figure 1.1 Inter-relation between various e^+e^- production processes.

which has aroused much interest in the past. The inter-relation between these processes has been, and remains, a fascinating theoretical problem. The decays of vector mesons into $\ell^+ \ell^-$ pairs led to the spectacular ψ discovery and associated revelations of recent years, including the latest the upsilon. The detection of final state leptons in hadron-hardon collisions will most probably remain one of the ways that quark degrees of freedom are probed in the future.

The short introduction above provides a basis for understanding the continued experimental and theoretical interest in lepton production with respect to transverse momentum in high-energy hadron-hadron collisions. When discussing transverse momentum, there is sometimes confusion about the meaning of "large" - large production angle in centre-of-mass or large $|\underline{p}_T|$ ($|\underline{p}_T|$ = modulus of momentum perpendicular to beam direction) or both. We shall try to emphasise which situation we are considering in each case. We shall be concerned predominantly with a source of electrons at large production angles but small $|\underline{p}_T|$ and we next review the recent data which has instigated this work.

First measurements of the ratio of the cross sections for electron and pion production in hadron-hardon collisions showed an e/π ratio which was $\sim 1 \times 10^{-4}$ and roughly constant with transverse momentum. (For a review of data up to 1976 see ref. [2]). Dividing the lepton yield by the pion yield at the same transverse momentum gives us an arbitrary way of comparing direct leptons with some "standard" particle production. The ratio is also,

importantly, much less dependent on absolute normalization, geometric acceptances, etc. The level of 1×10^{-4} for the e/π ratio is surprisingly large since, as we shall show later, a naive calculation based on the rho meson as a source of electrons predicts a level $< 1 \times 10^{-5}$. To understand the single electron yield more fully we need additional information - whether the electrons are associated with e^+e^- pairs and, if so, what mass region gives the major contribution. The answers to such questions are confused by the need to enforce experimental cuts to remove the large background from π^0 Dalitz pairs ($\pi^0 \to \gamma\, e^+e^-$) and from electrons due to external conversions in the apparatus of real photons coming from π^0 decays ($\pi^0 \to \gamma\gamma$).

The CCRS (Cern-Columbia-Rockefeller-Saclay) [3] experiment observed electrons emerging at 90° from proton-proton collisions at CERN ISR, over an energy range $\sqrt{s} = 23$ to 62 GeV. The electrons were of course identified by counters. Dalitz pairs and photon conversions in the vacuum chamber walls were rejected by the pulse height recorded in the hodoscope nearest to the beam pipe, this cut effectively removed all low mass pairs. The results of this experiment for $\sqrt{s} = 52.7$ GeV are shown in the compilation of data in fig. 1.2. Over a range of 0.6 GeV/c to 3.0 GeV/c in p_T, the e/π ratio is approximately constant $\sim 1 \times 10^{-4}$ but falling away as $p_T \to 0.6$ GeV/c. Over the available range in $\sqrt{s}$ of this experiment, the e/π ratio shows a slow increase with energy. (In ref. [2] the overall energy dependence of lepton/pion ratios was shown to be rather confused).

The next experiment was again at CERN ISR, with a production angle of 32° and $\sqrt{s} = 52.7$ GeV. Electrons and positrons were detected for 0.2 GeV/c $< p_T < 1.5$ GeV/c [4]. Background from photon conversions, Dalitz pairs and K_{e_3} decays was calculated by Monte Carlo techniques and subtracted. The experimental setup also effectively enforces a 5° pair minimum opening angle. This data is also shown in fig. 1.2. (We can compare sets of data with different production angles because hadron production decouples in p_T and x $(= 2p_{/\!/}/\sqrt{s})$ and we are presenting ratios). The results from ref. [4], CHORMN collaboration (Cern-Harvard-Orsay-Riverside-Munich-Northwestern!), show a remarkable rise at low p_T up to 6×10^{-4}. In view of the importance of the low p_T region, this collaboration performed a new experiment with an improved detection system to verify their first conclusions [5]. The detectors are again placed at 32°, Dalitz pairs etc. are subtracted by the Monte Carlo program and a dummy wall experiment is used to measure the background due to electrons from γ interactions. Again the small p_T rise is seen (fig. 1.2, CHORMN 2).

The discrepancy between CCRS and CHORMN results below $p_T = 1.0$ GeV/c will, at least in part, be due to the different experimental cuts.

There is support for the low p_T rise in the e/π ratio from the Pennsylvania-Stony Brook group [6]. This experiment has a proton beam incident on a liquid hydrogen target at energies 10, 15 and 24 GeV/c. Electrons are detected at a laboratory production angle $\theta_{lab} = 16^{o}$ which corresponds to 90° in the centre-of-mass over a range of $0.5 \rightarrow 1.5$ GeV/c in transverse momentum. Dalitz

pairs and internal conversions are rejected by ionization and single track requirements in the spectrometer and K_{e_3} decays are subtracted by a Monte Carlo calculation. Again small opening angle e^+e^- pairs are effectively excluded ($\sim 7^o$). We show the 24 GeV/c data in fig. 1.2. The increase at small p_T in CHORMN and Penn-S.B. results has an approximate p_T^{-1} behaviour.

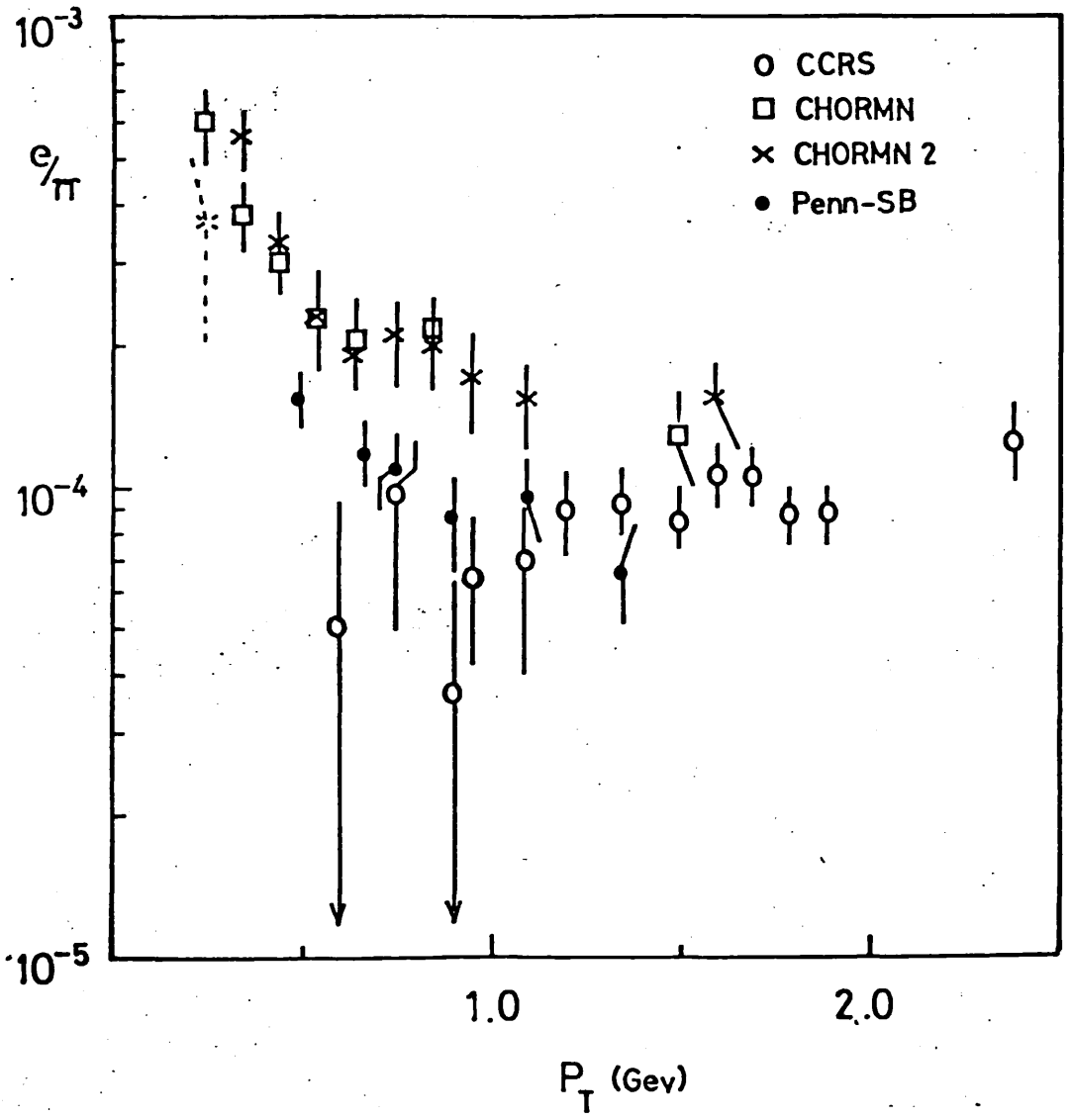

Figure 1.2 Compilation of data for electron/pion ratio plotted against transverse momentum.

(⋮ Markedly non-uniform acceptance)

A suggestion that there is a large excess of e^+e^- pairs over Dalitz pairs in the low mass region is found in recent results from SLAC [7]. Here, pairs are detected after the exposure of the one metre hydrogen bubble chamber to 18 GeV/c pion beams. The limit on unpaired electrons or positrons is at $< 2.4 \times 10^{-5}$, so this low energy experiment provides some indication that the copious single electron signal at low p_T will be associated with low mass pairs, although more information about production angles is needed.

The problems of very small mass pairs and π^0 Dalitz pairs are avoided by looking at prompt muons. (Muon experiments have other difficulties - usually concerned with dumping the beam). Available muon data is in the region $1.0 \rightarrow 5.0$ GeV/c in transverse momentum and is consistent with electron data where there is overlap, $\sim 1 \times 10^{-4}$ [1,2,8,9]. The observed single muon yield can be accounted for by low mass dimuons. Contributions from vector mesons and a low mass continuum are observed experimentally [10] and calculations based on these sources can account for the data [8]. We show some data [9] and the calculated yields for $1 \text{ GeV/c} < p_T < 3 \text{ GeV/c}$ in fig. 1.3.

Polarization has also been looked at in muon experiments. If direct muons have an electronmagnetic origin, then one would expect zero polarization due to parity conservation. But if direct muons are produced by the V - A weak decay of a heavy particle, a non-zero longitudinal polarization would be expected. An early Serpukov experiment observing muons at 90° found no evidence for longitudinal polarization [11]. Recent results from a Yale-BNL-Fermilab collaboration

are also consistent with an electromagnetic origin [12].

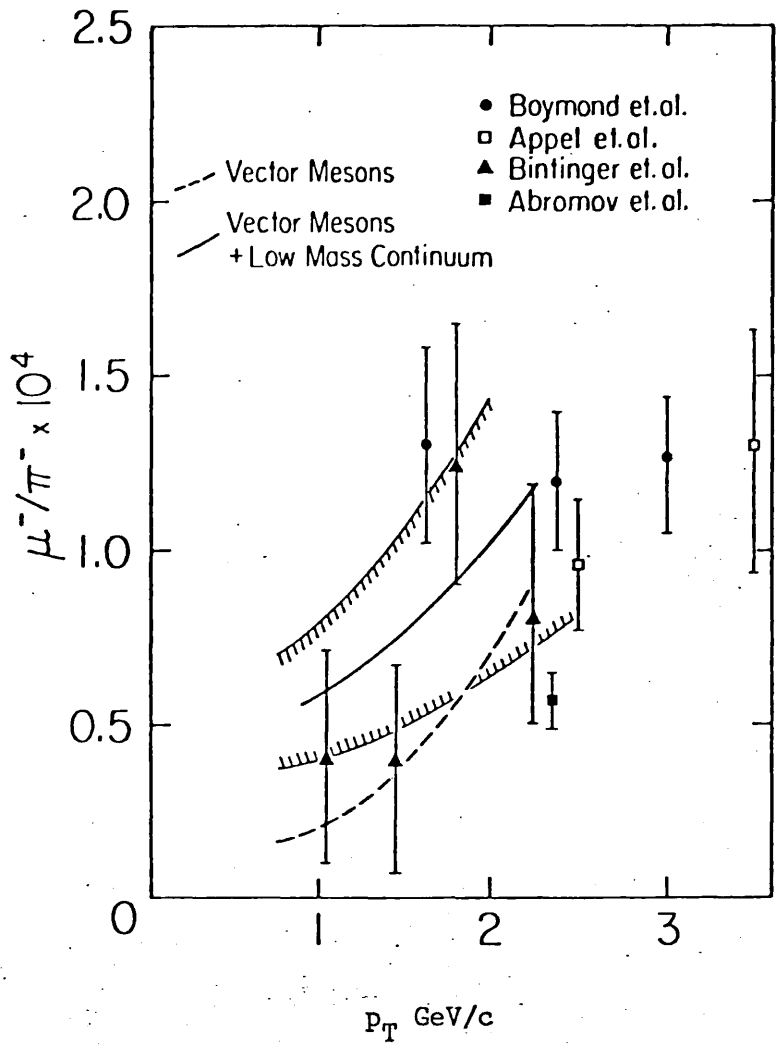

Figure 1.3 Calculated μ^-/π^- ratio compared with data of ref. 9 .

The only available data for real photons is in the high p_T region ($3 \rightarrow 4$ GeV/c). Measurements of (γ/π^0) excess (i.e. with contributions from π^0 and η removed) give 15 - 20%.

We are primarily interested in the surprisingly high yield of electrons below $p_T = 0.5$ GeV/c and we next discuss the possible sources of prompt electrons and their failure to explain the observed yield. The alternative sources can be divided into three main categories:

i) Weak decay of resonant hadronic states (π, K, D, F, D^*, ...),

ii) Electromagnetic decay of resonant hadronic states (π^o, η; ρ, ψ, ψ', ...),

iii) Production of virtual photon continuum by electronmagnetic processes.

We must also bear in mind such possibilities as $W^{\pm}$, W^o and heavy leptons $L^{\pm}$ ($\tau^{\pm}$). We have already seen that such well-established and copious sources as pions and kaons are removed from the data so that only the direct (and unknown) yield remains.

It is important to the calculations of e/π ratios to recall some well-known and useful kinematics. If direct leptons are produced by two-body decay of a parent particle, then the child (lepton) spectrum will fall away for $p_T < M/2$, where M is the parent mass, see fig. 1.4(a).

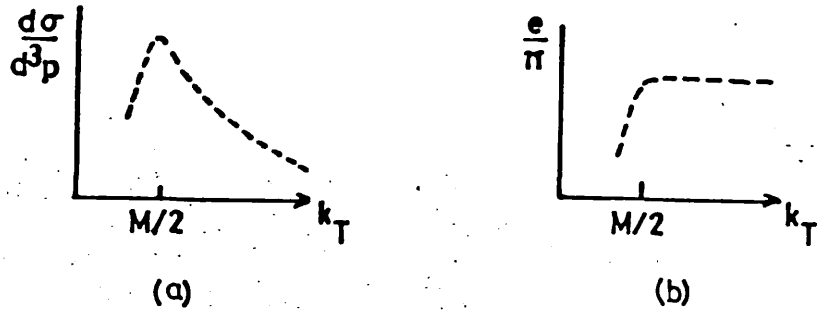

Figure 1.4 (a) Lepton spectrum from two-body decay of pion-like parent.
(b) e/π ratio corresponding to production in (a).

Correspondingly, if the parent has a pion-like production, the e/π ratio will also fall below $p_T \simeq M/2$ (fig. 1.4(b)). For three-body decay, one would expect a reduction since the parent transverse momentum has to be shared among three bodies. In fact there is strong kinematic suppression bu the lepton spectrum can peak at $p_T = 0$ in this case.

Initially, the prime suspects as sources of prompt leptons were the vector mesons. These particles are produced with hadronic cross sections and have leptonic branching ratios making them obvious candidates. Conventional calculations of the yield from vector mesons ($\rho \to e^+e^-$, $\omega \to e^+e^-$, $\phi \to e^+e^-$, $\psi \to e^+e^-$) are based on a narrow width approximation [13]. For the larger values of p_T, the narrow width e/π ratio has the following simple form [14]

$$\frac{e}{\pi} \simeq \frac{c_V}{c_\pi} \frac{B_{V\to e^+e^-}}{(n-1)} \quad . \qquad (1.1)$$

Here, the universality in p_T of hadronic single particle spectra has been assumed. The transverse momentum dependence is taken as a power law ($\sim p_T^{-8}$) which changes to an exponential ($\exp(-6\, p_T)$) below $p_T \simeq 1$ GeV/c. In equation (1.1), n is the effective power law parameter, c_V/c_π gives the ratio of vector meson to pion production and $B_{V\to e^+e^-}$ is the branching ratio for vector meson decay into a lepton pair. Typically, for the rho meson, $B_{V\to e^+e^-} = .43 \times 10^{-4}$, $c_\rho \simeq c_\pi$ and $n = 8$. This gives $e/\pi \simeq 6 \times 10^{-6}$, at least a factor of 10 too low to explain the level of the data. The total contribution from all vector mesons cannot raise the level above

5×10^{-5} at $p_T \approx 1$ GeV/c. The results of the narrow width calculation of Bourquin and Gaillard [13] are shown in fig. 1.5.

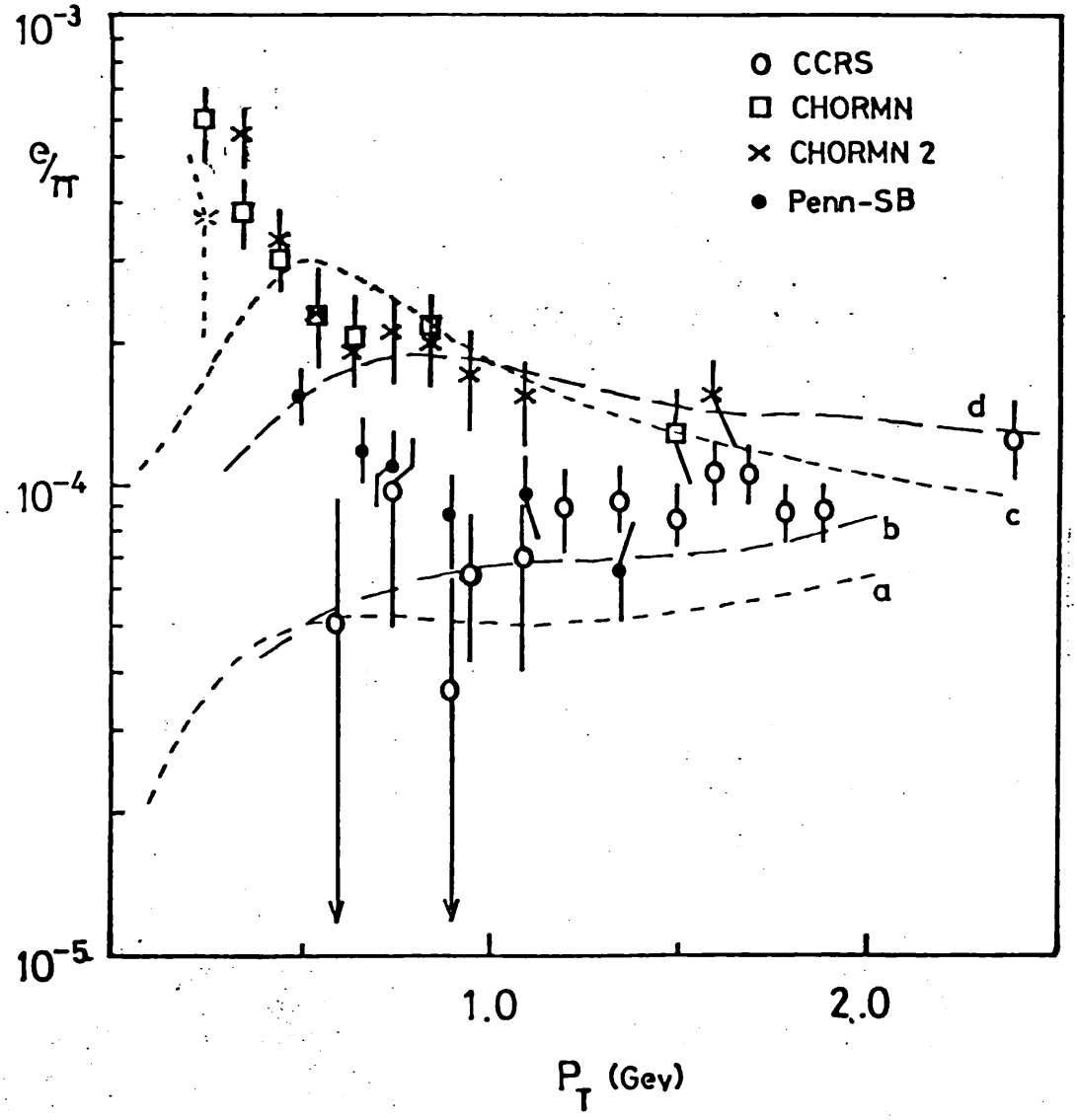

Figure 1.5 Data with conventional estimates of e/π ratio.
Curve a - narrow width vector meson calculation of ref. 13 .
Curve b - three-body decays (η,η',...) of ref. 14 .
Curves c and d - charmed meson decay (ref. 17) $D(1.8) \to K^* e\nu$ and $D(1.8) \to K e\nu$ repectively.

We must also take into account 3-body decays: $\omega \to \pi^0 e^+e^-$, $\eta' \to (\rho,\gamma) e^+e^-$, $\eta \to \gamma e^+e^-$ and $\phi \to \eta e^+e^-$. Calculations for these sources are analogous to Dalitz pairs [15]. The yield [14] from these additional Dalitz pairs is also shown in fig. 1.5. Craigie and Schildknecht [14] also point out that there is a contribution due to a low mass photon continuum, this piece is most important since it rises sharply as $p_T \to 0$ and we shall give the details in Chapter III.

The above considerations exhaust category (ii) in our list of sources. From category (i) there remains the currently interesting suggestion that charmed mesons may make a significant contribution [16, 17, 18]. Candidates are the now firmly established D mesons ($D^{+,0}$ pseudoscalar and $D^{*+,0}$ vector; masses — m_{D^0} = 1.863 GeV, m_{D^+} = 1.868 GeV, $m_{D^{*0}}$ = 2.006 GeV, $m_{D^{*+}}$ = 2.009 GeV; quark combinations — $M_c^+ = c\bar{d}$ and $M_c^0 = c\bar{u}$) and the less well observed F and F^* ($c\bar{s}$). While there is still some uncertainty about the size of charmed meson production cross sections and leptonic branching ratios, some estimates for lepton yields have been made. Purely leptonic decays $D^+ \to \ell^+ + \nu_\ell$ are suppressed compared to semi-leptonic decays, with the ratio (pure leptonic/semi-leptonic) $\sim 10^{-5}$ [19]. For semi-leptonic decays the $M_c \to K + \ell + \nu_\ell$ mode is dominant. The semi-leptonic branching ratio is fairly well fixed at $\sim$ 8%, but the estimated 10 μb production cross section is more uncertain [20]. The theoretical input of calculations can strongly influence the result: transverse momentum dependences and three body decay

distributions. The mass of the recoil hadron also has a noticeable effect on the e/π ratio. All calculations are agreed that the ratio will turn over in the p_T range $400 \rightarrow 500$ MeV/c, in contrast to the data which continues to rise up to $p_T = 200$ MeV/c, and that in general a rather large inclusive cross section for charm production is needed to reach the level of the data. Results of the model of ref. [17] are shown in fig. 1.5. One paper [18] claims that, within experimental uncertainties, charm can account for the observed lepton yield in the $0.5 \rightarrow 1.0$ GeV/c range in p_T; it is argued that experimental data connecting single electrons with e^+e^- pairs are not in conflict with this result - charm originated leptons are limited to Feynman $x \sim 0$ whereas existing pair data is for larger x_F. However, there still remains the issue of the continuing low p_T rise. In the central rapidity region, it is expected that $D\bar{D}$ production will dominate giving equal lepton and antilepton signals.

The "story so far" demands a further source of e^+e^- pairs and the absence of any low p_T threshold in the e/π ratio suggests an explanation in terms of a virtual photon continuum. Bremsstrahlung was long ago proposed as a possible mechanism for pair production in hadronic interactions [21]. For large mass pairs dubious assumptons about the detailed dynamics of photon production are inevitable. The contribution from low mass, low energy (= "soft") virtual photons was calculated by R. Rückl, being essentially model independent [22]. In this work, the author improves on the method of Cahn for

real photons [23] and extends to pair production. Unrealistic assumptions are made in ref. [22] when real photons are replaced by virtual photons producing pairs. The method involves the use of soft photon theorems. We shall extend and revise this calculation in the following chapters. We obtain a leading term (comparable to result of Rückl), a second order term and show how the vector meson dominated low mass continuum fits into the scheme of the calculation.

In Chapter II the soft photon theorem approach is explained, together with the real photon application. The extension to lepton pair production is made in Chapter III. Details of some numerical work and the evaluation of coefficients are given in Chapter IV. The results and their implications are discussed in Chapter V. Some additional work is left to appendices. The emphasis is always on the large angle production of electrons for comparison with the data (the 32° data of the CHORMN group may be considered "large" angle when compared with the angle of the forward hadronic cone) but we shall also present the small angle case.

CHAPTER II

We investigate the bremsstrahlung production of real photons in high-energy centre-of-mass proton-proton collisions. The cross section for the production of real photons with energy q_o $(= |\underline{q}|)$ can be expanded in increasing powers of q_o in the limit $q_o \to 0$,

$$q_o \frac{d\sigma}{d^3q} = \frac{c_1}{q_o^2} + \frac{c_2}{q_o} + c_3 + c_4 q_o + c_5 q_o^2 + \ldots \qquad (2.1)$$

The Low soft photon theorem [24] for spinless particles (or for polarized particles with spin) states that unique values of c_1 and c_2 can be obtained just from a knowledge of non-radiative cross sections. This result depends on the law of charge-current conservation or equivalently gauge invariance. Strictly speaking, the theorem holds only when the scattering amplitudes are sufficiently smooth to allow complete expansions in powers of q_o. Some problems may arise if there are rapid variations in amplitudes, for example when there is a narrow resonance with width less than q_o. Or, to express this condition another way, we need (change in amplitude for leg going off-shell) << (size of amplitude) [25]. (For this situation the theorem holds to a good approximation, but in ref. [25] an error term is discussed and the authors suggest that conversely conditions could be chosen to emphasise the error and obtain new information about an interaction). So the result will only be applicable when the effective expansion parameter $q_o/\langle E\rangle$, where $\langle E\rangle$ is an average energy of the particles

in the interaction, is small ($\ll 1$). We can expect this limit to be valid for high-energy collisions with $q_o \to 0$. Low's theorem has certainly been applied with some success in the past, see for example ref. [26].

The technique of Low has been extended to include cross sections with spin summations [27, 28] with similar results. The first two terms of the expansion in photon energy can be calculated from the non-radiative cross section (summed and averaged over spins). We give a derivation assuming spinless particles which demonstrates the role of gauge invariance and reproduces the results of ref. [27].

The radiative amplitude contains contributions both from terms in which the photon is radiated from an external line and from terms in which the photon is radiated from an internal line. The most singular $(1/q_o^2)$ term in equation (2.1) is the result of external radiation and arises from the off-mass-shell charged hadron propagators in initial and final state bremsstrahlung.

The external bremsstrahlung amplitude (fig. 2.1(a)) for a proton-proton collision producing an arbitrary n-particle final state $(a + b \to n)$ is given below. We note that the off-mass-shell progagator $((p + q)^2 - m^2)^{-1}$ reduces to $(2p.q)^{-1}$.

T_n^μ (bremsstrahlung)

$$= \sum_{i=1}^{n} Q_i \frac{(2p_i + q)^\mu}{2p_i \cdot q} T_n(p_a, p_b; p_1, \ldots, p_i + q, \ldots p_n)$$

$$- Q_a \frac{(2p_a - q)^\mu}{2p_a \cdot q} T_n(p_a - q, p_b; p_1, \ldots, p_n)$$

$$- Q_b \frac{(2p_b - q)^\mu}{2p_b \cdot q} T_n(p_a, p_b - q; p_1, \ldots, p_n) \tag{2.2}$$

where the ith particle has charge Q_i and four-momentum p_i and $T_n(p_a, p_b; p_1, \ldots, p_n)$ is the on-shell amplitude for $a + b \to n$ particles. The Feynman rules for scattering amplitudes are given in the Appendix.

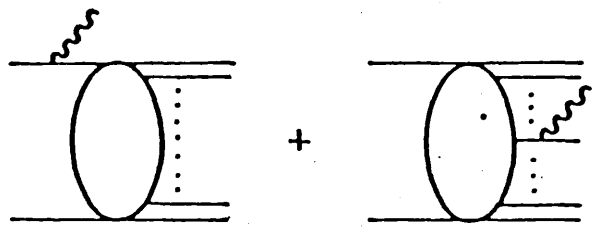

Figure 2.1 (a) Initial and final state bremsstrahlung amplitudes.

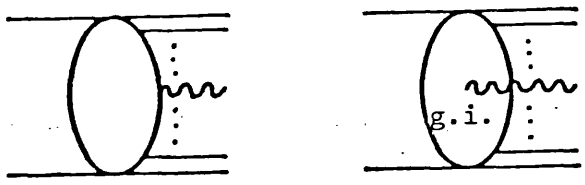

Figure 2.1 (b) Direct photon and gauge invariant amplitudes.

We note overall charge conservation means $Q_a + Q_b = \sum_{i=1}^{n} Q_i$. Performing simple Taylor expansions of the amplitudes T_n about $q_o = 0$ yields, for example,

$$T_n(p_a,p_b;p_1,\ldots,p_i+q,\ldots p_n)|_{q_o \to 0}$$

$$= T_n(p_a,p_b;p_1,\ldots p_n) + q.\nabla^i T_n(p_a,p_b;p_1,\ldots p_n) \qquad (2.3)$$

$$+ \ldots.$$

where ∇^i is the four-dimensional gradient with respect to the momentum of the ith particle. We now divide the full radiative amplitude into two parts, the contribution from external bremsstrahlung and the contribution from all other sources $(T_R{}^\mu)$(fig. 2.1(b)),

$$T_n{}^\mu \text{ (full)} = T_n{}^\mu \text{ (bremsstrahlung)} + T_R{}^\mu.$$

We can apply gauge invariance to the full amplitude and obtain

$$-q.T_R = + q.T_n \text{ (bremsstrahlung)}. \qquad (2.4)$$

Using charge conservation and equations (2.2) and (2.3), equation (2.4) reduces to

$$-q.T_R = \left\{ \sum_{i=1}^{n} Q_i \; q.\nabla^i - Q_a \; q.\nabla^a - Q_b \; q.\nabla^b \right\}$$

$$\times \; T_n(p_a,p_b;p_1,\ldots p_n).$$

Thus we have obtained an expression for $T_n{}^\mu$ (full) which we can write in increasing powers of q_o,

$$T_n^{\mu}\ (\text{full}) = \Big\{ \sum_{i=1}^{n} Q_i \left[\frac{(2p_i+q)^{\mu}}{2p_i\cdot q} + \frac{(2p_i+q)^{\mu}}{2p_i\cdot q}\ q.\nabla^i - \nabla^{i\mu} \right]$$

$$- Q_a \left[\frac{(2p_a-q)^{\mu}}{2p_a\cdot q} + \frac{(2p_a-q)^{\mu}}{2p_a\cdot q}\ q.\nabla^a - \nabla^{a\mu} \right]$$

$$- Q_b \left[\frac{(2p_b-q)^{\mu}}{2p_b\cdot q} + \frac{(2p_b-q)^{\mu}}{2p_b\cdot q}\ q.\nabla^b - \nabla^{b\mu} \right] \Big\}$$

$$\times\ T_n(p_a,p_b;p_1,\cdots p_n)$$

$$+ \Big(\text{gauge invariant terms of } o(q_o)\Big). \qquad (2.5)$$

The next-to-leading term in the cross section $(\sim 1/q_o)$ will be associated with interference terms in the squared amplitude. We now introduce some notation for the sum over initial and final states. We define

$$\sum_i{}' \ X_i = \sum_{j=1}^{n} X_j - \sum_{c=a,b} X_c$$

and whenever $(2p_i + q)$ occurs in X_i it is implicitly replaced in X_c by $(2p_c - q)$. Now the second order terms are given by

$$\left(\sum_i{}' Q_i \frac{(2p_i+q)^{\mu}}{2p_i\cdot q}\right) T_n \left[\sum_j{}' Q_j \left(\frac{(2p_j+q)^{\nu}}{2p_j\cdot q}\ q.\nabla^j - \nabla^{j\nu}\right)\right] T_n^{\dagger}$$

$$+ \left[\sum_i{}' Q_i \left(\frac{(2p_i+q)^{\mu}}{2p_i\cdot q}\ q.\nabla^i - \nabla^{i\mu}\right)\right] T_n \left(\sum_j{}' Q_j \frac{(2p_j+q)^{\nu}}{2p_j\cdot q}\right) T_n^{\dagger}$$

and noting that this will be contracted with a symmetric tensor, we can reduce to

$$\left(\sum_i{}' Q_i \frac{(2p_i+q)^{\mu}}{2p_i\cdot q}\right) \left[\sum_j{}' Q_j \left(\frac{(2p_j+q)^{\nu}}{2p_j\cdot q}\ q.\nabla^j - \nabla^{j\nu}\right)\right] |T_n|^2$$

So, up to second order, the hadronic tensor, $H^{\mu\nu}$, is given by

$$H^{\mu\nu} = \left(\sum_i{}' \; Q_i \; \frac{(2p_i+q)^\mu}{2p_i\cdot q}\right) \left[\sum_j{}' \; Q_j \; \left(\frac{(2p_j+q)^\nu}{2p_j\cdot q} + \frac{(2p_j+q)^\nu}{2p_j\cdot q} \; q.\nabla^j - \nabla^{j\nu}\right)\right] |T_n|^2 \qquad (2.6)$$

We recall that this is the result exactly corresponding to that of Burnett and Kroll [27] which included a summation over particle spins. In ref. [27], the authors point out that the momenta and energy at which T_n in equation (2.6) is to be evaluated are not unambiguously specified. We will evaluate T_n at on-shell, non-radiative values for the leading term. Off-shell effects for the second term are discussed later in this Chapter.

We are now able to calculate the coefficients c_1 and c_2 in equation (2.1). The constant (c_3) part of equation (2.1) will have a contribution from the interference between the leading bremsstrahlung amplitude and the gauge invariant amplitude. Any calculation of this term will require detailed dynamical assumptions, including a knowledge of phase. A priori, we can say little about this term but we shall consider some order of magnitude arguments. In examining the remaining contributions to c_3 and higher order terms $(c_4, c_5, \ldots)$, we must include a consideration of the production of photons via vector mesons [29].

We now proceed to an evaluation of the leading bremsstrahlung term ($\sim 1/q_o^2$ in equation (2.1)). We write the amplitude in a factorised form,

$$T_n^{\mu}(p_a,p_b;p_1,\ldots p_n,q) = J_n^{\mu}\, T_n(p_a,p_b;p_1,\ldots p_n) \qquad (2.7)$$

where

$$J_n^{\mu} = \sum_i{}' \, Q_i \, \frac{(2p_i+q)^{\mu}}{2p_i\cdot q}$$

and T_n is the physical production amplitude. The corresponding inclusive photon cross section is given by (see Appendix)

$$2q_o \frac{d\sigma}{d^3q} = \frac{\alpha}{2\pi^2}\,\frac{1}{2s}\sum_{n=2}^{\infty}\sum_{\lambda=\pm}\int\left(\prod_{i=1}^{n}\frac{d^3p_i}{2E_i(2\pi)^3}\right)(2\pi)^4$$

$$\delta^4(p_a+p_b-\sum_i^n p_i)\,|T_n(p_a,p_b;p_1,\ldots p_n)|^2\, J_n\cdot\varepsilon_\lambda J_n\cdot\varepsilon_\lambda^* \qquad (2.8)$$

where $\varepsilon_\lambda^{\mu}$ $(\lambda = \pm)$ are the transverse polarization vectors of the real photon and $q_\mu\,\varepsilon_\lambda^{\mu} = 0$.

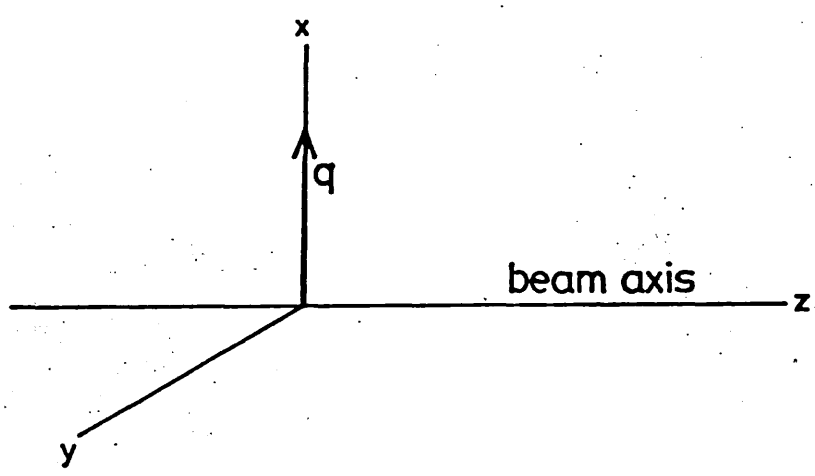

Figure 2.2 Photon produced at 90° to beam direction.

We choose initially to consider a <u>photon produced at 90°-to the beam direction</u> (beam is along z-axis and photon is taken for convenience along x-axis, see fig. (2.2)). In this configuration, the polarization vectors reduce to $\varepsilon_\pm = 1/\sqrt{2}\ (0,\ 0,\ i,\ \mp 1)$ and it is clear that to a leading approximation

$$\frac{p_i \cdot \varepsilon_\pm}{p_i \cdot q} = \pm \frac{\mathrm{sign}(y_i)}{q_o\sqrt{2}}\ , \qquad (2.9)$$

where y_i is the rapidity of the ith particle

$$\left(y_i = \tfrac{1}{2}\ \ell n\ \left(\frac{E_i + p_{i_z}}{E_i - p_{i_z}}\right)\right)$$

and $\mathrm{sign}(y) = +1$ for $y > 0$; -1 for $y < 0$. From equations (2.7), (2.8) and (2.9), it is now evident that the leading bremsstrahlung term in the photon cross section will be governed by the "charge fluctuation" $\langle\Delta^2 Q\rangle$ defined by

$$\langle\Delta^2 Q\rangle = \left\langle\left[\sum_{i=1}^{n} Q_i \mathrm{sign}(y_i) - Q_a \mathrm{sign}(y_a) - Q_b \mathrm{sign}(y_b)\right]^2\right\rangle. \qquad (2.10)$$

By making use of the charge sum rules [30], we can write the "charge fluctuation" in the following form (Appendix 2.1)

$$\langle\Delta^2 Q\rangle = -4 \sum_c \sum_d Q_c Q_d \int_0^{\frac{Y}{2}} dy_c \int_{-\frac{Y}{2}}^{0} dy_d\ C_{cd}(y_c, y_d) \qquad (2.11)$$

where Y is the total available rapidity and C_{cd} is the usual two-particle correlation function, (σ = inelastic cross section),

$$C_{cd}\,(y_c,y_d) = \frac{1}{\sigma}\,\frac{d\sigma}{dy_c dy_d} - \frac{1}{\sigma^2}\,\frac{d\sigma}{dy_c}\,\frac{d\sigma}{dy_d}\,. \tag{2.12}$$

This result is related closely to the Zone Graph analysis discussed by Baier in ref. [31].

From equations (2.8) and (2.10), we obtain

$$\left(q_o\,\frac{d\sigma}{d^3q}\right)^{90^o} = \frac{\alpha}{4\pi^2}\left(\langle\Delta^2 Q\rangle + C_T\right)\frac{\sigma}{q_o^2}\,. \tag{2.13}$$

C_T is a correction term which takes into account the transverse momentum of the hadrons in the final state which was neglected in the approximation of equation (2.9).

To estimate C_T, we use

$$\sum_\lambda J_n\cdot\varepsilon_\lambda\, J_n\cdot\varepsilon_\lambda^* = \frac{1}{q_o^2}\Bigg(\sum_i\sum_j Q_iQ_j\,\frac{(p_{i_y}p_{j_y}+p_{i_z}p_{j_z})}{(E_i-p_{i_x})(E_j-p_{j_x})}$$

$$- 2\left(Q_a\frac{p_{a_z}}{E_a} + Q_b\frac{p_{b_z}}{E_b}\right)\sum_i Q_i\,\frac{p_{i_z}}{(E_i-p_{i_x})}$$

$$+ \left(Q_a\frac{p_{a_z}}{E_a} + Q_b\frac{p_{b_z}}{E_b}\right)^2\Bigg). \tag{2.14}$$

Next, neglecting the masses of the beam particles w.r.t. $\sqrt{s}$ and recalling that $p_{a_z} = -\,p_{b_z}$ for centre-of-mass collisions, we can eliminate the last two terms in equation (2.14). We proceed to expand the first term in increasing powers of p_x/E and p_y/E.

$$\sum_\lambda J_n\cdot\varepsilon_\lambda\, J_n\cdot\varepsilon_\lambda^* = \frac{1}{q_o^2}\sum_i\sum_j Q_iQ_j\left(\frac{p_{i_y}}{E_i}\,\frac{p_{j_y}}{E_j}\right.$$

$$+\ \mathrm{sign}(y_i)\mathrm{sign}(y_j)\left[\left(1-\frac{m_{i_T}^2}{2E_i^2}+\ldots\right)\left(1+\frac{p_{i_x}}{E_i}+\frac{p_{i_x}^2}{E_i^2}+\ldots\right)\right.$$

$$\left.\left.\times\left(1-\frac{m_{j_T}^2}{2E_j^2}+\ldots\right)\left(1+\frac{p_{j_x}}{E_j}+\frac{p_{j_x}^2}{E_j^2}+\ldots\right)\right]\right) \qquad (2.15)$$

where $E^2 = m_T^2 + p_z^2$, $m_T^2 = m^2 + p_x^2 + p_y^2 = m^2 + p_T^2$ and m_T is known as the transverse mass. Equation (2.15) can be divided into two pieces, a term corresponding to the charge fluctuation $(\sim \mathrm{sign}(y_i)\mathrm{sign}(y_j))$ and the correction term C_T.

To obtain an expression for C_T, we assume the pions are produced symmetrically about the beam axis, so that any terms which are odd in p_{i_x} or p_{i_y} will vanish on integration. In similar spirit, we take $p_x^2 \simeq \frac{p_T^2}{2} \simeq p_y^2$ and $p_{c_x}p_{d_x} \simeq \frac{\vec{p}_{c_T}\cdot\vec{p}_{d_T}}{2} \simeq p_{c_y}p_{d_y}$

($\vec{p}_{c_T}$ is the two-dimensional transverse momentum vector).

Since

$$e^{2y} = \ln\left(\frac{E+p_z}{E-p_z}\right) = \ln\left(\frac{E+\sqrt{E^2-m_T^2}}{E-\sqrt{E^2-m_T^2}}\right)$$

$$\Rightarrow\ (e^{2y}+1)^2\,(E^2-m_T^2) = E^2\,(e^{2y}-1)^2$$

we have $E = m_T\cosh y$ and also $p_z = m_T\sinh y$.

$$C_T = \frac{1}{\sigma} \sum_c \int 2E_c \frac{d\sigma}{d^3p_c} \left(\frac{p_{c_T}^2 - m_c^2}{m_{c_T}^2 \cosh^2 y_c} \right) \frac{d^3p_c}{2E_c}$$

$$+ \frac{1}{\sigma} \sum_c \sum_d Q_c Q_d \int\int \frac{d\sigma}{d^3p_c d^3p_d} \, 2E_c 2E_d \, \frac{d^3p_c}{2E_c} \, \frac{d^3p_d}{2E_d}$$

$$x \left(\frac{1}{2} \frac{\vec{p}_{c_T} \cdot \vec{p}_{d_T}}{m_{c_T} m_{d_T} \cosh y_c \cosh y_d} \right.$$

$$+ \operatorname{sign}(y_c) \operatorname{sign}(y_d) \left[- \frac{m_c^2}{2m_{c_T}^2 \cosh^2 y_c} - \frac{m_d^2}{2m_{d_T}^2 \cosh^2 y_d} \right.$$

$$\left. \left. + \frac{\vec{p}_{c_T} \cdot \vec{p}_{d_T}}{2m_{c_T} m_{d_T} \cosh y_c \cosh y_d} \right] \right) \qquad (2.16)$$

The $(1/q_o)$ term in the bremsstrahlung spectrum (equation (2.1)) has coefficient c_2. We estimate this contribution by looking at the second order terms in equation (2.6). The relevant expression, including the photon polarization vectors, is

$$\sum_{\lambda=\pm} \left(\sum_{i=1}^{n} \sum_{j=1}^{n} Q_i Q_j \frac{p_i \cdot \varepsilon_\lambda}{p_i \cdot q} \left[\frac{p_j \cdot \varepsilon_\lambda^*}{p_j \cdot q} q \cdot \nabla^j - \nabla^j \cdot \varepsilon_\lambda^* \right] \right.$$

$$- \sum_{\ell=a,b} \sum_{j=1}^{n} Q_\ell Q_j \frac{p_\ell \cdot \varepsilon_\lambda}{p_\ell \cdot q} \left[\frac{p_j \cdot \varepsilon_\lambda^*}{p_j \cdot q} q \cdot \nabla^j - \nabla^j \cdot \varepsilon_\lambda^* \right]$$

$$- \sum_{i=1}^{n} \sum_{k=a,b} Q_i Q_k \frac{p_i \cdot \varepsilon_\lambda}{p_i \cdot q} \left[\frac{p_k \cdot \varepsilon_\lambda^*}{p_k \cdot q} q \cdot \nabla^k - \nabla^k \cdot \varepsilon_\lambda^* \right]$$

$$\left. + \sum_{\ell=a,b} \sum_{k=a,b} Q_\ell Q_k \frac{p_\ell \cdot \varepsilon_\lambda}{p_\ell \cdot q} \left[\frac{p_k \cdot \varepsilon_\lambda^*}{p_k \cdot q} q \cdot \nabla^k - \nabla^k \cdot \varepsilon_\lambda^* \right] \right)$$

$$x \; |T_n|^2 \qquad (2.17)$$

(where $T_n = T_n(p_a, p_b; p_1, \ldots p_n)$)

and again by the symmetry of the centre-of-mass proton-proton collision, we can take the first term as dominant. (The squared amplitude is taken as a constant with respect to initial state momenta). Summing over the transverse polarizations ($\varepsilon_\pm = \frac{1}{\sqrt{2}}(0,0,i,\mp 1)$ as before for photon at 90°), equation (2.17) becomes

$$\sum_i \sum_j Q_i Q_j \left(\frac{(p_{i_y} p_{j_y} + p_{i_z} p_{j_z})(\nabla_o^{\,j} \overset{+}{-} \nabla_x^{\,j})}{(E_i - p_{i_x})(E_j - p_{j_x})} - \frac{(p_{i_y} \nabla_y^{\,j} + p_{i_z} \nabla_z^{\,j})}{(E_i - p_{i_x})} \right) |T_n|^2 \qquad (2.18)$$

We define D_T to be the coefficient corresponding to this second order term, then (dividing throughout by σ)

$$D_T = \frac{1}{\sigma} \sum_c \int \frac{d^3p_c}{2E_c} \left(\frac{(p_{c_y}^{\,2} + p_{c_z}^{\,2})}{(E_c - p_{c_x})^2} \left(\frac{\partial}{\partial E_c} + \frac{\partial}{\partial p_{c_x}}\right) - \frac{\left(p_{c_y} \frac{\partial}{\partial p_{c_y}} + p_{c_z} \frac{\partial}{\partial p_{c_z}}\right)}{(E_c - p_{c_x})} \right) \frac{d\sigma}{d^3p_c} \, 2E_c$$

$$+ \frac{1}{\sigma} \sum_c \sum_d Q_c Q_d \int\int \frac{d^3p_c}{2E_c} \frac{d^3p_d}{2E_d}$$

$$\times \left(\frac{(p_{c_y} p_{d_y} + p_{c_z} p_{d_z})}{(E_c - p_{c_x})(E_d - p_{d_x})} \left(\frac{\partial}{\partial E_d} + \frac{\partial}{\partial p_{d_x}}\right) - \frac{\left(p_{c_y} \frac{\partial}{\partial p_{d_y}} + p_{c_z} \frac{\partial}{\partial p_{d_z}}\right)}{(E_c - p_{c_x})} \right) 2E_c 2E_d \frac{d\sigma}{d^3p_c \, d^3p_d} \qquad (2.19)$$

This term is now to be included in the expression for the large angle real photon cross section. Equation (2.13) is modified and now becomes

$$\left(q_o \frac{d\sigma}{d^3q}\right)^{90^o} = \frac{\alpha\sigma}{4\pi^2}\left(\frac{\langle\Delta^2 Q\rangle + C_T}{q_o^{\,2}} + \frac{D_T}{q_o}\right) \qquad (2.20a)$$

It is appropriate to note here that this equation is only valid for the $q_o \to o$ limit and that the last term will be most sensitive to increases in the value of q_o. The "soft" photon expansion we use is expected to be valid for $2q_oE << m^2$ (where E and m are respectively the energy and mass of the radiating hadron). As q_o is allowed to grow towards this limit, off-shell damping effects will become increasingly important. The off-shell behaviour of hadronic production amplitudes is partly determined by natural damping of multi-Regge amplitudes in the Toller variables [32]. (Fig 2.3 illustrates the dependence of production amplitudes on the Toller variable η). This effect can be related through unitarity and analyticity to the transverse mass dependence of the single-particle-inclusive cross section.

In this case, the transverse mass is defined by $m_T = (p^2 + p_T^{\,2})^{\frac{1}{2}}$ where p^2 is the virtual mass squared and p_T is the transverse momentum of the off-mass-shell leg. Those higher order terms in the expansion of the photon cross section which are not strongly dominated by the small q_o limit will be affected by this off-shell behaviour. Bearing in mind the expected $F(m_T) = \exp(-am_T)$ behaviour of inclusive cross sections, we insert a simple $\exp(-aq_o)$ factor to control this damping.

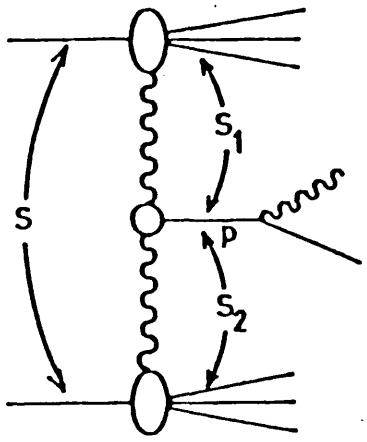

$$\frac{s_1 s_2}{s} = \eta^2 = p^2 + p_T^2$$

Figure 2.3 Diagram illustrating the dependence of the off-shell behaviour of production amplitudes on the Toller variable η.

Then

$$\left(q_o \frac{d\sigma}{d^3q}\right)^{90^o} = \frac{\alpha}{4\pi^2}\left(\frac{\langle\Delta^2 Q\rangle + C_T}{q_o^{\,2}} + \frac{D_T}{q_o}\, e^{-aq_o}\right) \qquad (2.20b)$$

We now consider <u>photons produced along the beam direction</u> ($\theta = 0^o$). In this case, we shall see that the familiar problem of soft photon summation arises. The transverse polarization vectors are now $\varepsilon_\pm = 1/\sqrt{2}\ (0,1,\pm i,0)$ and

$$\frac{p_i\cdot\varepsilon_\pm}{p_i\cdot q} = -\frac{1}{\sqrt{2}}\ \frac{p_{i_x} \pm i p_{i_y}}{q_o(E_i - p_{i_z})}$$

$$= -\frac{1}{\sqrt{2}} \frac{e^{\pm i\Phi_i} p_{i_T}}{q_o m_{i_T} e^{-y_i}} \tag{2.21}$$

where Φ_i is the hadronic azimuthal angle ($p_i = (E_i, p_{i_T} \cos \Phi_i, p_{i_T} \sin \Phi_i, p_{i_z})$).

We proceed naively to calculate the $1/q_o^2$ term to order α. The relevant contribution will be (c.f. eqn. (2.14)) (note $p_{a_T} = p_{b_T} = 0$)

$$\sum_i \sum_j Q_i Q_j \frac{1}{2q_o^2} \left(\frac{p_{i_T} e^{i\Phi_i}}{m_{i_T} e^{-y_i}} \frac{p_{j_T} e^{-i\Phi_j}}{m_{j_T} e^{-y_{i_j}}} + \frac{p_{i_T} e^{-i\Phi_i}}{m_{i_T} e^{-y_i}} \frac{p_{j_T} e^{-i\Phi_j}}{m_{j_T} e^{-y_j}} \right)$$

$$= \sum_i \sum_j Q_i Q_j \frac{1}{q_o^2} \left(\frac{\vec{p}_{i_T} \cdot \vec{p}_{j_T}}{m_{i_T} m_{j_T} e^{-y_i} e^{-y_j}} \right) \tag{2.22}$$

where $\vec{p}_{i_T}$ is the two dimensional vector, $\vec{p}_{i_T} = (p_{i_T} \cos \Phi_i, p_{i_T} \sin \Phi_i)$. Then the real photon cross section at 0° assumes the following form, when we exhibit only the diagonal part of equation (2.22).

$$\left(q_o \frac{d\sigma}{d^3q}\right)^{0^o} = \frac{\alpha}{4\pi^2} \frac{1}{q_o^2} \left(\sum_c \int \frac{d^3p_c}{2E_c} \frac{p_{c_T}^2}{m_{c_T}^2} e^{2y_c} 2E_c \frac{d\sigma}{d^3p_c} + \ldots \right). \tag{2.23}$$

We shall show below that this expression has a linear rise in s and hence that the perturbation expansion in α is in some sense spurious.

We assume a simple form for the inclusive cross-section of the produced hadron 30

$$E_c \frac{d\sigma}{d^3p_c} = \frac{d\sigma}{dy_c d^2p_{c_T}} = F(p_{c_T})\, g(y_c) \tag{2.24}$$

with the transverse momentum dependence normalized so that $\int F(p_{c_T})\, d^2p_{c_T} = 1$, and as usual

$$\int \frac{p_{c_T}^2}{m_{c_T}^2} F(p_{c_T})\, d^2p_{c_T} = \left\langle \frac{p_{c_T}^2}{m_{c_T}^2} \right\rangle .$$

Hadronic scaling (i.e. inclusive cross sections as functions of p_T and $x = 2P_z/\sqrt{s}$ only) is largely satisfied at higher s values and one consequence is that $d\sigma/dy = g(y)$ has a constant plateau over the central region. This effect is shown in fig. 2.4.

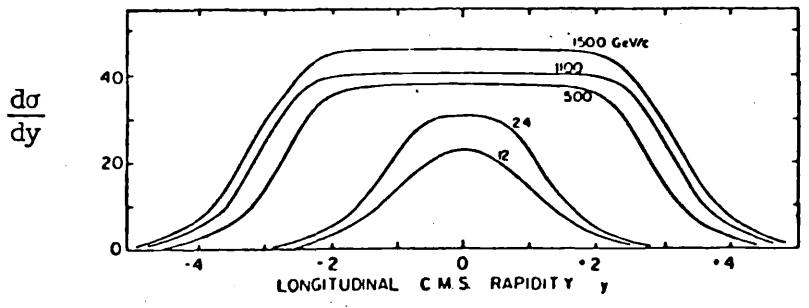

Figure 2.4 Showing the plateau in rapidity of inclusive cross sections ($p+p \to \pi+X$) at different energies.

Thus we take $g(y) \simeq \text{constant} = g(0)$. The total available rapidity $Y \sim \ln (s/m^2)$ and so

$$\left(q_o \frac{d\sigma}{d^3q}\right)^{0^o} \simeq \frac{\alpha}{4\pi^2} \frac{1}{q_o^2} \left(\sum_c \left\langle \frac{p_{c_T}^2}{m_{c_T}^2} \right\rangle g_c(0) \frac{s}{2m^2} + \ldots\right) \quad (2.25)$$

This strong peaking of real photon emission parallel to the beam direction has long been known to experimentalists. It has also been seem in early work on radiative corrections and cancellations of infrared divergences [33]. When $\alpha s/m^2 \sim 1$, we should do a complete photon summation (i.e. sum over number of photons emitted) particularly in view of the difficulty of isolating single photons experimentally.

Henceforward we shall concentrate on large angle production which will be more relevant to our aim of large p_T leptons. It is at least apparent that real photons follow broadly the distribution of the hadronic final state - what might be described as a halo effect.

The strong collimation of photons with the forward hadronic jet can be demonstrated by examining the angular distribution. To obtain a rough estimate, we consider a photon at 0° together with the radiating hadron at θ^o, then

$$\frac{|p.\varepsilon_\lambda|^2}{(p.q)^2} \simeq \frac{|\underline{p}|^2 \sin^2\theta}{(E - |\underline{p}| \cos\theta)^2}$$

$$\simeq \frac{\sin^2\theta}{(1 + \frac{2m^2}{s} - \cos\theta)^2}$$

which suggests, $((1 - \cos\theta) \simeq -\theta^2/2)$, an angular spread $\Delta\theta \sim 2m/\sqrt{s}$, which will be small.

APPENDIX 2.1

We use the following fundamental formulae [30] :-

Phase space:

$$d\Pi_n = \int \left(\prod_{i=1}^{n} \frac{d^3p_i}{2E_i(2\pi)^3} \right) (2\pi)^4 \, \delta^4(p_a+p_b-\sum_i^n p_i) \qquad (1)$$

Total cross section:

$$\sigma_{TOT} = \frac{1}{2s} \sum_{n=2}^{\infty} \int d\Pi_n \, |T_{2\to n}|^2 \qquad (2)$$

Inclusive cross section for particle type c:

$$E_c \frac{d\sigma}{d^3p_c} = \frac{1}{2s} \sum_{n=2}^{\infty} \sum_{k\sim c} \int d\Pi_n \, E_k \delta^3(p_k-p_c) \, |T_{2\to n}|^2 \qquad (3)$$

Twice-inclusive cross section for particles c and d:

$$E_c E_d \frac{d\sigma}{d^3p_c d^3p_d} = \frac{1}{2s} \sum_{n=2}^{\infty} \sum_{\substack{k\sim c \\ k\neq \ell}} \sum_{\ell\sim d} \int d\Pi_n \, E_k \, \delta^3(p_k-p_c)$$

$$\times \, E_\ell \, \delta^3 (p_\ell-p_d) \, |T_{2\to n}|^2 \qquad (4)$$

Average multiplicities:

$$\int E_c \frac{d\sigma}{d^3p_c} \frac{d^3p_c}{E_c} = \langle n_c \rangle \, \sigma \qquad (5)$$

$$\int E_c E_d \frac{d\sigma}{d^3p_c d^3p_d} \frac{d^3p_c}{E_c} \frac{d^3p_d}{E_d} = \langle n_c n_d - \delta_{cd} n_c \rangle \sigma \qquad (6)$$

Charge Sum Rules:

$$(Q_a+Q_b)\sigma = \sum_c \int \frac{d^3p_c}{E_c} \; E_c \; \frac{d\sigma}{d^3p_c} \; Q_c \tag{7}$$

$$(Q_a+Q_b-Q_c)\; E_c \; \frac{d\sigma}{d^3p_c} = \sum_d \int E_c E_d \; \frac{d\sigma}{d^3p_c d^3p_d} \; Q_d \; \frac{d^3p_d}{E_d} \tag{8}$$

<u>Derivation of charge fluctuation formula</u>:

$$\sigma\langle\Delta^2 Q\rangle = \frac{1}{2s} \sum_{n=2}^{\infty} \int d\Pi_n \; |T_{2\to n}|^2$$

$$\times \left(\sum_{i=1}^{n} Q_i \; \mathrm{sign}(y_i) - Q_a \; \mathrm{sign}(y_a) - Q_b \; \mathrm{sign}(y_b) \right)^2 \tag{9}$$

For centre-of-mass collisions of identical particles, ($Q_a = Q_b$, $\mathrm{sign}(y_a) = -\mathrm{sign}(y_b)$),

$$\sigma\langle\Delta^2 Q\rangle = \frac{1}{2s} \sum_{n=2}^{\infty} \int d\Pi_n \; |T_{2\to n}|^2$$

$$\times \left(\sum_i \sum_j Q_i Q_j \; \mathrm{sign}(y_i) \; \mathrm{sign}(y_j) \right)$$

$$= \sum_c \int \frac{d\sigma}{d^3p_c} \; d^3p_c$$

$$+ \sum_c \sum_d Q_c Q_d \int\int dy_c dy_d \; \frac{d\sigma}{dy_c dy_d} \; \mathrm{sign}(y_c) \; \mathrm{sign}(y_d)$$

and using equations (7) and (8)

$$\sigma\langle\Delta^2 Q\rangle = \langle n\rangle\sigma + (Q_a + Q_b)^2\sigma - \langle n\rangle\sigma$$

$$- 2 \sum_c \sum_d Q_c Q_d \left[\int_{-\frac{Y}{2}}^{0} \int_{0}^{\frac{Y}{2}} + \int_{0}^{\frac{Y}{2}} \int_{-\frac{Y}{2}}^{0} \right] \frac{d\sigma}{dy_c dy_d} \, dy_c dy_d$$

$$= - 2\sigma \sum_c \sum_d Q_c Q_d \left[\int_{-\frac{Y}{2}}^{0} \int_{0}^{\frac{Y}{2}} + \int_{0}^{\frac{Y}{2}} \int_{-\frac{Y}{2}}^{0} \right] C_{cd}(y_c, y_d) dy_c dy_d$$

by symmetry of collision.

So (c.f. [31]).

$$\langle\Delta^2 Q\rangle = - 4 \sum_c \sum_d Q_c Q_d \int_{-\frac{Y}{2}}^{0} \int_{0}^{\frac{Y}{2}} C_{cd}(y_c, y_d) dy_c dy_d \quad .$$

CHAPTER III

In this chapter we consider how the methods of Chapter II can be extended to the case of low mass e^+e^- pair production. The pair creation process relevant to this discussion is shown in fig. 3.1

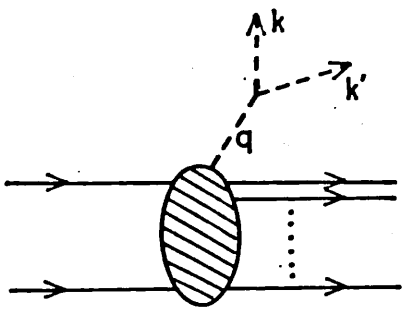

Figure 3.1 Amplitude for pair production via a virtual photon.

and involves the decay of a soft virtual photon ($q^2 \to 0$, $q_o \to 0$). We use k and k' for the lepton momenta ($q = k + k'$).

To obtain an expression for the e^+e^- pair production via this soft virtual photon emission, we work with an analogy of equations (2.6) and (2.8). The hadronic tensor $H^{\mu\nu}$ (equation (2.6)) is continued to small $q^2 \neq 0$ and the denominators (off-shell hadronic propagators) will now become $(2p_i.q + q^2)$. The sum over real photon polarization vectors which appears in equation (2.8) is replaced for the virtual photon decay process by a leptonic tensor $L_{\mu\nu}$. A squared photon propagator will also be required. Thus we have

$$4k_o k_o' \frac{d\sigma}{d^3k d^3k'} = \frac{e^4}{(2\pi)^6} \frac{1}{2s} \sum_{n=2}^{\infty} \int \left(\prod_{i=1}^{n} \frac{d^3p_i}{2E_i(2\pi)^3} \right)$$

$$\times (2\pi)^4 \delta^4(p_a+p_b-\sum_i^n p_i) \frac{H^{\mu\nu}L_{\mu\nu}}{q^4} \qquad (3.1)$$

We use Feynman rules (see Appendix) to obtain $L_{\mu\nu}$. Setting the electron mass squared equal to zero ($m_e^2 = 0$),

$$L_{\mu\nu} = \sum_{s,s'} (\bar{u}\,\gamma_\mu v)(\bar{v}\,\gamma_\nu u)$$

$$\simeq \mathrm{Tr}\quad \gamma_\mu \not{k}' \gamma_\nu \not{k}$$

$$\simeq -2q^2 g_{\mu\nu} + 4k'_\mu k_\nu + 4k_\mu k'_\nu \qquad (3.2)$$

Since $H_{\mu\nu}$ is gauge invariant, we can rewrite equation (3.1) in terms of an effective photon cross section $(2q_o\, d\sigma/d^3q)_{eff}$. This effective cross section is obtained by replacing $\varepsilon_\pm^\mu$ in the real photon cross section by ε_λ^μ ($\lambda = \pm,0$) (i.e. $q^2 \neq 0$) with the properties $q.\varepsilon_\lambda = 0$, $-g_{\mu\nu}\, \varepsilon_\lambda^\mu\, \varepsilon_{\lambda'}^{*\nu} = \delta_{\lambda\lambda'}$ and

$$\sum_\lambda \varepsilon_\lambda^\mu\, \varepsilon_\lambda^{*\nu} = -g^{\mu\nu} + \frac{q^\mu q^\nu}{q^2}\,. \qquad (3.3)$$

Now clearly we can write

$$H^{\mu\nu} L_{\mu\nu} = H^{\mu\nu'}\, g^{\nu}{}_{\nu'}\, g_\mu{}^{\mu'} L_{\mu'\nu}$$

and, by making use of equation (3.3) and gauge invariance, this becomes

$$H^{\mu\nu}L_{\mu\nu} = \sum_{\lambda=\pm,0} \sum_{\lambda'=\pm,0} H^{\mu\nu'} \varepsilon_{\lambda\nu'} \varepsilon^{*\nu}_{\lambda} \quad \varepsilon^{*}_{\lambda'\mu} \varepsilon_{\lambda'}{}^{\mu'} L_{\mu'\nu} \quad (3.4)$$

and equation (3.1) can be written

$$4k_o k_o' \frac{d\sigma}{d^3k d^3k'} = \frac{\alpha}{2\pi^2} \int \frac{dq^2}{q^2} \delta(q^2-2k.q)\, d^3\underline{q}\, \delta^3(\underline{q}-\underline{k}-\underline{k}')$$

$$\times \left(2q_o \frac{d\sigma}{d^3q}\right)_{eff} \quad 4\, \mathrm{Tr}(\rho W) \qquad (3.5)$$

where we have introduced the density matrix

$$\rho_{\lambda\lambda'} = \frac{\sum_{n=2}^{\infty} \int \left(\prod_{i=1}^{n} \frac{d^3p_i}{2E_i(2\pi)^3}\right) H^{\mu\nu} \varepsilon_{\lambda\nu} \varepsilon^{*}_{\lambda'\mu}}{\sum_{\lambda''=\pm,0} \sum_{n=2}^{\infty} \int \left(\prod_{i=1}^{n} \frac{d^3p_i}{2E_i(2\pi)^3}\right) H^{\mu'\nu'} \varepsilon_{\lambda''\mu'} \varepsilon^{*}_{\lambda''\nu'}} \qquad (3.6)$$

and the virtual photon decay distribution

$$W_{\lambda\lambda'} = \frac{\varepsilon_{\lambda'}{}^{\mu} \varepsilon_{\lambda}{}^{*\nu} \left(-2g_{\mu\nu} + \frac{4}{q^2}(k'_{\mu}k_{\nu} + k_{\mu}k'_{\nu})\right)}{-g^{\mu'\nu'} \left(-2g_{\mu'\nu'} + \frac{4}{q^2}(k'_{\mu'}k_{\nu'} + k_{\mu'}k'_{\nu'})\right)} \qquad (3.7)$$

For the case of a single electron (or positron) detected at a production angle of θ^o to the beam direction, we define the x-axis perpendicular to the beam direction in the plane containing the beam and the detected lepton. The angle between the virtual photon and the lepton is designated θ and the azimuthal angle denoted by ϕ. This configuration is shown in fig. 3.2 for $\theta = 90^o$. Using the conservation of momentum delta function, we can integrate over the undetected lepton momentum.

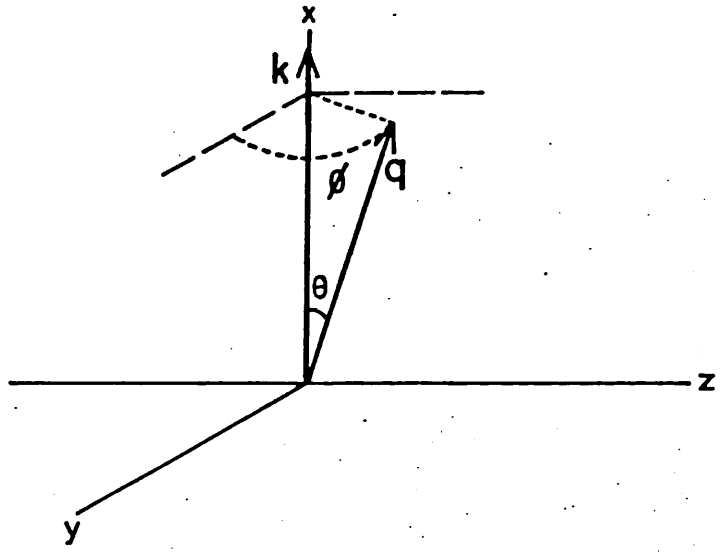

Figure 3.2 Showing the orientation of the virtual photon with respect to a lepton produced along the x-axis.

We note

$$dq^2\ d^3\underline{q}\ \delta(q^2 - 2k.q)\ \delta^3(\underline{q} - \underline{k} - \underline{k}') = d^4q\ \delta^4(q - k - k')$$

$$= |\underline{q}|\ dq_o\ \frac{dq^2}{2}\ d\cos\theta\ d\phi\ \delta^4(q - k - k')$$

and integrating over $\frac{d^3k'}{2k_o'}$ obtain

$$dq^2\ d^3\underline{q}\ \delta(q^2 - 2k.q)\ \delta^3(\underline{q} - \underline{k} - \underline{k}')\ \frac{d^3k'}{2k_o'}$$

$$= |\underline{q}|\ dq_o\ \frac{dq^2}{2}\ \frac{1}{2k_o'}\ d\cos\theta d\phi\ \ \delta(q_o - k_o - k_o')$$

$$= \frac{dq^2}{4|\underline{k}|}\ dq_o\ d\phi$$

where $$\cos\theta = \frac{2k_oq_o - q^2}{2|\underline{k}|\ |\underline{q}|} \quad . \qquad (3.8)$$

Now we can express the single lepton inclusive cross section in terms of an integral over the effective photon cross section.

$$2k_o \frac{d\sigma}{d^3k} = \frac{\alpha}{2\pi^2} \int \frac{dq^2}{q^2} \int \frac{dq_o}{4|\underline{k}|} \int d\phi \left(2q_o \frac{d\sigma}{d^3q}\right)_{eff}$$

$$\times\ 4\ \mathrm{Tr}(\rho W) \qquad (3.9)$$

We are interested in those contributions for which the hadronic propagators stay near the mass shell and the virtual photons remain soft. The integrals in equation (3.9) are dominated by their lower limits - the region where our approximations are valid. If we look at the region where $q^2 << 4k_o^2$, the well known parent-child kinematics lead to the Sternheimer formula [34]. This formula gives $\cos\theta \simeq 1$ and $q_o \sim k_o$, which means that the produced lepton follows closely the direction of the parent virtual photon and is created with energy $\sim q_o$. We can derive this result easily from equation (3.8).

Using $q^2 = q_o{}^2 - |\underline{q}|^2$, equation (3.8) will yield a quadratic equation in q_o with solutions

$$q_o = \tfrac{1}{2} \frac{\left(k_o q^2 \pm |\underline{k}|\cos\theta[q^2(q^2 - 4k_o{}^2 + 4|\underline{k}|^2\cos^2\theta)]^{\frac{1}{2}}\right)}{(k_o{}^2 - |\underline{k}|^2 \cos^2\theta)} \qquad (3.10)$$

The condition for real roots gives

$$\cos^2\theta \geq 1 - \frac{(q^2 - 4m_e{}^2)}{4|\underline{k}|^2}$$

$$\simeq 1 - \frac{q^2}{4k^2} \qquad (3.11)$$

for $m_e^2 \simeq 0$ and $k_o \simeq |\underline{k}| = k$. For the Sternheimer limit, $q^2/4k^2 << 1$, equation (3.11) implies $\cos^2\theta \simeq 1$. Evidently, $\cos\theta \neq 1$ since this would involve $q^2 > 2kq_o \Rightarrow q^4/4k^2 > q_o^2 \geqq q^2 \Rightarrow q^2 > 4k^2$. Hence $\cos\theta \simeq 1$. The lower limit of the energy integration is found from equation (3.10) by putting $\cos\theta = 1$ and taking the minus sign. (The electron mass must be retained during the intermediate stages of the derivation).

$$q_{o_{min}} = \frac{k_o q^2 - |\underline{k}|[q^2(q^2 - 4m_e^2)]^{\frac{1}{2}}}{2m_e^2}$$

$$= k + \frac{q^2}{4k} \qquad \text{with} \quad m_e^2 \to 0 \qquad (3.12)$$

Thus $q_o \sim k$ and we have the Sternheimer result.

The single lepton cross section now appears as

$$2k_o \frac{d\sigma}{d^3k} = \frac{\alpha}{2\pi^2} \int_{4m_e^2} \frac{dq^2}{q^2} \int_{q_{o_{min}}} \frac{dq_o}{4k} \int d\phi \left(2q_o \frac{d\sigma}{d^3q}\right)_{eff}$$

$$\times\ 4\ \mathrm{Tr}\ (\rho W) \qquad (3.13)$$

and we shall discuss further the question of the range of integrations in Chapter IV.

We concentrate on the production of leptons perpendicular to the beam direction ($\theta = 90^o$). In the configuration of fig. 3.2,

$$k = (k,k,0,0)$$

$$q = (q_o, |\underline{q}|\cos\theta, |\underline{q}|\sin\theta\cos\phi, |\underline{q}|\sin\theta\sin\phi)$$

$$\varepsilon_+ = \frac{1}{\sqrt{2}}(0, -\sin\theta, \cos\theta\cos\phi + i\sin\phi, \cos\theta\sin\phi - i\cos\phi)$$

$$\varepsilon_- = \frac{1}{\sqrt{2}}(0, \sin\theta, -\cos\theta\cos\phi + i\sin\phi, -\cos\theta\sin\phi - i\cos\phi)$$

$$\varepsilon_o = \frac{1}{\sqrt{q^2}}(|\underline{q}|, q_o\cos\theta, q_o\sin\theta\cos\phi, q_o\sin\theta\sin\phi).$$

The numerator of $W_{\lambda\lambda'}$ (equation (3.7)) can be modified,

$$\varepsilon^{\mu}_{\lambda'}\varepsilon_{\lambda}^{*\nu}\left(-2g_{\mu\nu} + \frac{4}{q^2}(k'_{\mu}k_{\nu} + k_{\mu}k'_{\nu})\right)$$

$$= \varepsilon^{\mu}_{\lambda'}\varepsilon_{\lambda}^{*\nu}\left(-2g_{\mu\nu} - \frac{8}{q^2}k_{\mu}k_{\nu}\right)$$

by using the property $q.\varepsilon_{\lambda} = 0$. Also,

$$k_{\mu} \simeq \frac{k}{q_o}q_{\mu} + (0, -\frac{k}{q_o}|\underline{q}|\cos\theta + k, -\frac{k}{q_o}|\underline{q}|\sin\theta\cos\phi, -\frac{k}{q_o}|\underline{q}|\sin\theta\sin\phi)$$

then put $|\underline{q}| = q_o - \frac{q^2}{2q_o}$, $\cos\theta = 1 - \frac{\sin^2\theta}{2}$ and get (to order $\sin^2\theta$)

$$k_{\mu} \simeq \frac{k}{q_o}q_{\mu} + (0, k(\frac{q^2}{2q_o^2} + \frac{\sin^2\theta}{2}), -k\sin\theta\cos\phi, -k\sin\theta\sin\phi).$$

So we have k_{μ} in terms of q_{μ} and an expansion up to order q^2. (We have $\sin^2\theta$ of order q^2 from equation (3.11)). For the tensor $k_{\mu}k_{\nu}$, removing q_{μ} and q_{ν} terms, only y and z components will be $O(q^2)$, remaining terms are higher order. So, as a

matrix, we can approximate to

$$k_\mu k_\nu \sim k^2 \sin^2\theta \begin{pmatrix} 0 & 0 & 0 & 0 \\ 0 & 0 & 0 & 0 \\ 0 & 0 & \cos^2\phi & \cos\phi\sin\phi \\ 0 & 0 & \cos\phi\sin\phi & \sin^2\phi \end{pmatrix}$$

If we integrate the term proportional to $k_\mu k_\nu H^{\mu\nu}$, in $\mathrm{Tr}\,(\rho W)$, over the azimuthal angle, only the diagonal terms will survive. This is a consequence of the following integral results

$$\int_0^{2\pi} \cos^2\phi \, d\phi = \pi = \int_0^{2\pi} \sin^2\phi \, d\phi$$

$$\int_0^{2\pi} \sin\phi \cos\phi \, d\phi = 0.$$

So, removing ϕ dependence, we can equivalently use

$$k_\mu k_\nu \sim \frac{k^2 \sin^2\theta}{2} \begin{pmatrix} 0 & 0 & 0 & 0 \\ 0 & 0 & 0 & 0 \\ 0 & 0 & 1 & 0 \\ 0 & 0 & 0 & 1 \end{pmatrix} \quad (3.14)$$

and note that $k_\mu k_\nu/q^2 = O(1)$. In the low q^2 region, we expect that only the transverse polarizations will survive, so we replace $(2q_o \; d\sigma/d^3q)_{eff}$ by the real photon cross section and assume that the error involved in this substitution will be small. We see from equation (3.14) and equation (2.14) that the effect of the leptonic tensor $k_\mu k_\nu$ will be proportional to a sum over real polarization vectors. Thus we replace

$$\left(2q_o \; \frac{d\sigma}{d^3q}\right)_{eff} \quad 4 \; \mathrm{Tr} \; (\rho W)$$

by

$$\left(2q_o \; \frac{d\sigma}{d^3q}\right) \; 2 \; [1 - \frac{2k^2}{q^2} \; \sin^2\theta]$$

and obtain

$$2k_o \; \frac{d\sigma}{d^3k}^{90^o} = \frac{\alpha}{2\pi^2} \int_{4m_e^2} \frac{dq^2}{q^2} \int_{q_{o_{min}}} \frac{dq_o}{4k} \int d\phi$$

$$\times \left(2q_o \; \frac{d\sigma}{d^3q}\right) \; 2 \; [1 - \frac{2k^2}{q^2} \; \sin^2\theta]$$

$$= \frac{\alpha}{2\pi^2}^{2} \; \frac{\sigma}{2k} \int_{4m_e^2} \frac{dq^2}{q^2} \int_{q_{o_{min}}} dq_o \int d\phi$$

$$\times \; [1 - \frac{2k^2}{q^2} \sin^2\theta] \left(\frac{\langle \Delta^2 Q \rangle + C_T}{q_o^{\,2}} + \frac{D_T e^{-aq_o}}{q_o} \right) \qquad (3.15)$$

with

$$\sin^2\theta = 1 - \left[\frac{2kq_o - q^2}{2k(q_o^{\,2} - q^2)^{\frac{1}{2}}} \right]^2 .$$

We discuss the numerical integration of equation (3.15) fully in Chapter IV, but an analytic approximation can easily be found. Expanding $\sin^2\theta$ in powers of q^2 gives

$$\sin^2\theta \simeq \frac{q^2}{q_o}\left(\frac{1}{k} - \frac{1}{q_o}\right) + \dots \quad (3.16)$$

and if, for this estimate only, we let $q_{o_{min}} = k$, $q_{o_{max}} \to \infty$ and $q^2_{max} = 4k^2$, we can use equation (3.15) in the form

$$2k_o \frac{d\sigma}{d^3k}^{90^o} \simeq \frac{\alpha}{2\pi^2}^{2} \frac{\sigma}{2k} \int_{4m_e^2}^{4k^2} \frac{dq^2}{q^2} \int_{q_o}^{\infty} dq_o \int_o^{2\pi} d\phi$$

$$x\left[1 - \frac{2k^2}{q_o}\left(\frac{1}{k} - \frac{1}{q_o}\right)\right]\left(\frac{\langle\Delta^2 Q\rangle + C_T}{q_o^2} + \frac{D_T e^{-aq_o}}{q_o}\right)$$

$$= \frac{\alpha}{2\pi^2}^{2} \frac{\pi\sigma}{k} \ln\left(\frac{k^2}{m_e^2}\right) \frac{2}{3k}\left(\langle\Delta^2 Q\rangle + C_T\right)$$

$$+ D_T\left[E_1(ak)(1 + ak)^2 - e^{-ak}(1 + ak)\right] \quad (3.17)$$

where E_1 is the Exponential Integral. This result is derived in the first appendix to this chapter (Appendix 3.1)

Much of the yield will originate from pairs with small opening angle (ψ), so we must consider the influence of experimental cuts when comparing with the data. A discussion of opening angles and their kinematic relations is given in the second appendix to this chapter. (Appendix 3.2).

This estimate of the bremsstrahlung contribution to electron yield at low transverse momentum has a k_T^{-2} rise ($k = k_T$ at 90°). The electron to pion ratio is obviously found by dividing equation (3.17) by a relevant parameterization of the large angle pion production data.

Finally, we point out that there is some uncertainty if one extrapolates to virtual photons away from 90°. Since, at 90°, $q_z^2 = 0$ and $q_o^2 = q^2 + q_T^2$ whereas for $\theta < 90^o$, $q_o^2 - q_z^2 = q^2 + q_T^2$. By looking at the propagators we can expect that $q_o^2 \rightarrow q^2 + q_T^2$ would be the proper replacement.

At this point, we outline the method for calculating the production of prompt electrons at low transverse momentum via the vector meson dominated low mass continuum. This contribution to the e/π ratio, as we discussed in Chapter I, dominates all other conventional sources in the low k_T region.

Vector meson dominated low mass continuum.

Craigie and Schildknecht [14] point out that the low mass vector meson continuum ($q^2 << m_V^2$) strongly influences the low transverse momentum lepton yield. This result is in contrast with previous estimates [13] based on the narrow width approximation, which fall off steeply for $k_T < m_V/2$, as we discussed in Chapter I. We shall briefly describe the method of

ref. [14]. This contribution is related to the higher order terms in the soft photon expansion.

Traditionally, the single lepton spectrum resulting from the production of a parent particle and its subsequent decay is expressed in the following form (narrow width)

$$2k_o \frac{d\sigma}{d^3k} = B_e \int \frac{d^3q}{2q_o} \left(2q_o \frac{d\sigma}{d^3q}\right) \frac{1}{\Gamma_e} 2k_o \frac{d\Gamma_e}{d^3k} . \qquad (3.18)$$

The parent has momentum q, Γ_e is the relevant partial width and B_e is the branching ratio for decays producing the required lepton. This format is generalized to a broad resonance or continuous mass source by incorporating a running mass variable. (Production and decay mechanisms are assumed to be factorizable).

$$2k_o \frac{d\sigma}{d^3k} = \int dq^2 \, \rho(q^2) \, B_e(q^2) \int \frac{d^3q_o}{2q_o} \left(2q_o \frac{d\sigma}{d^3q}\right)$$

$$\times \frac{1}{\Gamma_e(q^2)} \, 2k_o \frac{d\Gamma_e}{d^3k} \qquad (3.19)$$

The branching ratio is given by

$$B_e(q^2) = B_{V\to e^+e^-} \frac{m_V^2}{q^2}$$

and the two body decay probability per invariant phase space element reduces to

$$\frac{1}{\Gamma} 2k_o \frac{d\Gamma}{d^3k} = \frac{2}{\pi} \delta(q^2 - 2q.k) .$$

Changing the integration variable in equation (3.19) to the non-observed lepton momentum yields $(k' = q - k)$

$$2k_o \frac{d\sigma}{d^3k} = \frac{2}{\pi} B \int dq^2 \, \rho(q^2) \frac{m_v^2}{q^2} \int \frac{d^3k'}{2k_o'} \left(2q_o \frac{d\sigma}{d^3q}\right)$$

$$\times \quad \delta((k + k')^2 - q^2)$$

and performing the $|\underline{k}'|$ integration $(m_e^2 = 0)$ gives

$$2k_o \frac{d\sigma}{d^3k} = \frac{2}{\pi} B \int_{4\mu^2}^{\infty} dq^2 \, m_v^2 \, \rho(q^2) \int \frac{d\Omega}{8k^2(1 - \cos\psi)^2}$$

$$\times \quad \left(2q_o \frac{d\sigma}{d^3q}\right) \qquad (3.20)$$

where ψ is the lepton pair opening angle and Ω is the solid angle. For the low mass continuum, the following identifications are made

$$\rho(q^2) \, 2q_o \frac{d\sigma}{d^3q} \simeq 2q_o \frac{d\sigma}{d^3q} \frac{m_v \Gamma_v}{\pi(q^2 - m_v^2)^2}$$

$$\simeq 2q_o \frac{d\sigma}{d^3q} \frac{m_v \Gamma_v}{\pi m_v^4} ,$$

$$B_{v \to e^+e^-} = \frac{\Gamma_{v \to e^+e^-}}{\Gamma_v}$$

$$= \frac{\alpha^2 m_v}{12} \left(\frac{4\pi}{\gamma_v^2}\right) \frac{1}{\Gamma_v}$$

where the vector meson-photon coupling $4\left(\frac{\gamma_v^2}{4\pi}\right) \simeq 2.4$.

So equation (3.20) becomes

$$2k_o \frac{d\sigma}{d^3k} = \frac{2}{\pi} \int_{4\mu^2}^{\infty} dq^2 \int d\Omega \frac{1}{8k^2(1-\cos\psi)^2} \left(2q_o \frac{d\sigma}{d^3q}\right)$$

$$\times \frac{\alpha^2}{3\gamma_v^2} .$$

We can substitute the parent cross section $2q_o\ d\sigma/d^3q = c_v F(q_T)f(y)$ and neglect the rapidity dependence $f(y) \simeq f(0)$. For a 90° trigger angle (observed electron along x-axis), we can express the undetected lepton momentum in terms of the pair opening angle (ψ) and an azimuthal angle (ϕ'). In the limit $m_e^2 \to 0$,

$$k' = k'(1, \cos\psi, \sin\psi \sin\phi', \sin\psi \cos\phi').$$

The parent transverse momentum is known,

$$q_T^2 = k^2 + k'^2(\cos^2\psi + \sin^2\psi \sin^2\phi') + 2kk'\cos\psi$$

$$= k^2 + \frac{q^4(\cos^2\psi + \sin^2\psi \sin^2\phi')}{4k^2(1 - \cos\psi)^2} + \frac{q^2\cos\psi}{(1-\cos\psi)}$$

(by conservation of momentum).

As $k \to 0$, q_T^2 is approximated by the k^{-2} term and

$$q_T dq_T = \frac{q^2 dq^2}{4k^2} \frac{(\cos^2\psi + \sin^2\psi\sin^2\phi')}{(1 - \cos\psi)^2}$$

and

$$2k_o \frac{d\sigma}{d^3k} = \frac{2}{\pi} \frac{\alpha^2}{12\gamma_v^2 k} \; c_v f(0) \int_o^\infty dq_T \; F(q_T)$$

$$x \int d\Omega \; \frac{1}{(1-\cos\psi)\,[1-\sin^2\psi\cos^2\phi']^{\frac{1}{2}}} \; .$$

Then, assuming a similar form for the pion distribution, the leading term of the electron to pion ratio is

$$\frac{e}{\pi} \simeq \frac{1}{k} \frac{\alpha^2}{(\gamma_v^2/4\pi)24\pi^2} \; \frac{c_v}{c_\pi} \; J.F \tag{3.21}$$

with

$$F = \int_o^\infty F(q_T)dq_T \; .$$

and

$$J = \int_{-1}^{1-\varepsilon} \frac{d\cos\psi}{(1-\cos\psi)} \; 2 \int_o^\pi \frac{d\phi'}{[1-\sin^2\psi\cos^2\phi']^{\frac{1}{2}}}$$

(ε is connected with opening angle considerations in the $m_e^2 \to 0$ limit, see Appendix 3.2).

APPENDIX 3.1

For simplicity, since we see that the energy integration in equation (3.17) is dominated by the lower limit, $q_{o_{min}} \simeq k$, we let $q_{o_{max}} \to \infty$. Now, trivially, we have

$$\int_k^\infty \frac{1}{q_o^2}\left(1 - \frac{2k}{q_o} + \frac{2k^2}{q_o^2}\right)dq_o \simeq \frac{2}{3k} . \qquad \text{(i)}$$

We also need to consider

$$\int_k^\infty \frac{e^{-aq_o}}{q_o}\left(1 - \frac{2k}{q_o} + \frac{2k^2}{q_o^2}\right) dq_o$$

$$= \int_{ak}^\infty \frac{e^{-t}}{t} dt - 2ak \int_{ak}^\infty \frac{e^{-t}}{t^2} dt + 2a^2k^2 \int_{ak}^\infty \frac{e^{-t}}{t^3} dt$$

$$= \Gamma(o,ak) - 2ak\Gamma(-1,ak) + 2a^2k^2\Gamma(-2,ak) \qquad \text{(ii)}$$

where Γ is the incomplete gamma function [35]

$$\Gamma(\beta,x) = \int_x^\infty e^{-t}\, t^{\beta-1}\, dt$$

which satisfies the functional relation

$$\Gamma(\beta+1\ ,x) = \beta\Gamma(\beta,x) + x^\beta e^{-x} \qquad \text{(iii)}$$

and in particular

$$\Gamma(-1,x) = x^{-1}e^{-x} - \Gamma(o,x)$$

$$\Gamma(-2,x) = \tfrac{1}{2}\left(x^{-2}e^{-x} - \Gamma(-1,x)\right)$$

$$= \tfrac{1}{2}\left(x^{-2}e^{-x} - x^{-1}e^{-x} + \Gamma(0,x)\right). \qquad \text{(iv)}$$

Then using (iii) and (iv) in (ii),

$$\int_k^\infty dq_o \frac{e^{-aq_o}}{q_o}\left(1 - \frac{2k}{q_o} + \frac{2k^2}{q_o^{\,2}}\right) = \Gamma(o,ak)(1+ak)^2 - e^{-ak}(1+ak). \quad \text{(v)}$$

Now

$$\Gamma(o,ak) = \int_{ak}^\infty \frac{e^{-t}}{t}\, dt$$

$$= E_1(ak).$$

Hence equation (3.17).

APPENDIX 3.2

Discussion of opening angles:

We can obtain, from equation (3.10), the upper limit of energy integration.

$$q_{o_{max}} = \frac{q^2}{2m_e^2}\left[k_o + |\underline{k}|\left(1 - \frac{4m_e^2}{q^2}\right)^{\frac{1}{2}}\right]$$

$$\simeq \frac{q^2 k}{m_e^2} \quad \text{as} \quad m_e^2 \to 0, \quad k_o \simeq |\underline{k}| = k. \qquad \text{(i)}$$

Similarly for $m_e^2 = 0$, with opening angle ψ,

$$q^2 = 2kk'(1 - \cos\psi)$$

and so

$$q_o = k + \frac{q^2}{2k(1 - \cos\psi)}. \qquad \text{(ii)}$$

Then from (i) and (ii), we clearly have the restriction

$$k + \frac{q^2}{2k(1 - \cos\psi)} \leqq \frac{q^2 k}{m_e^2}$$

=>

$$(1 - \cos\psi) \geqq \frac{q^2 m_e^2}{2k^2(q^2 - m_e^2)}$$

$$\simeq \frac{m_e^2}{2k^2}.$$

Hence, in taking a zero electron mass limit, we have as a consequence to impose the condition (c.f. equation (3.22)).

$$(1 - \cos\psi) \geqq \varepsilon_o = \frac{m_e^2}{2k^2}.$$

When opening angle cuts are imposed experimentally, $\psi \geqq \psi_c$, the effect is reproduced by modifying $q_{o_{max}}$:

$$q_{o_{max}}(\text{cut}) = k + \frac{q^2}{2k(1 - \cos\psi_c)} .$$

Clearly for all cases of practical interest $(1 - \cos\psi_c) >> \varepsilon_o$. The (considerable) effect of 5° and 10° cuts on the leading term of our calculation are shown in the figure.

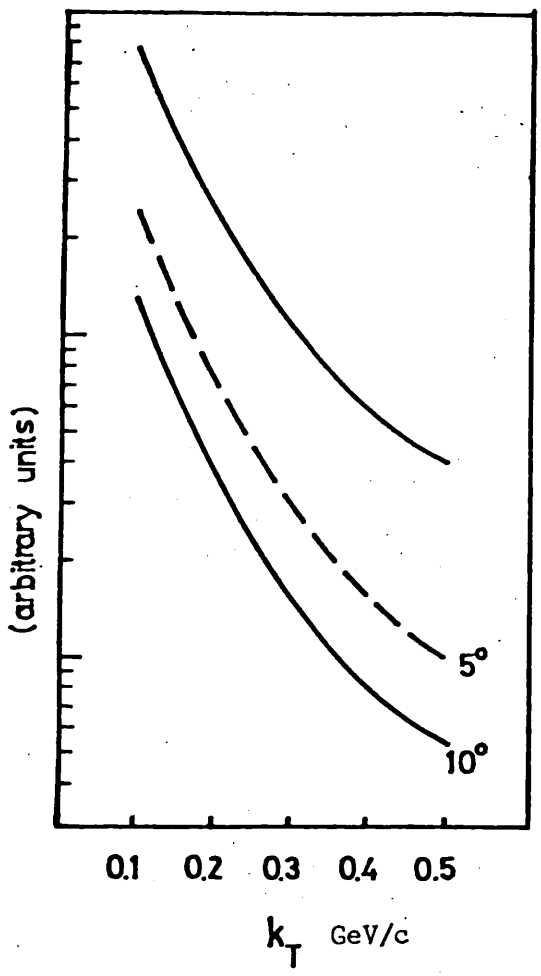

Figure Showing the effect of opening angle cuts on single lepton inclusive cross sections.

CHAPTER IV

It is natural that any production mechanism which involves bremsstrahlung must in some sense be controlled by the charge distribution in the final state. Indeed, the coefficients $\langle\Delta^2 Q\rangle$, C_T and D_T which arise in our expressions for real photon and lepton yields are clearly most sensitive to charge structure. Our "charge fluctuation", $\langle\Delta^2 Q\rangle$, defined in equation (2.10) is related (equation (2.11)) to the charged particle rapidity correlation functions. The correction term C_T (equation (2.16)) and the second order coefficient D_T (equation (2.19)) have similar, but more complicated, expressions. To begin this chapter, we will discuss the available experimental information and then use the relevant data to estimate our coefficients.

The accumulated data on centre-of-mass charge fluctuation in proton-proton collisions shows a slow rise with energy. (Note that $\langle u^2\rangle = \frac{1}{4}\langle\Delta^2 Q\rangle$ is strictly defined as the fluctuation and is measured experimentally). In fig. 4.1

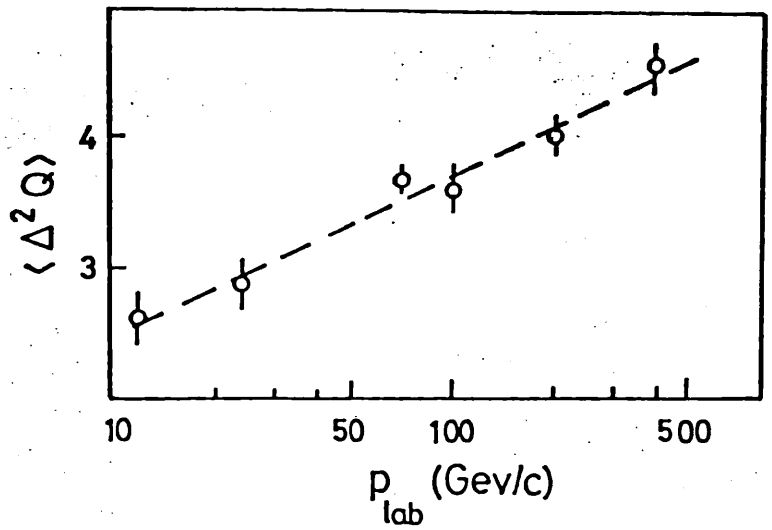

Figure 4.1 Compilation of data for 'charge fluctuation'.

we show a compilation of data for $\langle\Delta^2 Q\rangle$ plotted against p_{lab}, (see for example ref. [36]). The line is a (by hand) parameterization given in ref. [37], $\langle\Delta^2 Q\rangle = .56\ln(s) + .76$. Detailed investigation of the charge structure of many-particle events was originally proposed to differentiate between theoretical models for the underlying production process. For example, the behaviour of $\langle\Delta^2 Q\rangle$ has been examined to compare fragmentation and multiperipheral cluster models. The multiperipheral philosophy predicts [38] that the charge fluctuation will approach a constant at asymptotic energies, but the fragmentation picture [39] results in an increase proportional to $\sqrt{s}$.

The observed approximate $\ln(s)$ rise in the $\langle\Delta^2 Q\rangle$ data could be explained by a simple quark-parton model [37]. Under the assumption that valence quarks populate predominantly the ends of the rapidity plot, the fluctuation of quantum number in the central region is taken to be the result of fluctuation in the quark sea. Then, since recombination and resonance decay can be considered short range effects and consequently energy independent, the energy dependent part of $\langle\Delta^2 Q\rangle$ can be associated with fluctuations of quarks and antiquarks from the sea. Quark-parton models with a random distribution of charges of sea quarks can predict a $\ln(s)$ dependence for $\langle\Delta^2 Q\rangle$ (proportional to the number of quarks and antiquarks present).

The charge structure of multiparticle final states has also been tested for evidence of "local compensation of charge" [36]. A Zone graph analysis (see for example ref. [31]) is often used, where $-Z(y)$ is defined as

the charge transfer across the rapidity value y and $Z(0)$ is the c.m. charge transfer. In ref. [36], the authors compare the experimental results with a random charge allocation model and conclude that in the central region charge is compensated over a mean length of .75 units of rapidity. The well known "leading particle effect" is also observed.

A direct implication of local charge compensation and the leading particle effect should be that the dominant contribution to the charge fluctuation must come from the centre of the central region.

Experimentally, charged particle distributions have been studied in the 30" hydrogen bubble chamber at Fermilab, which of course allows charge identification, and at ISR. Data from FNAL is available at $p_{lab} = 205$ GeV/c [40] and at $p_{lab} = 102, 400$ GeV/c [41, 42, 43, 44]. We can use the results of the Rochester-Michigan collaboration [41, 42, 43] to examine the consistency condition for $\langle\Delta^2 Q\rangle$ and the charged particle rapidity correlation functions $C_{cd}(y_c,y_d)$, equation (2.11), since the ++, -- and +- charge combinations are separated. The quantity measured is not simply C_{cd}, but the "normalized correlation function"

$$R_{cd}(y_c,y_d) = \frac{C_{cd}(y_c,y_d)}{(\frac{1}{\sigma}\frac{d\sigma}{dy_c})(\frac{1}{\sigma}\frac{d\sigma}{dy_d})} \quad . \tag{4.1}$$

(This form of the correlation function is chosen by experimentalists because of its insensitivity to secondary interactions [45]). Clearly

$$C_{cd}(y_c,y_d) = \frac{1}{\sigma^2}\frac{d\sigma}{dy_c}\frac{d\sigma}{dy_d} \quad R_{cd}(y_c,y_d) \ .$$

We show, in fig. 4.2 a) b) c) respectively,

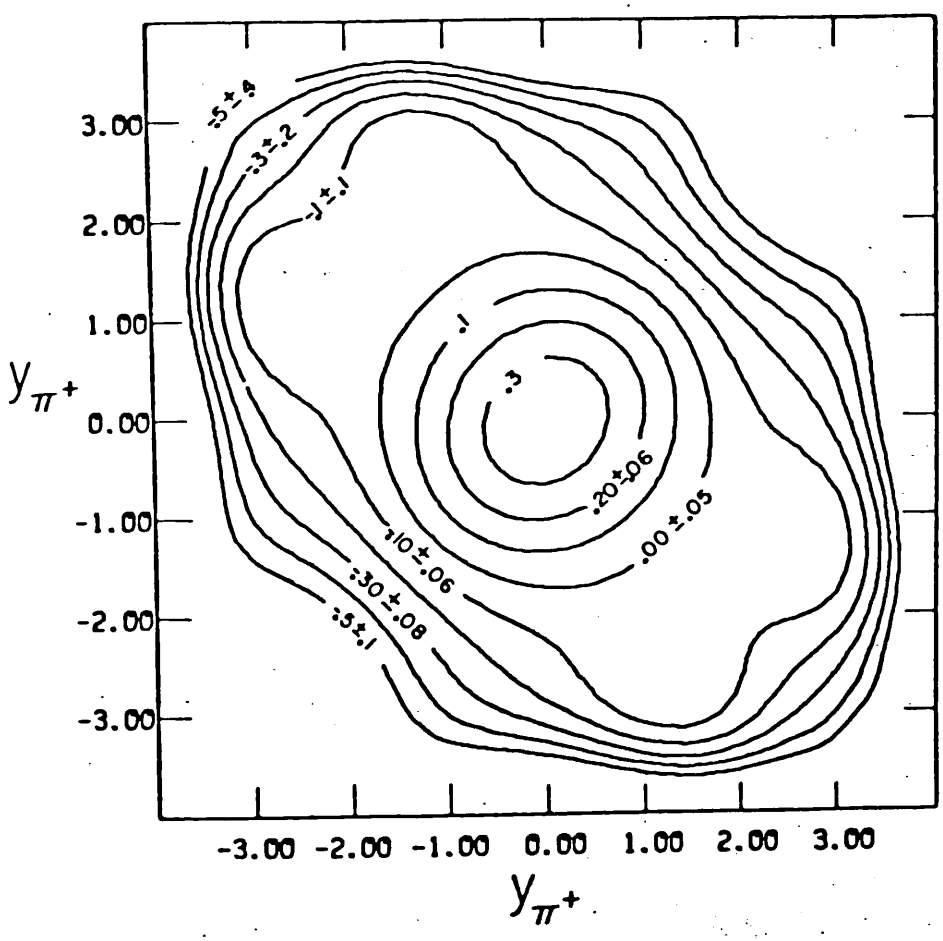

Figure 4.2 (a) Contour plot for correlation function R_{++} at P_{lab} = 102 GeV/c against c.m. rapidity.

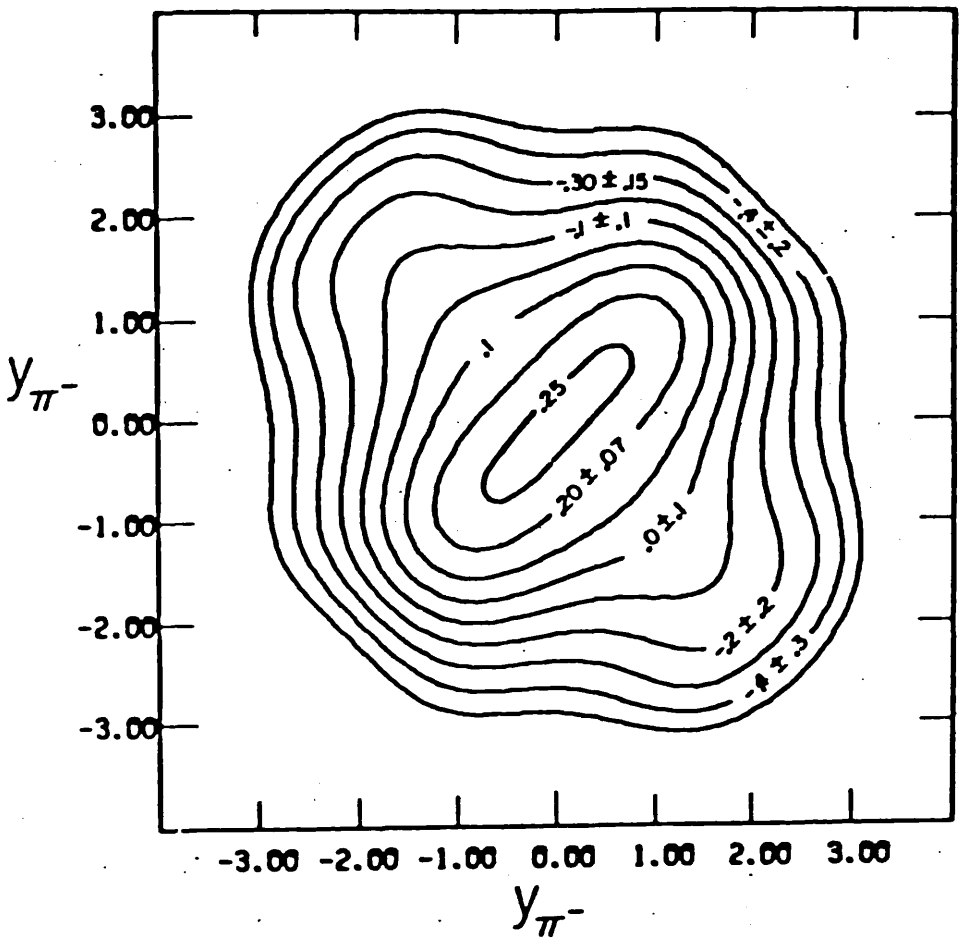

Figure 4.2 (b) Contour plot for correlation function R_{--} at p_{lab} = 102 GeV/c against c.m. rapidity.

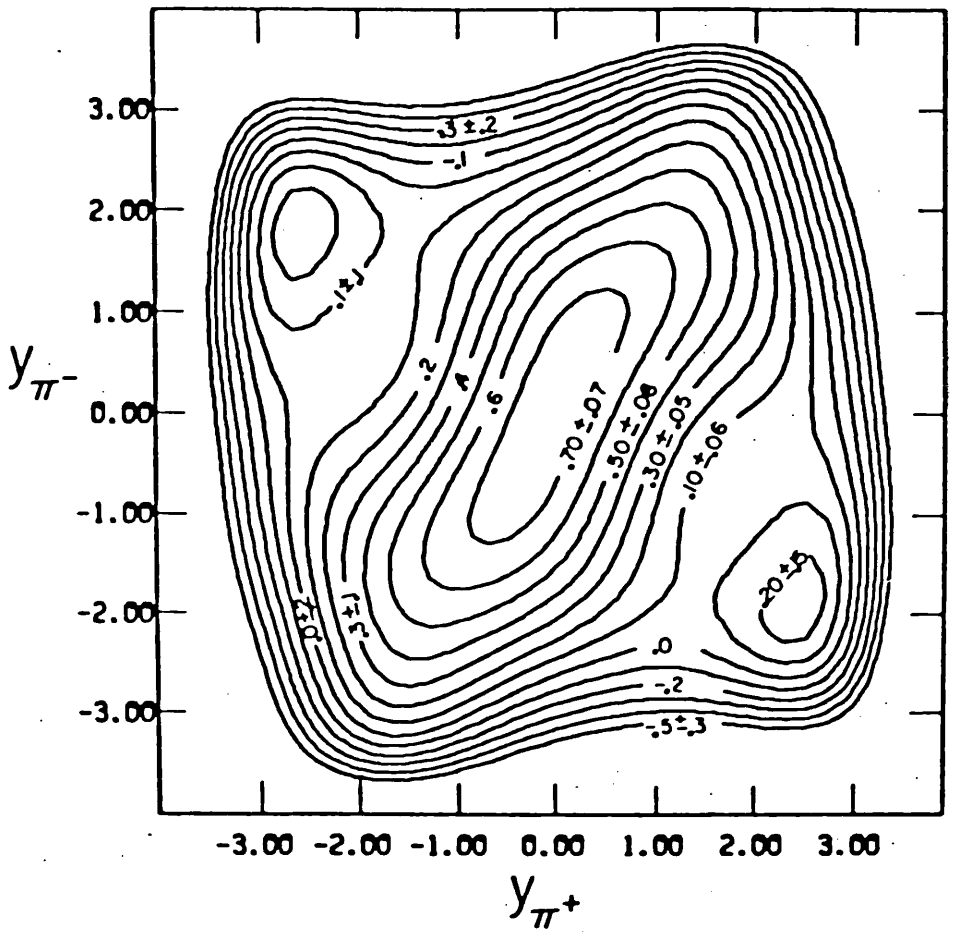

Figure 4.2 (c) Contour plot for correlation function R_{+-} at p_{lab} = 102 GeV/c against c.m. rapidity.

the contour plots of R_{cd} for ++, -- and +- charge combinations of produced pions, for p_{lab} = 102 GeV/c, plotted against centre-of-mass rapidity. Data taken from these plots and integrated numerically over the asymmetric region indicated by equation (2.11) (with bin size 0.4), yields a value of 2.9 ± .4 for the charge fluctuation. This is compared with the quoted value of 3.60 ± .16. In identifying particles for these two-pion correlations, those particles which were identifiable as protons by track ionization were removed and all particles with longitudinal momentum > 4 GeV/c were also excluded (thus removing fast forward protons). The symmetry of the pp incident channel was used to reflect data about expected axes of symmetry. Misidentification of particles (approximately 1% e^-, 7% K^-, 2% $\bar{p}$; 1% e^+, 10% K^+ and 13% p in central region) and the removal of protons as described above mean that we cannot calculate the true charge fluctuation from this data and thus partially explain the discrepancy between given and calculated values of $\langle\Delta^2 Q\rangle$. However, we consider that this data can be used to provide (at worst) a good estimation of the size of our coefficients. Before going on to evaluate the coefficients C_T and D_T, we make some observations on the overall shape of the C_{cd} correlations.

The energy dependence of inclusive pion correlations is shown to be weak by comparison of results at p_{lab} = 102 GeV/c and at p_{lab} = 400 GeV/c (see fig. 4.3 [43] for a comparison of the two charged particle correlations R_{cc} for these two energies). The most

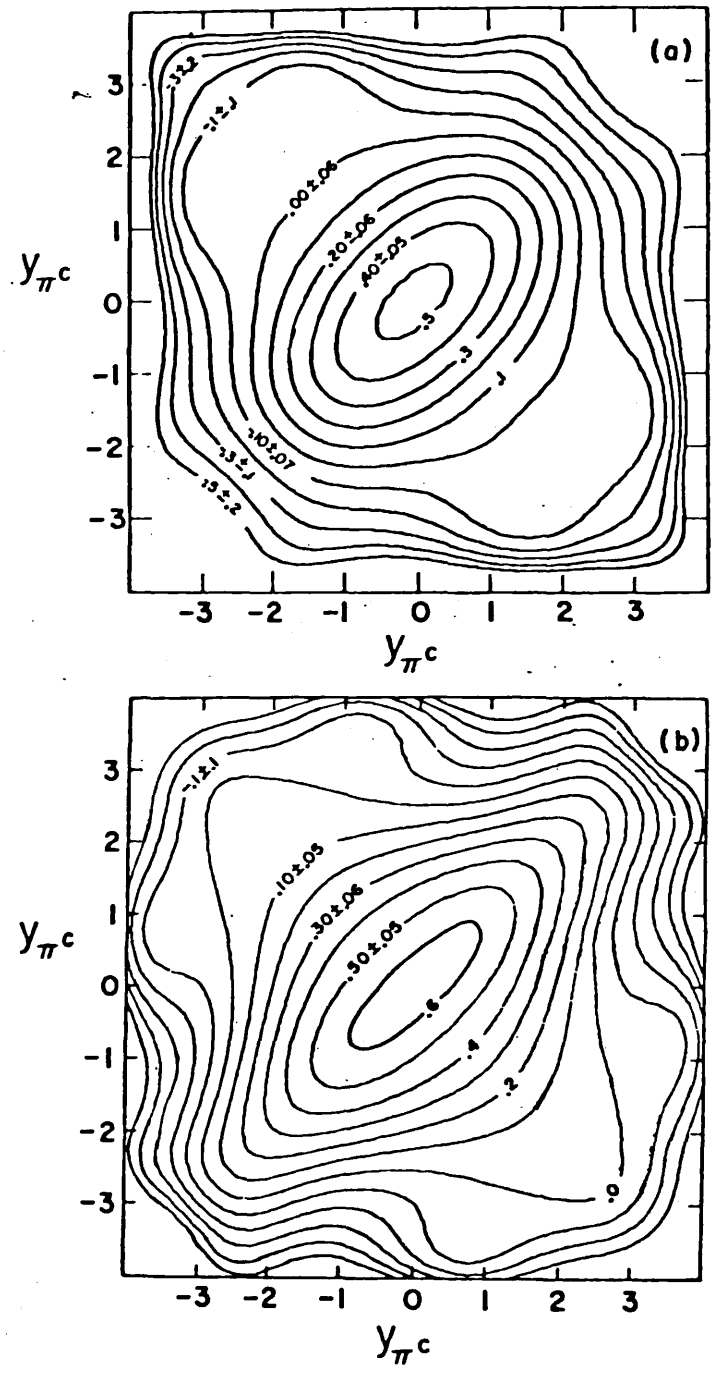

Figure 4.3 Contour plots for R_{cc} for charged pions against c.m. rapidity at (a) p_{lab} = 102 GeV/c,
(b) p_{lab} = 400 GeV/c.

striking feature in fig. 4.2 is the elongation of the contours along values of constant $\Delta y = |y_c - y_d|$ for +- and, to a lesser extent, for -- charge combinations. This short range correlation appears translationally invariant, at least in the central region. Thus we are seeing the evidence for local compensation of charge. (Some evidence for simultaneous dissociation of protons and long-range diffractive correlations can also be found [42]). At this point, it is interesting to note that simple energy-momentum sum rules can produce positive values of R in the central region of rapidities. If we define

$$f_2^{cd} = \langle n_c n_d - \delta_{cd} n_c \rangle - \langle n_c \rangle \langle n_d \rangle,$$

the second Mueller correlation moment, then

$$\int \int R_{cd}(y_c, y_d) \frac{d\sigma}{dy_c} \frac{d\sigma}{dy_d} \, dy_c dy_d = f_2^{cd} \, \sigma^2$$

and f_2^{cd} cannot vanish by energy-momentum sum rules [30].

For azimuthal angle correlations (the angle between the transverse momenta of the two produced particles, defined by $\cos\phi_{cd} = \vec{p}_{c_T} \cdot \vec{p}_{d_T} / |\vec{p}_{c_T}||\vec{p}_{d_T}|$), we show data (fig. 4.4) again from the Rochester-Michigan collaboration at $p_{lab} = 102$ GeV/c [41]. (Protons and events with less than six charged particles have been removed). Here too, there is more structure for pions with unlike charges.

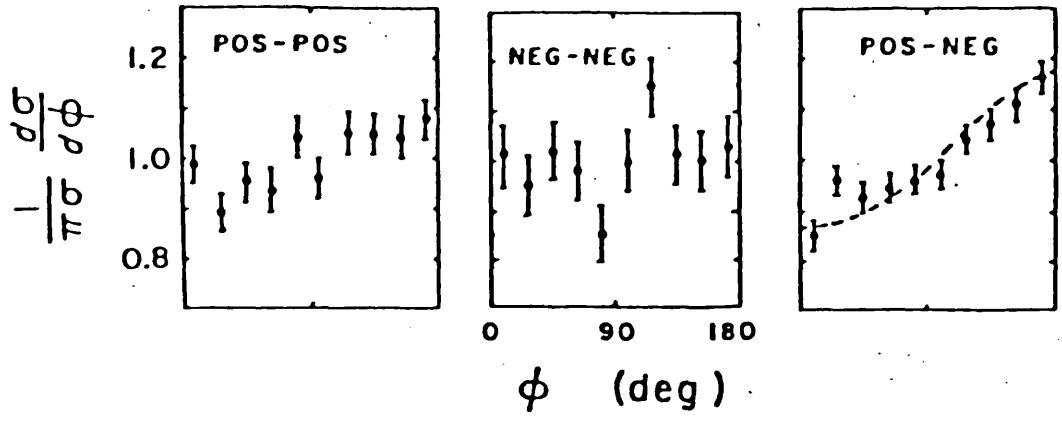

Figure 4.4 Azimuthal angle dependence (normalised to 1).

Momentum conservation requires some anti-correlation; the short range anti-correlation in ϕ_{cd} for +- may be associated with local transverse momentum conservation for particles which are strongly correlated in rapidity. The smaller anti-correlation for -- and ++ results from the corresponding reduced rapidity correlation. The azimuthal dependence for the charge combination +- can be approximated by a simple function $\sim (1 - B_{cd} \cos \phi_{cd})$. The the "average value" of $\cos \phi_{cd}$,

$$\langle \cos \phi_{cd} \rangle \sim \int_0^{2\pi} d\phi_{cd} \cos\phi_{cd} \left(1 - B_{cd} \cos \phi_{cd}\right)$$

is given trivially by $(- \frac{B_{cd}}{2})$.

The short range behaviour in azimuthal rapidity correlations of like-charged particles, which is often known as the Goldhaber effect, has been observed in some experiments [46]. These correlations, which have

a rise at $\Delta y = 0$, $\phi_{cd} = 0$, can be explained in multiperipheral or cluster models by the effect of Bose-Einstein statistics [47, 48]. We do not take into account this enhancement since the effect is very subtle compared to overall structure.

For transverse momentum correlations, no systematic trends have been isolated [49].

With these patterns of behaviour in mind, we can expect the two-particle correlation function to have the following simple form

$$C_{cd}\,(y_c, p_{c_T}; y_d, p_{d_T})$$
$$= C'_{cd}\; e^{-\alpha|y_c - y_d|} F(m_{c_T}) F(m_{d_T}) \left(1 - B_{cd} \cos \phi_{cd}\right) \quad (4.2).$$

(For the azimuthal dependence, we let $B_{cd} \to 0$ for ++ and -- charge combinations). The parameter α is associated with the correlation length and $\alpha^{-1} \simeq 2 \pm 1$ [40].

In equation (4.2) we have assumed independent transverse momentum distributions in analogy with the single particle inclusive crosssection. (See equation (2.24) and fig. 2.4). For inclusive charged pion production, the cross section is given in the form [49, 50]

$$E_c \frac{d\sigma}{d^3 p_c} = A \exp\left(- B\, m_{c_T}\right). \quad (4.3)$$

If we take average values over charges of the parameters, then at $p_{lab} \simeq 102$ GeV/c, $A \simeq 145$ mb $(\text{GeV})^{-2}$ and $B \simeq 6.0\ (\text{GeV})^{-1}$. This corresponds to the central region.

Rewriting equation (4.3) as

$$E_c \frac{d\sigma}{d^3p_c} = \rho_o F(p_{c_T}) \qquad (4.4)$$

where $F(p_T) \alpha \exp(-B\, m_T)$ and $\int F(p_T)\, d^2 p_T = 1$, we have $\rho_o = 19.5$ mb $(\mathrm{GeV})^{-2}$. We can of course use this expression to predict the "average values" of functions of p_T, i.e. $\langle h(p_T)\rangle = \int h(p_T)F(p_T)d^2p_T$. Some useful values obtained in this way are given in Table 4.1. The experimental value for $\langle p_T\rangle$ is $.341 \pm .005$.

TABLE 4.1

$h(p_T)$	$\langle h(p_T)\rangle$
p_T	.36
p_T/m_T	.83
p_T/m_T^2	2.4
p_T^2/m_T^2	.73
$1/m_T$	3.2
$1/m_T^2$	12.1
$1/m_T^3$	53.6

While we have continuously used a "central region" approximation (both in equation (4.2) and equation (4.4)), we must notice that the rapidity plateau is not fully developed at $p_{lab} = 102$ GeV/c (fig. 4.5).

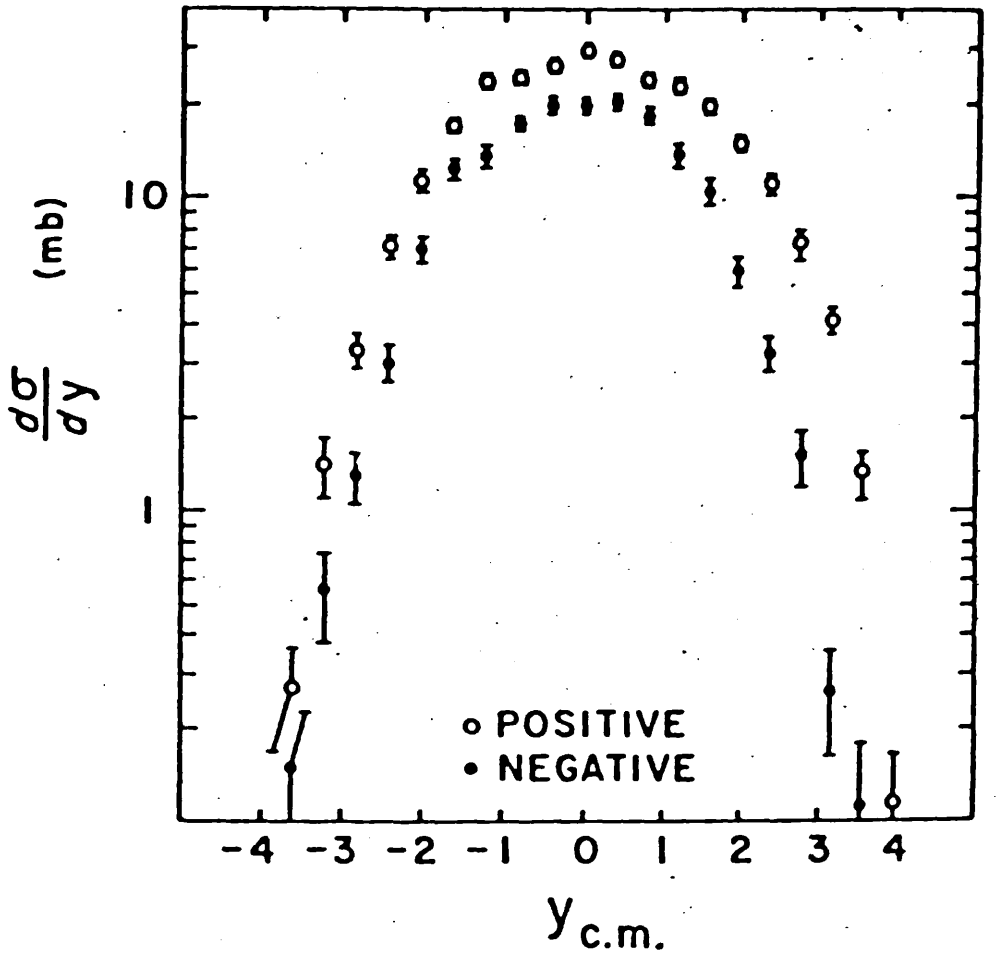

Figure 4.5 Single pion inclusive cross section plotted against c.m. rapidity.

Since we know that at asymptotic energy the central region will dominate the rapidity space, we consider we are justified in using this approximation to estimate the yields.

We have now reviewed all the information we shall need to calculate C_T and D_T.

Coefficient C_T

From equation (2.16),

$$C_T = \frac{1}{\sigma} \sum_c \int \frac{d^3p_c}{2E_c} \left(\frac{p_{c_T}^{\ 2} - m_c^{\ 2}}{m_{c_T}^{\ 2}\cosh^2 y_c} \right) 2E_c \frac{d\sigma}{d^3p_c}$$

$$+ \frac{1}{\sigma} \sum_c \sum_d Q_c Q_d \int\int \frac{d^3p_c}{2E_c} \frac{d^3p_d}{2E_d} \quad 2E_c 2E_d \frac{d\sigma}{d^3p_c d^3p_d}$$

$$\times \left(\frac{1}{2} \frac{\vec{p}_{c_T} \cdot \vec{p}_{d_T}}{m_{c_T} m_{d_T} \cosh y_c \cosh y_d} \right.$$

$$+ \operatorname{sign}(y_c)\operatorname{sign}(y_d) \left[- \frac{m_c^{\ 2}}{2m_{c_T}^{\ 2}\cosh^2 y_c} \right.$$

$$\left. \left. - \frac{m_d^{\ 2}}{2m_{d_T}^{\ 2}\cosh^2 y_d} + \frac{\vec{p}_{c_T} \cdot \vec{p}_{d_T}}{2m_{c_T} m_{d_T} \cosh y_c \cosh y_d} \right] \right)$$

By the symmetry of the single-particle-inclusive cross sections, we can replace the double-inclusive cross section by the correlation function. (The integrals over single-inclusive cross sections are odd in integration variables and vanish by symmetry). Then we easily get

$$C_T = \frac{1}{\sigma} \sum_c \left(\left\langle \frac{p_{c_T}^{\ 2}}{m_{c_T}^{\ 2}} \right\rangle - m_c^{\ 2} \left\langle \frac{1}{m_{c_T}^{\ 2}} \right\rangle \right) \rho_o \int dy_c \operatorname{sech}^2 y_c$$

$$+ \sum_c \sum_d Q_c Q_d \int \int dy_c dy_d \; C_{cd}(y_c, y_d)$$

$$x \left(\frac{1}{2} \left\langle \frac{p_{c_T}}{m_{c_T}} \right\rangle \left\langle \frac{p_{d_T}}{m_{d_T}} \right\rangle \langle \cos\phi_{cd} \rangle \operatorname{sech} y_c \operatorname{sech} y_d \right.$$

$$x \left[1 - \operatorname{sign}(y_c) \operatorname{sign}(y_d) \right]$$

$$+ \operatorname{sign}(y_c) \operatorname{sign}(y_d) \left[- \frac{m_c^{\ 2}}{2} \left\langle \frac{1}{m_{c_T}^{\ 2}} \right\rangle \operatorname{sech}^2 y_c \right.$$

$$\left. \left. - \frac{m_d^{\ 2}}{2} \left\langle \frac{1}{m_{d_T}^{\ 2}} \right\rangle \operatorname{sech}^2 y_d \right] \right) \quad (4.5)$$

and the value obtained using this equation and results given above (numerical integration over rapidities) is 1.189.

<u>Coefficient D_T</u>

From equation (2.19),

$$D_T = \frac{1}{\sigma} \sum_c \int \frac{d^3 p_c}{2E_c} \left(\frac{(p_{c_y}^{\ 2} + p_{c_z}^{\ 2})}{(E_c - p_{c_x})^2} \left(\frac{\partial}{\partial E_c} + \frac{\partial}{\partial p_{c_x}} \right) \right.$$

$$\left. - \frac{\left(p_{c_y} \frac{\partial}{\partial p_{c_y}} + p_{c_z} \frac{\partial}{\partial p_{c_z}} \right)}{(E_c - p_{c_x})} \right) 2E_c \frac{d\sigma}{d^3 p_c}$$

$$+ \frac{1}{\sigma} \sum_c \sum_d Q_c Q_d \int\int \frac{d^3p_c}{2E_c} \frac{d^3p_d}{2E_d} \frac{(p_{c_y} p_{d_y} + p_{c_z} p_{d_z})}{(E_c - p_{c_x})(E_d - p_{d_x})}$$

$$\times \left(\frac{\partial}{\partial E_d} + \frac{\partial}{\partial p_{d_x}} \right)$$

$$- \frac{\left(p_{c_y} \frac{\partial}{\partial p_{d_y}} + p_{c_z} \frac{\partial}{\partial p_{d_z}} \right)}{(E_c - p_{c_x})} \quad 2E_c 2E_d \frac{d\sigma}{d^3p_c d^3p_d}$$

and we shall use the same approach as for coefficient C_T to estimate this term.

We take the approximations given by equation (4.4) for the single-particle inclusive cross section and by equation (4.2) for the two-particle correlation function and use these to estimate the derivatives. For this we will need to use

$$\frac{\partial}{\partial E} = \frac{1}{m_T \sinh_y} \frac{\partial}{\partial y} ,$$

$$\frac{\partial}{\partial y_d} \exp(-\alpha|y_c - y_d|) \simeq \alpha \operatorname{sign}(y_c - y_d) \exp(-\alpha|y_c - y_d|)$$

and

$$\frac{\partial}{\partial p_x} \exp(-Bm_T) = - B \frac{p_x}{m_T} \exp(-Bm_T).$$

Again we shall make use of symmetry by setting odd integrands equal to zero. In this we find that, as before, double-inclusive cross sections can be replaced by two-particle correlation functions. We do the usual expansions in powers of $\frac{p_x}{E}$ and $\frac{p_y}{E}$ and keep only the leading terms. Then we have

$$D_T = \frac{B}{\sigma} \sum_c \frac{-1}{2} \left\langle \frac{p_{c_T}^2}{m_{c_T}^2} \right\rangle \rho_c \int \operatorname{sech} y_c \, dy_c$$

$$+ \sum_c \sum_d Q_c Q_d \int\int dy_c dy_d$$

$$\Bigg(\frac{B}{2} \left\langle \frac{p_{c_T}}{m_{c_T}} \right\rangle \left\langle \frac{p_{d_T}}{m_{d_T}} \right\rangle \langle \cos\phi_{cd} \rangle \left[1 - \mathrm{sign}(y_c)\mathrm{sign}(y_d) \right]$$

$$- \frac{B}{2} \left\langle \frac{p_{d_T}^2}{m_{d_T}^2} \right\rangle \mathrm{sech} y_d \, \mathrm{sign}(y_c)\mathrm{sign}(y_d)$$

$$+ \alpha \frac{\mathrm{sign}(y_c - y_d)}{\sinh y_d} \Bigg[\left\langle \frac{p_{c_T}}{m_{c_T}} \right\rangle \left\langle \frac{p_{d_T}^2}{m_{d_T}^2} \right\rangle \mathrm{sech} y_c \, \mathrm{sech} y_d \langle \cos\phi_{cd} \rangle$$

$$+ \mathrm{sign}(y_c)\mathrm{sign}(y_d)\Big(1 - m_c^2 \left\langle \frac{1}{m_{c_T}^2} \right\rangle \left\langle \frac{1}{m_{d_T}} \right\rangle \mathrm{sech}^2 y_c$$

$$- m_d^2 \left\langle \frac{1}{m_{d_T}^3} \right\rangle \mathrm{sech}^2 y_d + \left\langle \frac{p_{c_T}}{m_{c_T}} \right\rangle \left\langle \frac{p_{d_T}}{m_{d_T}} \right\rangle \mathrm{sech} y_c \, \mathrm{sech} y_d \, \langle \cos\phi_{cd} \rangle \Big) \Bigg]$$

$$- \alpha \, \mathrm{sign}(y_c - y_d)\mathrm{sign}(y_c) \mathrm{sech} y_d \left[\left\langle \frac{1}{m_{d_T}} \right\rangle - m_d^2 \left\langle \frac{1}{m_{d_T}^3} \right\rangle \mathrm{sech}^2 y_d \right] \Bigg)$$

$$\times \, C_{cd}(y_c, y_d).$$

Now we revert to numerical integration over correlations using the data from the contour plots to find D_T. For this coefficient we get $D_T \sim 20$. In view of the successive approximations that have been made (some accuracy is inevitably lost by the averaging methods) this value can only be regarded as an order of magnitude result. Without using explicit models for the production amplitudes, we cannot obtain an exact value.

The values obtained above for $\langle\Delta^2 Q\rangle$, C_T and D_T are inserted in equation (3.15) and then the integrations over virtual photon energy (q_o) and mass squared (q^2) were performed numerically for a range $.05 \rightarrow .40$ GeV/c in k_T. A Romberg type integration package was used [51]. An upper limit of $\sqrt{s}/2$ was enforced on photon energy when the maximum kinematically allowed $(q_{o_{max}})$ was in excess. The upper limit of energy integration was taken as $4\lambda k^2$ with $\lambda = 0.1$. The lepton spectra depend only logarithmically on this upper limit and consequently are relatively insensitive to variations in λ. To illustrate this, the effect of changing from $\lambda = 0.1$ to a k-independent upper limit of 1 GeV (two very extreme situations) result in a factor of 0.8 increase at $k = .1$. We also calculate the muon production yield although the large muon mass brings the whole "soft" photon approach into question and we feel that the results should only be trusted qualitatively.

The lepton/pion ratios are calculated at $\sqrt{s} = 52.7$ GeV for comparison with CHORMN data (although we work at 90°, we have already seen in Chapter I that we expect "large angle" results to apply at 32°). The fit of ref. [52] for 90° pions is used and σ is taken from ref. [53], we take $\pi = \frac{1}{2}(\pi^+ + \pi^-)$.

CHAPTER V

The lepton/pion ratios resulting from the two bremsstrahlung terms we have calculated and from the low mass continuum are shown (separately) in fig. 5.1 together with the maximum total effect. The e/π ratio shows a steep rise for small k_T, but the μ/π ratio (fig. 5.2) is flatter. These estimates do not include the contribution from interference between the gauge invariant part of the direct photon piece and the leading bremsstrahlung term (see Chapter II). If this is maximally constructive, it could give rise to a 20-30% increase in these results (from considering the magnitudes of the respective diagonal terms). We also show (fig. 5.3) the same electron expressions but with a 5° opening angle cut and the low k_T data.

Although the combined effect does not completely reproduce the data, we can nevertheless see that these QED effects give a substantial contribution to a rising signal at low k_T. (This work has been reported in ref. [54]).

The proliferation of models for single lepton and pair production in hadronic collisions, covering the whole range of q^2 and transverse momentum, testifies to the great interest in this field. Of the equivalent languages used for discussing electromagnetic processes, it seems that quark-parton (especially Drell-Yan) ideas work well for large masses but lose their clarity for lower mass regions where vector meson dominance takes over.

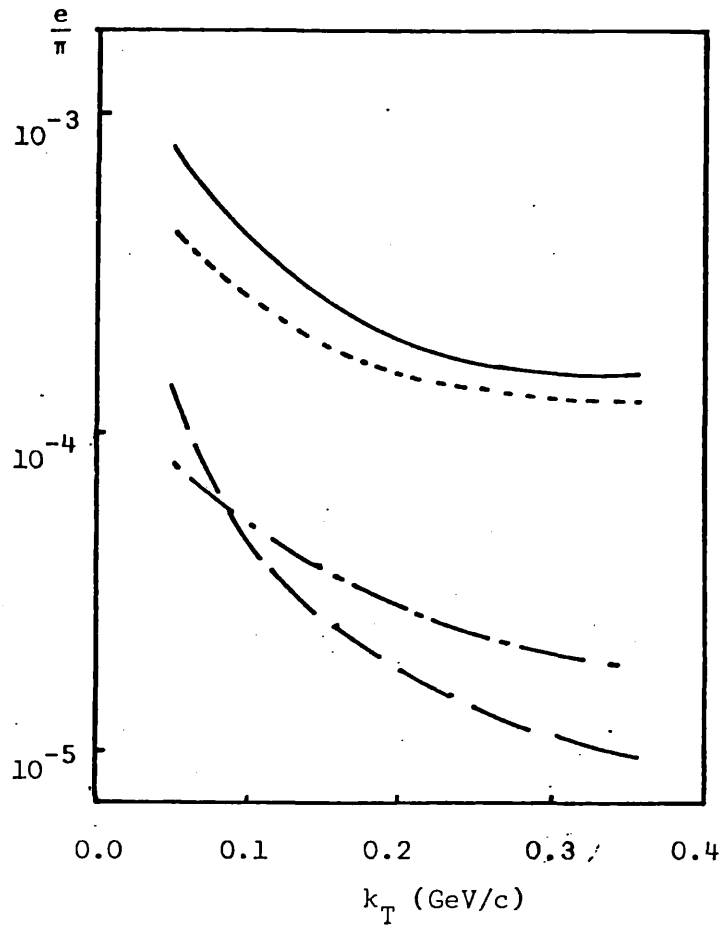

Figure 5.1 Contributions to e/π ratio. Curves shown are
- - - - - leading order calculation,
— — next-to-leading,
- — calculation of low mass conitnuum,
——— maximum total effect.

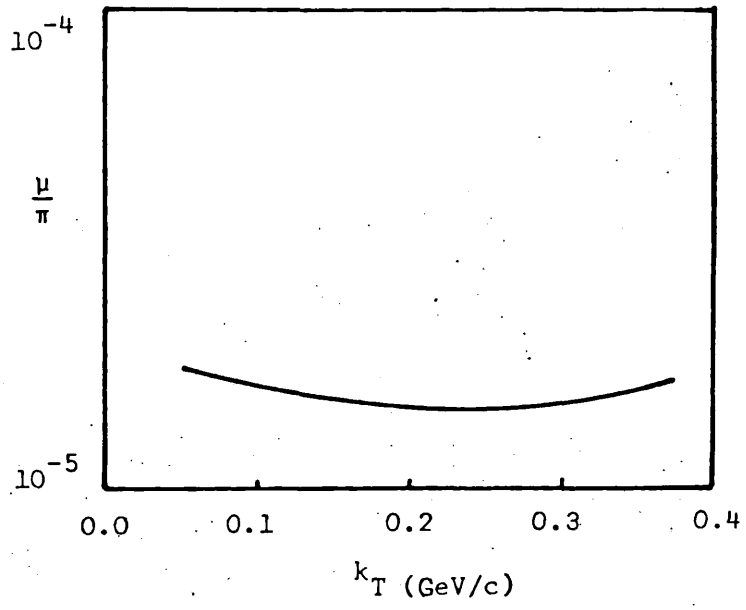

Figure 5.2 Leading order μ/π calculation.

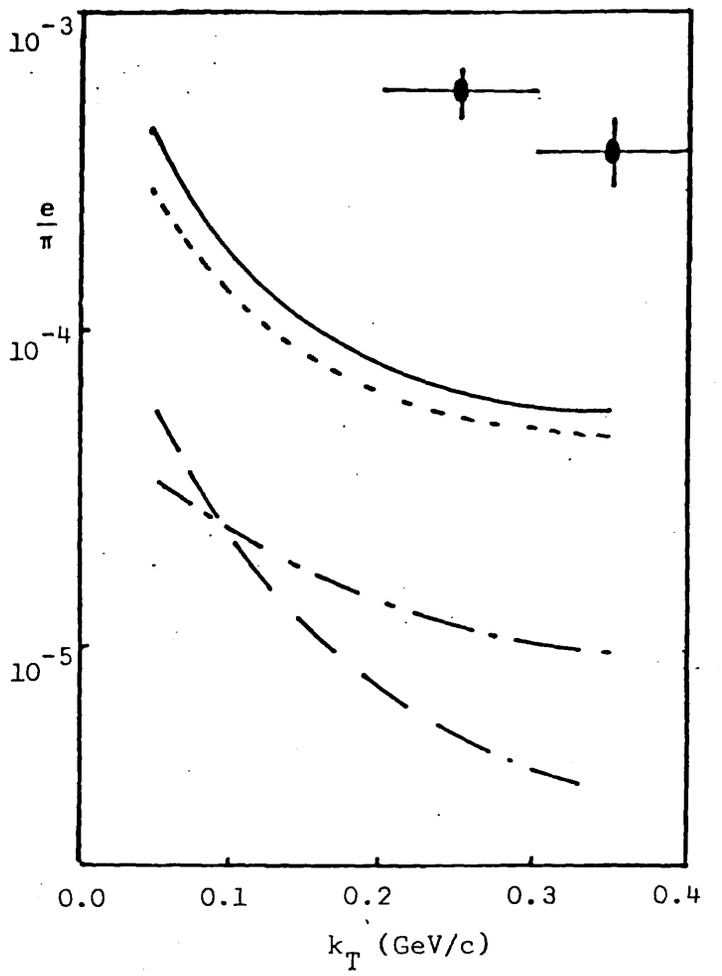

Figure 5.3 e/π ratio with 5° opening angle cut enforced and low k_T data. Curves as in figure 5.1.

Modifications of these basic processes abound: Drell-Yan models with quarks coming not from incident hadrons [55], constituent interchange models where quarks and mesons interact [56], massive virtual photon decay [57] - to list only a few of the more well-known suggestions. The inter-relation between the two fundamental methods is still not clear and calculations such as the present one, which have some success in explaining the data, point the way to further modifications - the obvious one is quark bremsstrahlung.

Further experimental measurements at still lower k_T and low mass pair data will provide a clear test of this calculation. (A brief analysis of the mass spectrum of this calculation is given in Appendix 5.1). If, when the levels of charm lepton production have been clarified (possibly by looking at correlations [58] or neutrino measurements to study charm cross sections), the known sources still cannot explain the data, there always remains the suggestion [59] that an unobserved light mass particle is responsible. But the chances of such a particle having avoided detection seem prohibitively low.

The search for the W many years ago led to the startling advances in theoretical understanding during the last decade. Now unified theories of weak and electronmagnetic interactions suggest [60] that the W has a mass $\sim$ 100 GeV and we must speculate what superaccelerators will reveal.

APPENDIX 5.1

The mass spectrum of the pairs produced via bremsstrahlung is given by

$$\frac{d\sigma}{dq^2} \sim \frac{1}{q^2} \int_{\sqrt{q^2}}^{\infty} |\underline{q}| \frac{dq_o}{q_o^2} e^{-aq_o} \qquad \text{(i)}$$

where the upper limit is controlled by the exponential damping (see Chapter II). If we put $Z = q_o/\sqrt{q^2}$, we can rewrite equation (i) as

$$\frac{d\sigma}{dq^2} \sim \frac{1}{q^2} \int_1^{\infty} \frac{\sqrt{Z^2-1}}{Z^2} dZ \; e^{-aZ\sqrt{q^2}} . \qquad \text{(ii)}$$

The parameter a comes from the transverse momentum dependence of single-particle-inclusive cross sections and is often approximated by $a \simeq 2/\langle p_T \rangle$. This leads us to expect, from equation (ii), that the $1/q^2$ behaviour of the mass spectrum will persist up to $\sqrt{q^2} \sim \langle p_T \rangle$.

REFERENCES

1. N.S. Craigie, Physics Reports (to appear).
(preliminary version, Imperial College, Jan. 1978).

2. L. Lederman, Physics Reports 26C (1976) 149.

3. F.W. Busser et al., Phys. Lett. 53B (1974) 212.
F.W. Busser, Proceedings of International Symposium, Stanford (1975).

4. L. Baum et al., Phys. Lett. 60B (1976) 485.

5. M. Barone et al., Nucl. Phys. B132 (1978) 29.

6. E.W. Beier et al., Phys. Rev. Lett. 37 (1976) 117.

7. SLAC-Duke-IC collaboration contribution to International Symposium on Lepton and Photon interactions, Hamburg (1977).
J. Ballam et al., Phys. Rev. Lett. 40 (1978) 741.

8. M.J. Schochet, Proceedings of SLAC Summer Institute (1977).

9. J.P. Boymond et al., Phys. Rev. Lett. 33 (1974) 112.
J.A. Appel et al., Phys. Rev. Lett. 33 (1974) 722.
D. Bintinger et al., Phys. Rev. Lett. 35 (1975) 72.
V.V. Abramov et al., Phys. Lett. 64B (1976) 365.

10. K. Bunnel et al., Phys. Rev. Lett. 40 (1978) 136.

11. V.V. Abramov et al., Proceedings of XVII International Conference on High Energy Physics, Rutherford Laboratory (1974).
V.V. Abramov et al., Proceedings of International Symposium, Stanford (1975).
See also ref. 9.

12. L.B. Leipuner et al., Phys. Rev. Lett 36 (1976) 1011.
M.J. Lauterbach et al., Phys. Rev. Lett. 37 (1976) 1436

13. J.J. Sakurai and H.B. Thacker, Nucl. Phys. B76 (1974) 445.
M. Bourquin and J.M. Gaillard, Phys. Lett. 59B, (1975) 191.

14. N.S. Craigie and D. Schildknecht, Nucl. Phys. B118 (1977) 311.

15. R.H. Dalitz, Proc. Phys. Soc. A64 (1951) 667.

16. J.D. Sullivan, Proceedings of Vanderbilt Conference on Particle Searches and Discoveries (A.I.P. No. 30) (1976).

17. I. Hinchliffe and C.H. Llewellyn Smith, Phys. Lett. 61B (1976) 472.

I. Hinchliffe and C.H. Llewellyn Smith, Nucl. Phys. B114 (1976) 45.

18. C. Fontan and R. Odorico, Nuovo Cim. 42A (1977) 141.

19. M. Perl, Proceedings of SLAC Summer Institute (1977).

20. G. Feldman, Proceedings of SLAC Summer Institute (1977).

21. S.M. Berman, D.J. Levy and T.L. Neff, Phys. Rev. Lett. 23 (1969) 1363.

22. R. Rückl, Phys. Lett. 64B (1976) 39.

R. Rückl, "Weiche, elektromagnetische Bremsstrahlung in hadronischen Vielteilchen Reaktionen", Ph.D. Thesis, Munich (unpublished).

23. R.N. Cahn, Phys. Rev. D7 (1973) 247.

R.N. Cahn, Phys. Rev. Lett. 29 (1972) 1481.

24. F.E. Low, Phys. Rev. 110 (1958) 974.

25. H. Feshbach and D.R. Yennie, Nucl. Phys. 37 (1962) 150.

26. B.M.K. Nefkens and D.I. Sober, Phys. Rev. D9, (1976) 2434.

M.K. Liou and W.T. Nutt, Phys. Rev. D16 (1977) 2176.

27. T.H. Burnett and N.M. Kroll, Phys. Rev. Lett. 20 (1968) 86.

See also

T.H. Burnett, Phys. Rev. D1 (1970) 3098.

28. H.W. Fearing, Phys. Rev. C6 (1972) 1136.

H.W. Fearing, Phys. Rev. D7 (1973) 243.

29. D. Schildknecht, Springer Tract in Modern Physics No. 63.

30. D. Horn and F. Zachariasen, "Hadron Physics at Very High Energies", Benjamin (1973).

See also

J. Whitmore, Phys. Reports 10C (1974) 273.

31. R. Baier, Proceedings of EPS International Conference on High Energy Physics, Palermo (1975).

32. R.C. Brower, C.E. DeTar and J.H. Weis, Phys. Reports 14C (1974) 257.

33. D.R. Yennie, S.C. Frautschi and H. Suura, Annals of Phys. 13 (1961) 379.

34. R.M. Sternheimer, Phys. Rev. 99 (1955) 277.

35. I.S. Gradshteyn and I.M. Ryzhik, "Tables of Integrals Series and Products", Academic Press (1965).

36. C. Bromberg et al., Phys. Rev. D12 (1975) 1224.

37. V. Černý and J. Pišút, Acta Phys. Polonica B8 (1976) 469.

38. C. Quigg and G.H. Thomas, Phys. Rev. D7 (1973) 2752.

39. T.T. Chou and Chen Ning Yang, Phys. Rev. D7 (1973) 1425.

40. T. Kafka et al., Phys. Rev. Lett. 34 (1975) 687.
R. Singer et al., Phys. Lett. 49B (1974) 481.
R. Singer et al., Phys. Rev. D16 (1977) 1261.

41. C.M. Bromberg et al., Phys. Rev. D9 (1974) 1864.

42. C.M. Bromberg et al., Phys. Rev. D10 (1974) 3100.

43. C.M. Bromberg et al., Phys. Rev. D15 (1977) 1215.

44. C.M. Bromberg et al., Nucl. Phys. B107 (1976) 82
C.M. Bromberg et al., Phys. Rev. Lett. 31 (1973) 1563.

45. S.R. Amendolia et al., Phys. Lett. 48B (1974) 359.

46. K. Eggert et al., Nucl. Phys. B86 (1975) 201.

47. J. Ranft and G. Ranft, Nucl. Phys. B92 (1975) 207.

48. G. Goldhaber et al., Phys. Rev. 120 (1960) 300.

49. T. Kafka et al., Phys. Rev. D16 (1977) 1261.

50. P. Capiluppi et al., Nucl. Phys. B76 (1974) 1.

51. P. Davies and P. Rabinowitz, "Methods of Numerical Integration", Academic Press (1975).

52. B. Alper et al., Phys. Lett. 47B (1973) 75.

53. U. Amaldi et al., Phys. Lett. 44B (1973) 112.

54. N.S. Craigie and H.N. Thompson, Imperial College Preprint, ICTP/77-78/9 (to appear in Nuclear Physics).

55. J.D. Bjorken and H. Weisberg, Phys. Rev. D13 (1976) 1405.

56. J.F. Gunion, S.J. Brodsky and R. Blankenbecler, Phys. Rev. D6, (1973) 2652.

57. G. Farrar and S. Frautschi, Phys. Rev. Lett. 36 (1976) 1017.

58. N.S. Craigie, H.F. Jones and P. Milani, Imperial College Preprint, ICTP/77-78/12.

59. L.M. Lederman and S. White, Phys. Rev. Lett. 35 (1975) 1543.

60. S. Weinberg, Phys. Rev. Lett. 19 (1967) 1264.

PART TWO

An absorbed Mueller-Regge model for the process $\pi^- + p \rightarrow p + X$.

CHAPTER I

Regge theory, since its introduction into particle physics ($\sim$ 1960), has been applied to strong interaction processes with considerable success [1, 2, 3]. The theory is based on the generalization of angular momentum (ℓ) from a discrete to a complex variable. Regge showed that, for a wide class of potentials, the only singularities arising in the S-matrix were simple poles which move with energy, $\ell = \alpha(s)$ where $\alpha(s)$ is called a Regge trajectory. Trajectories passing close to integral or half-integral values of α describe strong interaction resonances or bound states. High-energy, two-body reactions are dominated by Regge poles in the crossed channel. When trajectories are displayed on a Chew-Frautschi plot (s vs. Re(α)), they become straight lines connecting hadron families with the same isospin, baryon number and strangeness (see e.g. [4]). Hence we have a correlation between Regge poles and the observed spectrum of hadronic bound states and resonances. Another important aspect of the theory is the connection with the quantum exchange idea which has been so successful in the field theoretic description of electromagnetic interactions. Constraints on the theory are imposed by such considerations as duality and consequently the predictive power is increased.

The successes of Regge theory in coherently explaining a wide range of two-body scattering data have caused the underlying ideas to become an accepted basis for strong interaction theories and models [5]. While the quark model studies the problem in a completely different way, it is no coincidence that it can explain the linear trajectory at low energy. A simple pole model can always be used to estimate results in two body scattering; it is the only model which is broadly predictive with an acceptable accuracy. Characteristically Regge poles can successfully predict for 2-body exchange processes: the magnitude of differential cross sections up to a factor of 2; the helicity structure; the energy dependence over a range 4 → 400 GeV/c and the approximate behaviour with respect to momentum transfer.

There is strong theoretical and experimental evidence to support the inclusion of Regge cuts as corrections to the simple poles. To cite a popular example, pole-only models predict zero polarization for $\pi^- + p \rightarrow \pi^0 + n$ whereas experiments give a non-zero result [5]. Regge cuts (corresponding to cuts in the complex angular momentum plane) are required theoretically by unitarity arguments [1].

Pion-nucleon backward scattering, (when the direction of motion of the nucleon is reversed after a centre-of-mass collision), provides an opportunity to investigate the exchange of baryon Regge trajectories. There are some special peculiarities of baryon exchange processes [3, 5, 6, 7]. Consideration of kinematic

singularities for baryon exchange of given signature requires that there must be two trajectories of opposite parity (hence opposite naturality = signature x parity, $n = \tau P$). The two trajectories are known as parity doublets and the result is known as MacDowell symmetry [8]. If we take u as the squared momentum transfer between the incoming meson (pion) and the outgoing baryon (nucleon), then both the trajectories (α) and the Regge residues (residue of amplitude at pole, β) are analytic functions of $\sqrt{u}$ and obey

$$\alpha^{+}(\sqrt{u}) = \alpha^{-}(-\sqrt{u}), \qquad \beta^{+}(\sqrt{u}) = \beta^{-}(-\sqrt{u}).$$

For linear trajectories, parity partner states are degenerate in mass. This mechanism (a consequence of the analyticity assumptions) is an example of "conspiracy". Experimentally the parity doublets are not well observed. A dynamical solution to the problem was suggested by Carlitz and Kislinger[9]; they proposed that a fixed angular momentum plane cut should be introduced. A branch point is inserted at α_0 (where $\alpha(\sqrt{u}) = \alpha_0 + \alpha'(\sqrt{u})^2$) and the unwanted parity partner states are placed on the unphysical side of the cut for $u > 0$. Thus we see that for baryon exchange it is particularly important to introduce Regge cuts. Absorption corrections are commonly assumed to include the effect of Regge cuts which correspond to iteration of Pomeron (Regge trajectory with zero quantum numbers) exchange.

Two-body pion-nucleon backward scattering has been studied extensively with different Regge cut models [10, 11]. Good agreement with the available differential cross section data can be obtained, and broadly speaking the cuts reduce the overall normalization but do not greatly alter the shape. Polarization data is not so well explained and the predictions of different models vary appreciably.

We now turn to a field which has aroused much interest during the past few years - production processes. From an experimental standpoint this is an important subject since production accounts for $\sim 80\%$ of the total cross sections at presently available energies. The adoption of the inclusive approach is particularly useful in the investigation of production processes. We shall concentrate on the single-particle inclusive case $a + b \to c + X$, where one particular type of particle (c) alone is selected in the final state. This procedure allows the theoretician to extract information from an otherwise unmanageably complicated system. Similarly, inclusive experiments are comparatively simple when contrasted with exclusive many-body experiments which present various difficulties, particularly with neutral particles.

The introduction of Mueller's Generalised Optical theorem [12] has made inclusive reactions accessible to Regge analysis and Regge phenomenology has developed rapidly. Single particle inclusive reactions have been widely studied using both pole-only and pole + cut

models. Again there are both theoretical [13] and phenomenological [14] arguments for the inclusion of cuts. An impressive array of cut-corrected models for basic reactions with meson pole exchange testifies to the wide interest in this field (see for example refs. [15, 16, 17, 18]). We shall be interested in the backward inclusive reaction $\pi^- + p \to p + X$ and we shall develop an absorbed Mueller-Regge model for this process. In the first place we look at the general framework of inclusive reactions.

The single particle inclusive cross section corresponding to the reaction $a + b \to c + X$ is given by [19, 20]

$$(2\pi)^3\, 2\, E_c \frac{d\sigma}{d^3p_c} = \frac{1}{F} \sum_{n=1}^{\infty} \left(\prod_t \frac{1}{n_t!}\right) \int \left(\prod_{i=1}^{n} \frac{d^3p_i}{(2\pi)^3 2E_i}\right)$$

$$\times\ (2\pi)^4 \delta^4\left(p_a + p_b - p_c - \sum_{i=1}^{n} p_i\right)$$

$$\times\ |\langle p_c, p_1, \ldots p_n | A | p_a, p_b \rangle|^2 \qquad (1.1)$$

where $1/n_t!$ is the statistical factor and F is the flux, which is given by

$$F = 2\, \Delta^{\frac{1}{2}}\, (s,\ m_2{}^2,\ m_b{}^2)$$

and Δ is the Kibble function,

$$\Delta(x,y,z) = x^2 + y^2 + z^2 - 2xy - 2yz - 2xz.$$

The single particle inclusive process is a function of three independent invariants. We follow the backward scattering convention and define (see fig. 1.1)

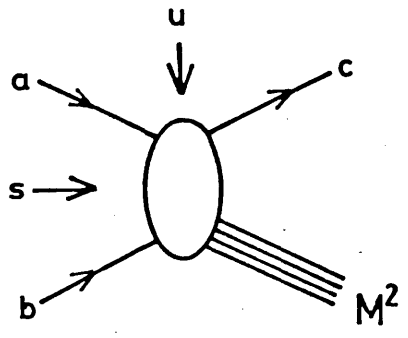

Figure 1.1 Single particle inclusive process $a + b \to c + X$ with invariants s, u and M^2.

$$s = (p_a + p_b)^2,$$

$$u = (p_a - p_c)^2$$

and

$$M^2 = (p_a + p_b - p_c)^2,$$

(M = mass of missing state X). Then if we put $t = (p_b - p_c)^2$ we have

$$s + t + u = m_a^2 + m_b^2 + m_c^2 + M^2.$$

The limits of the physical region are given by [21]

$$|u_{\substack{min\\max}}| = \left[\sqrt{\frac{(s+m_c^{\,2}-M^2)^2}{4s} - m_c^{\,2}} \mp \sqrt{\frac{(s+m_a^{\,2}-m_b^{\,2})^2}{4s} - m_a^{\,2}} \right]^2 - \left(\frac{M^2+m_a^{\,2}-m_b^{\,2}-m_c^{\,2}}{2\sqrt{s}} \right)^2 . \qquad (1.2)$$

In terms of invariants,

$$(2\pi)^3\, 2E_c \frac{d\sigma}{d^3p_c} = 16\pi^2\, \Delta^{\frac{1}{2}}(s,m_a^{\,2},m_b^{\,2}) \frac{d\sigma}{dudM^2} \qquad (1.3)$$

$$= f(ab \to c).$$

The Mueller Generalized Optical theorem [12] relates the inclusive cross section to the forward discontinuity in M^2 of the $3 \to 3$ amplitude i.e.

$$f(ab \to c) \sim \mathrm{disc}_{M^2} \langle a'b'\bar{c}'|A|ab\bar{c}\rangle \qquad (1.4)$$

with $p_a = p_{a'}$, $p_b = p_{b'}$, $p_{\bar{c}} = p_{\bar{c}'}$. The required six-particle amplitude is not the physical $3 \to 3$ amplitude, but one that has been analytically continued so that the subenergies s_{ab} and $s_{a'b'}$ are above and below their respective cuts ($s_{ab} = s + i\varepsilon$, $s_{a'b'} = s - i\varepsilon$) [22]. This is illustrated in fig. 1.2.

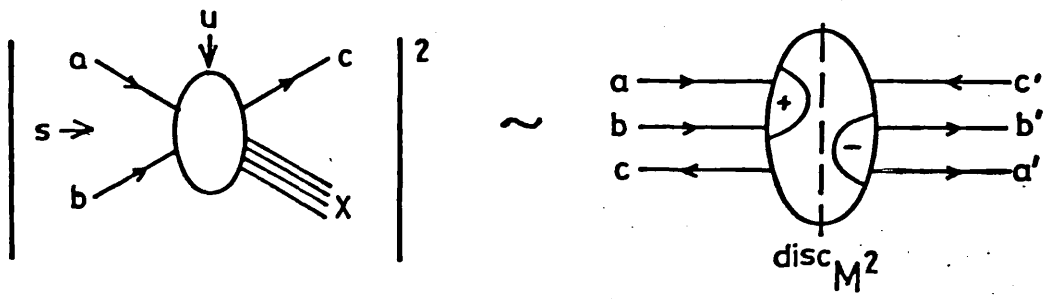

Figure 1.2 Diagramatic representation of Mueller's Generalized Optical theorem.

If we write the physical $3 \to 3$ amplitude as $A(s + i\varepsilon, M^2, s + i\varepsilon)$ then equivalently equation (1.4) becomes

$$f(ab \to c) \sim \text{disc}_{M^2} A(s-i\varepsilon, M^2, s+i\varepsilon). \qquad (1.5)$$

The spin effects in inclusive processes can be studied by incorporating helicity dependence into the Generalized Optical theorem. To this end we use six particle s-channel helicity amplitudes with the freedom of having different final and initial helicities [23]. The Mueller theorem now takes the form

$$\langle\lambda_{a'},\lambda_{b'}|A\dagger|\lambda_{c'},\kappa\rangle\langle\lambda_c,\kappa|A|\lambda_a,\lambda_b\rangle$$

$$\sim \text{disc}_{M^2} \langle\lambda_{a'},\lambda_{b'},\lambda_{\bar{c}'}|A|\lambda_a,\lambda_b,\lambda_{\bar{c}}\rangle \qquad (1.6)$$

where λ's are helicities of particles and κ denotes summation of the helicities of the missing mass X. We can now consider the constraints imposed on the Mueller amplitudes by parity and time reversal invariance [24, 25]. To obtain the parity relation, we first consider the pseudo-two-body amplitude,

$$\langle -\lambda_c, -\kappa | A(-\phi_i) | -\lambda_a, -\lambda_b \rangle$$

$$= \frac{\eta_c \eta_X}{\eta_a \eta_b} (-1)^{s_c + s_X - s_a - s_b + (\kappa - \lambda_c) - (\lambda_a - \lambda_b)}$$

$$\times \langle \lambda_c, \kappa | A(\phi_i) | \lambda_a, \lambda_b \rangle$$

where s_i denotes the spin of a particle or conglomerate, η_i = intrinsic parity and ϕ_i are angles of the particles internal to the composite state X. Integrating over these angles we obtain the final result,

$$\mathrm{disc}_{M^2} \langle \lambda_a, \lambda_b, \lambda_{\bar{c}} | A | \lambda_{a'}, \lambda_{b'}, \lambda_{\bar{c}'} \rangle$$

$$= (-1)^{(\lambda_a - \lambda_{a'}) + (\lambda_b - \lambda_{b'}) + (\lambda_{\bar{c}} - \lambda_{\bar{c}}')}$$

$$\times \mathrm{disc}_{M^2} \langle -\lambda_a, -\lambda_b, -\lambda_{\bar{c}} | A | -\lambda_{a'}, -\lambda_{b'}, -\lambda_{\bar{c}'} \rangle. \quad (1.7)$$

If we now consider time reversal, we immediately see that the time reversed Mueller amplitude is not a Mueller amplitude (because of the special continuations in subenergy variables, see fig. 1.3).

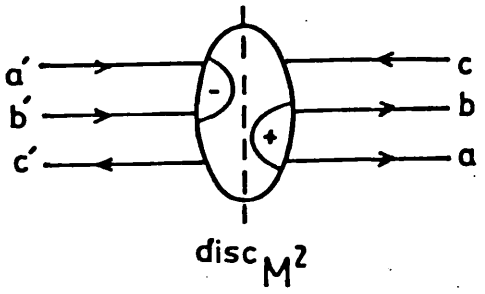

Figure 1.3 Time reversed Mueller amplitude.

Consequently time reversal can give no additional relationships between Mueller helicity amplitudes.

The Mueller amplitudes satisfy the hermiticity condition [24]

$$\langle\lambda_{a'},\lambda_{b'},\lambda_{\bar{c}'}|A|\lambda_a,\lambda_b,\lambda_{\bar{c}}\rangle$$

$$= \langle\lambda_a,\lambda_b,\lambda_{\bar{c}}|A\ |\lambda_{a'},\lambda_{b'},\lambda_{\bar{c}'}\rangle^*$$

This relation is illustrated in fig. 1.4.

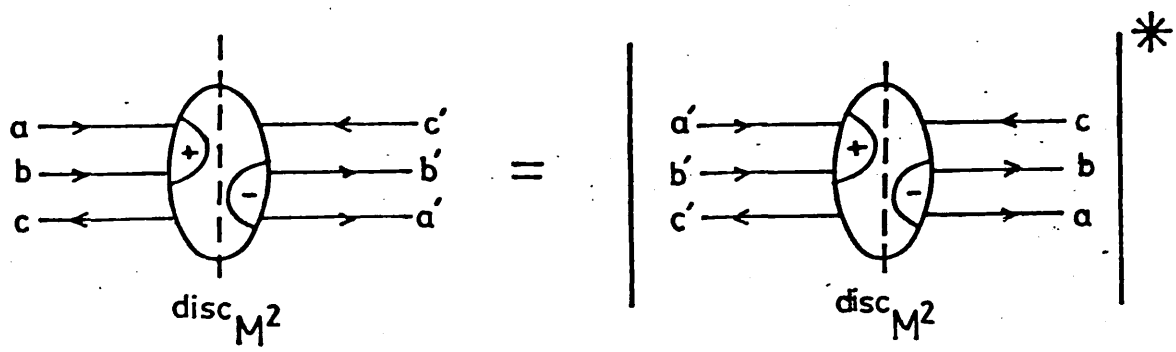

Figure 1.4 Representing hermiticity condition for Mueller amplitudes.

The total number of Mueller helicity amplitudes is given by $N_a^2 \times N_b^2 \times N_c^2$ where $N_i = 2s_i + 1$ are the number of helicity states of the particle. Parity invariance reduces the number of independent amplitudes by a factor of two and so does hermiticity Hence the number of independent amplitudes is $\frac{1}{4} N_a^2 \times N_b^2 \times N_c^2$.

The quantities available to be measured experimentally are the inclusive cross section, the polarization of the produced particle and the target asymmetry. We have (see Appendix 1.1)

$$\frac{s}{\pi} \frac{d\sigma}{dudM^2} = \frac{1}{64\pi^2 k^2 N_a N_b} \times \sum_{\lambda_a,\lambda_b,\lambda_c} H^{\lambda_a\lambda_b\lambda_c}_{\lambda_a\lambda_b\lambda_c} \tag{1.8}$$

where k is the initial state c.m. three-momentum and

$$H^{\lambda_{a'}\lambda_{b'}\lambda_{c'}}_{\lambda_a\lambda_b\lambda_c} = \text{disc}_{M^2} \langle\lambda_{a'},\lambda_{b'},\lambda_{c'}|A|\lambda_a,\lambda_b,\lambda_c\rangle \quad (1.9)$$

The polarization of a produced spin $\frac{1}{2}$ particle is given by [16, 25, 26]

$$P_c = -i \frac{\sum_{\lambda_a\lambda_b} H^{\lambda_a\lambda_b+}_{\lambda_a\lambda_b-} - H^{\lambda_a\lambda_b-}_{\lambda_a\lambda_b+}}{\sum_{\lambda_a\lambda_b\lambda_c} H^{\lambda_a\lambda_b\lambda_c}_{\lambda_a\lambda_b\lambda_c}} \quad (1.10)$$

and similarly, for target particle with spin $\frac{1}{2}$, the target asymmetry is given by

$$\Sigma_b = i \frac{\sum_{\lambda_a\lambda_c} H^{\lambda_a+\lambda_c}_{\lambda_a-\lambda_c} - H^{\lambda_a-\lambda_c}_{\lambda_a+\lambda_c}}{\sum_{\lambda_a\lambda_b\lambda_c} H^{\lambda_a\lambda_b\lambda_c}_{\lambda_a\lambda_b\lambda_c}} \quad (1.11)$$

With the results of the Mueller Generalized Optical theorem, we are able to apply Regge theory to an inclusive reaction. The general rule for invoking Regge behaviour is that if any energy variable is large, then in the channel crossed to that variable there is a leading Regge pole.

For the purposes of Regge analysis, we find it convenient to divide phase space into three regions: the beam (p_a) fragmentation region, the central region and the target (p_b) fragmentation region.

In the <u>beam fragmentation region</u>, the square of the four-momentum transfer between the beam particle (p_a) and the produced particle (p_c), u, is fixed and finite. The beam fragmentation region is further subdivided into the following three Regge limits [19].

a) The fixed $-M^2$ limit where u and M^2 are fixed and small and $\frac{s}{M^2} \to \infty$. The Regge behaviour is given by

$$f(ab\to c) \sim \frac{1}{s} \sum_{i,j} \beta_i^{a\bar{c}}(u)\, s^{\alpha_i(u)+\alpha_j(u)}\, \beta_j^{a\bar{c}}(u) \quad f^{ib\to jb}(M^2,u) \tag{1.12}$$

where β_i is the Reggeon-particle coupling, α_i is the pole trajectory and $f^{ib\to jb}$ is the forward Reggeon-particle scattering discontinuity.

b) The triple-Regge limit where u is fixed and small and $\frac{s}{M^2} \to \infty$ and $M^2 \to \infty$. In this limit, the inclusive cross section retains the form of equation (1.12), but the forward Reggeon-particle scattering discontinuity becomes

$$f^{ib\to jb}(M^2,u) \underset{M^2\to\infty}{\sim} \sum_k \beta_k^{b\bar{b}}(0)(M^2)^{\alpha_k(0)-\alpha_i(u)-\alpha_j(u)} \times g_{ijk}(u,\, u,\, 0) \tag{1.13}$$

c) The single-Regge limit where u and $\frac{s}{M^2}$ are fixed and finite. (Note that sometimes in the literature the fragmentation region refers

specifically to the single-Regge limit). In this case, the ac channel can no longer Reggeize and we have

$$f(ab\to c) \sim \frac{1}{s}\sum_k \beta_k^{b\bar{b}}(0)(M^2)^{\alpha_k(0)} F_k^{ac}(\frac{M^2}{s}, u) \qquad (1.14)$$

where $F_k^{ac}(\frac{M^2}{s}, u)$ takes into account the five-point function.

The Mueller-Regge diagrams corresponding to the above limits are shown in figs. 1.5(a), (b), (c) respectively. The wavy lines indicate exchanged Reggeons.

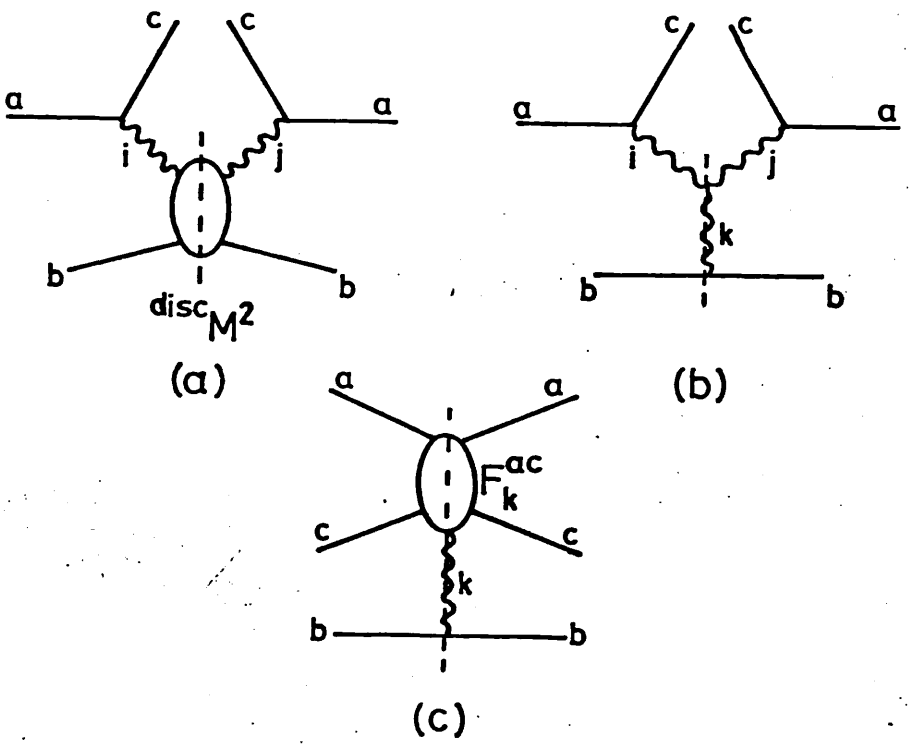

Figure 1.5 Mueller-Regge diagrams for the beam fragmentation region in (a) fixed-M^2, (b) triple-Regge and (c) single-Regge limits.

The situation for the target fragmentation region is essentially the same as above, but with the square of the four-momentum transfer between target particle (p_b) and produced particle (p_c), t, remaining fixed and finite i.e. the "other end" of phase space.

The central region (or double-Regge limit) is in the centre of phase space. Both t and u are large with $\frac{tu}{s}$ fixed and finite, we have $tu = m_T^2 s$ where m_T is the transverse mass. The corresponding Mueller-Regge diagram is given in fig. 1.6.

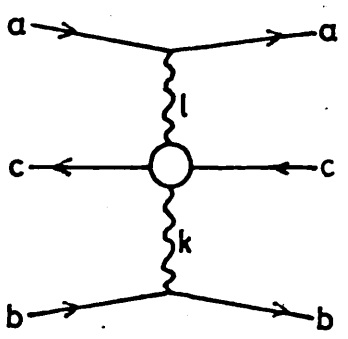

Figure 1.6 Mueller-Regge diagram for the Central region.

The inclusive cross section is given by

$$f(ab\to c) \sim \frac{1}{s} \sum_{k,\ell} \beta_\ell^{a\bar{a}}(0)\, u^{\alpha_\ell(0)}\, G_{k\ell}^{c}(\tfrac{ut}{s})\, u^{\alpha_k(0)}\, \beta_k^{b\bar{b}}(0) \tag{1.15}$$

where $G_{k\ell}^{c}(\frac{ut}{s})$ is the coupling of the Reggeons k, ℓ to $c\bar{c}$.

In terms of the familiar rapidity variable, $y = \frac{1}{2}\,\ell n\,(\frac{E + p_{\parallel}}{E - p_{\parallel}})$, the phase space regions for

$a + b \to c + X$ with relevant Regge limits are shown in fig. 1.7.

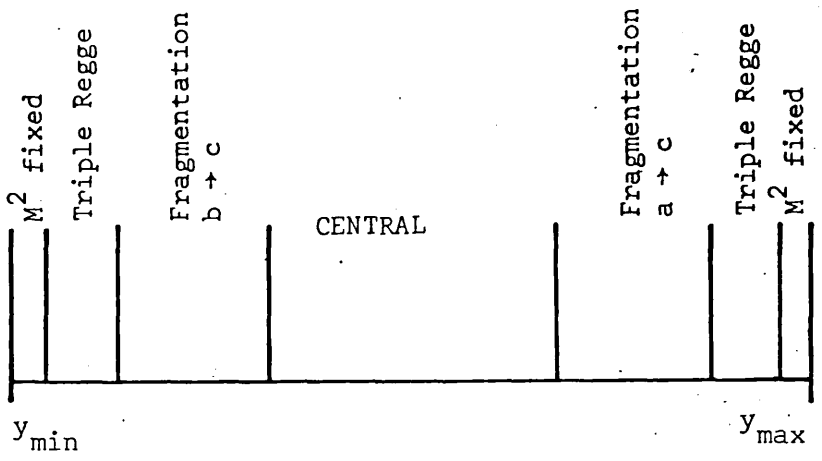

Figure 1.7 Rapidity space divided into Regge limits.

The leading asymptotic behaviour of the inclusive cross sections is provided by Pomeron exchange. The Pomeron trajectory has intercept one, $\alpha(0) = 1$. Hence, in the single- and triple-Regge regions we have $(s \to \infty)$

$$f(ab \to c) \sim g(\frac{M^2}{s}, u)$$

i.e. "scaling". In the central region

$$f(ab \to c) \sim h(\frac{ut}{s}) = h(m_T{}^2).$$

These results had been previously predicted; AFS scaling [27] and Feynman scaling [28]. The contribution from the exchange of meson trajectories, with $\alpha(0) \sim 0.5$, provide the scale breaking terms and control the approach to scaling.

In Chapter II we shall develop an absorbed Mueller-Regge model for the reaction $\pi^- + p \to p + X$ and we compare our results with the available data in Chapter III.

APPENDIX 1.1

We look at the normalization of the single particle inclusive cross section. The total cross section for $a + b \to c + X$ can be written

$$\langle n\rangle\, \sigma_{TOT}(ab\to c) = \frac{1}{F}\int dM^2 \int \frac{d^3p_c}{(2\pi)^3 2E_c}\,\frac{d^3P_X}{(2\pi)^3 2E_X}$$

$$\times\ (2\pi)^4\delta^4(p_a+p_b-p_c-P_X)\ \sum\!\!\!\!\!\!\int\ |\langle c,X|A|a,b\rangle|^2 \qquad \text{(i)}$$

where $\sum\!\!\!\!\!\!\int$ denotes summation over particles in the missing mass, integration over three-momenta of those particles and an averaging over initial helicity states. $\langle n\rangle$ is the average multiplicity of c. The differential quantity is obtained from (i) by the insertion of appropriate delta functions.

$$\langle n\rangle\, \frac{\partial\sigma}{\partial u\,\partial M^2} = \frac{1}{F}\int dM^2 \int \frac{d^3p_c}{(2\pi)^3 2E_c}\,\frac{d^3P_X}{(2\pi)^3 2E_X}$$

$$\times\ (2\pi)^4\delta^4(p_a+p_b-p_c-P_X)\,\delta(u - (p_a-p_c)^2)$$

$$\times\ \delta(M^2 - (p_a+p_b-p_c)^2)\sum\!\!\!\!\!\!\int |\langle c,X|A|a,b\rangle|^2. \qquad \text{(ii)}$$

Evaluating this expression in the c.m. frame, and putting $F = 4k\sqrt{s}$ where k is initial state c.m. three-momentum, we get (using Mueller's theorem)

$$\langle n\rangle \frac{\partial\sigma}{\partial u\partial M^2} = \frac{1}{64\pi sk^2}\frac{1}{N_aN_b}\sum_{\lambda_a,\lambda_b,\lambda_c} H^{\lambda_a\lambda_b\lambda_c}_{\lambda_a\lambda_b\lambda_c} \quad . \qquad \text{(iii)}$$

Since we work in the normal Regge limit (fixed M^2), we are effectively in that subregion of phase space where the produced particle c is at large rapidity gap from the rest of the produced particles (M^2 - cluster). So we expect that $\langle n\rangle \sim 1$ since we are unlikely to encounter another particle in the rapidity neighbourhood of c. So we write (iii) in the more conventional form

$$\frac{s}{\pi}\frac{d\sigma}{dudM^2} = \frac{1}{64\pi^2k^2}\frac{1}{N_aN_b}\sum_{\lambda_a,\lambda_b,\lambda_c} H^{\lambda_a\lambda_b\lambda_c}_{\lambda_a\lambda_b\lambda_c} \quad .$$

CHAPTER II

We develop a Mueller-Regge model for the study of a single particle inclusive process in the normal Regge region. We look at backward $\pi^- + p \to p + X$ $(a + b \to c + X)$ scattering where u is small and M^2 is fixed.

The single particle inclusive cross section is related by the Mueller Generalized Optical theorem [12] to six-point Mueller-Regge amplitudes. This relationship is shown in Fig. 2.1.

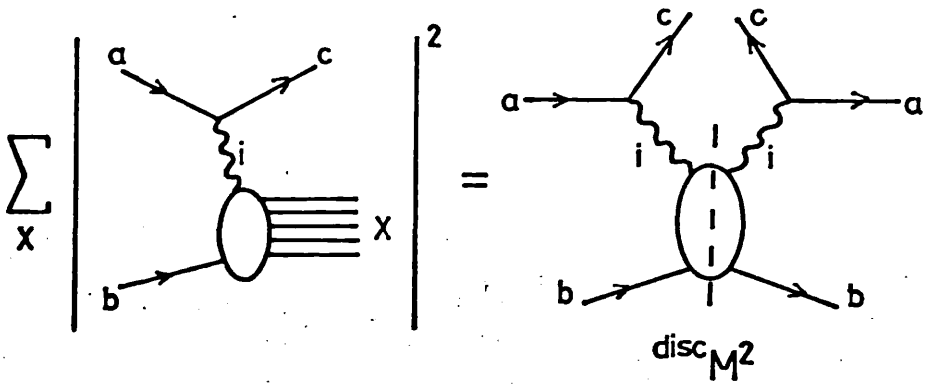

Figure 2.1 Generalized Optical theorem in normal Regge limit.

Here and throughout, particle a represents the incoming negative pion, particle b represents the target proton and particle c is the produced proton. The Mueller-Regge helicity amplitudes corresponding to fig. 2.1 are given by

$$H^{\lambda_a'\lambda_b'\lambda_c'}_{\lambda_a\lambda_b\lambda_c} = \sum_{\kappa} J_{\mu}^{\lambda_c\lambda_a} \nabla^{\mu\nu} \Gamma_{\nu}^{\lambda_b\kappa} (J_{\mu}^{\lambda_c\lambda_a} \nabla^{\mu'\nu'} \Gamma_{\nu'}^{\lambda_b\kappa})^{\dagger} \quad (2.1)$$

where $\nabla^{\mu\nu}$ is the Reggeized propagator, J_{μ} is the (on-shell) current at the particle-particle-Reggeon vertex and Γ is the structure function at the inclusive vertex.

In general we have the following relationship (see equation (1.8))

$$\frac{s}{\pi} \frac{d\sigma}{dudM^2} = \frac{1}{64\pi^2k^2} \frac{1}{(2s_a+1)(2s_b+1)} \sum_{\lambda_a,\lambda_b,\lambda_c} H^{\lambda_a\lambda_b\lambda_c}_{\lambda_a\lambda_b\lambda_c}$$

where s_a and s_b are the spins of the initial state particles and $\underline{k}$ is the centre-of-mass three-momentum ($k = |\underline{k}|$). For $\pi^- + p \to p + X$, particle a is clearly spinless, so we can simplify to

$$\frac{s}{\pi} \frac{d\sigma}{dudM^2} = \frac{1}{64\pi^2k^2} \frac{1}{(2s_b+1)} \sum_{\lambda_b,\lambda_c} H^{\lambda_b\lambda_c}_{\lambda_b\lambda_c} \quad (2.2)$$

and using the expression for the helicity amplitude given in equation (2.1),

$$\frac{s}{\pi} \frac{d}{dudM^2} = \frac{1}{64\pi^2k^2} \frac{1}{(2s_b+1)}$$

$$\times \sum_{\lambda_b,\lambda_c} \sum_{\kappa} J_{\mu}^{\lambda_c} \nabla^{\mu\nu} \Gamma_{\nu}^{\lambda_b\kappa} \Gamma_{\nu'}^{*\kappa\lambda_b} \nabla^{*\nu'\mu'} J_{\mu'}^{\lambda_c} \quad (2.3)$$

With the Mueller-Regge amplitude given by fig. 2.2,

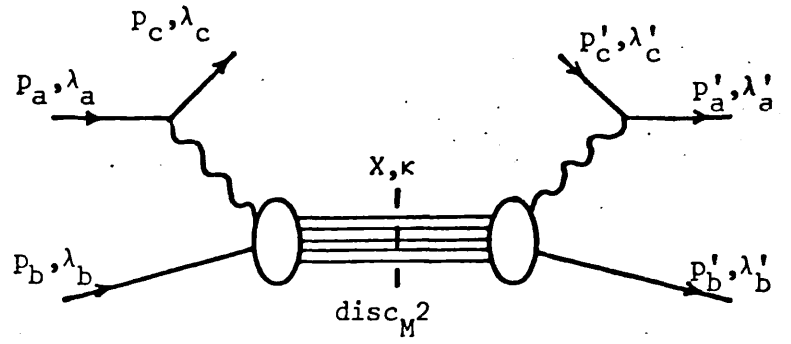

Figure 2.2 Helicity amplitude in normal Regge limit.

the only Regge trajectory which will contribute is the $I = \frac{3}{2}$, $Y = +1$, $P = +$, $\tau = -1$ baryon trajectory (Δ_δ). This trajectory is taken as the conventional linear trajectory $\alpha(u) = \alpha_o + \alpha' u$ where as usual α_o and α' will be the intercept and slope on the Chew-Frautschi plot [4, 5, 6] . Initially, we take the trajectory as a straight line through the $\Delta_\delta(1236, \frac{3}{2})$ and the $\Delta_\delta(2420, \frac{11}{2})$ which gives us the values $\alpha_o = 0.05$ and $\alpha' = 0.9$. This trajectory is shown in fig. 2.3, plotted with its parity partner (MacDowell symmetry) which exhibits the absent state.

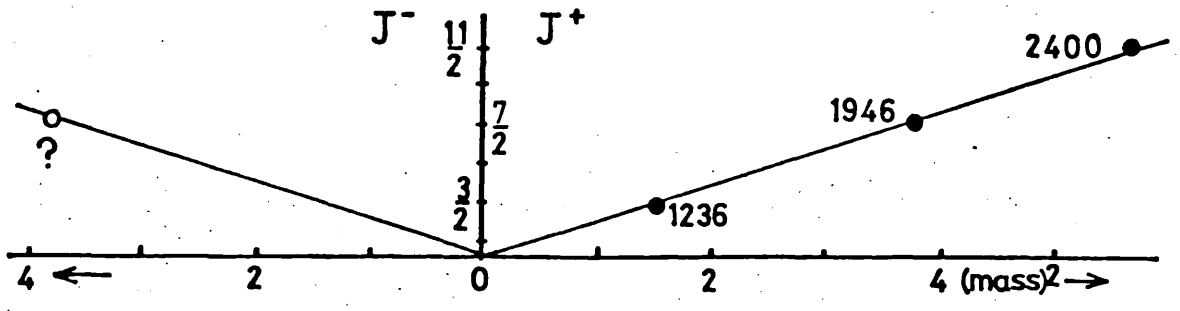

Figure 2.3 Δ_δ trajectory and parity partner showing extinguished state.

The current at the particle-particle-Reggeon vertex for this exchange is

$$J_{\mu}^{\lambda_c} = \bar{u}(p_c, \lambda_c) Q^{\mu} g$$

where the particles are on-shell and Q is the difference of the incoming and outgoing baryon momenta. The coupling constant g has been related to the $\Delta(1236)$ width via partial wave expansions [30] and the value obtained is $g^2/4\pi \simeq 15$.

The spin $\frac{3}{2}$ propagator $\nabla^{\mu\nu}$ is given by (see Appendix)

$$\begin{aligned}
\nabla_{\mu\nu} = \frac{1}{(u-m^2)} \Bigg(& (\not{P}+m) \Big[-g_{\mu\nu} + \frac{2}{3m^2} P_{\mu}P_{\nu} + \frac{1}{3} \gamma_{\mu}\gamma_{\nu} \\
& + \frac{1}{3m} (\gamma_{\mu}P_{\nu} - P_{\mu}\gamma_{\nu}) \Big] \\
& - \frac{2}{3m^2} (P^2 - m^2) \Big[\gamma_{\mu}P_{\nu} - P_{\mu}\gamma_{\nu} + (\not{P}+m)\gamma_{\mu}\gamma_{\nu} \Big] \Bigg) \\
= & (u - m^2)^{-1} D_{\mu\nu} . \qquad (2.4)
\end{aligned}$$

where $P = p_a - p_c$ and m = mass of delta. So we have

$$\begin{aligned}
H^{\lambda_c}_{\lambda_c} &= \sum_{\lambda_b} H^{\lambda_b\lambda_c}_{\lambda_b\lambda_c} \\
&= g^2 \, \bar{u}(p_c, \lambda_c) p_{a_{\mu}} \left[\frac{D^{\mu\nu}}{(u-m^2)} \right] \\
&\quad \times \left(\frac{1}{(2s_b+1)} \sum_{\lambda_b, \kappa} \Gamma_{\nu}^{\lambda_b \kappa} \, \Gamma_{\nu'}^{*\kappa\lambda_b} \right) \\
&\quad \times \left[\frac{D^{\nu'\mu'}}{(u-m^2)} \right]^* p_{a_{\mu'}} \, u(p_c, \lambda_c) \qquad (2.5)
\end{aligned}$$

Now we can write 31

$$\frac{1}{(2s_b+1)} \sum_{\lambda_b,\kappa} \Gamma_\nu^{\lambda_b \kappa} \Gamma_{\nu'}^{*\kappa\lambda_b} = \mathrm{Im}\,(W_{\nu\nu'}) \qquad (2.6)$$

where we have summed over the helicities λ_b and κ and averaged for particle b. Contracting this tensor with $\bar{\Delta}^{++}$ wave functions (see Appendix) and summing and averaging over delta helicites will allow us to apply the Optical Theorem for two-body scattering (M^2 is the relevant energy variable),

$$\frac{\mathrm{Im}}{(2s'+1)} \sum_r \bar{v}_\nu(P,r) \; W^{\nu\nu'} \; v_{\nu'}(P,r) = M^2 \sigma_{TOT}^{\bar{\Delta}p}(M^2) \qquad (2.7)$$

where s' is the spin of the delta.

We can pick out a dominant contribution to $\mathrm{Im}\, W^{\nu\nu'}$ by looking at the forward $\bar{\Delta}p \to \bar{\Delta}p$ scattering amplitude and again using the Optical theorem. We make the following identification,

$$\frac{\mathrm{Im}}{(2s'+1)} \sum_r \bar{v}_\nu(P,r) \; W^{\nu\nu'} \; v_{\nu'}(P,r)$$

$$= M^2 \; \sigma_{TOT}^{\bar{\Delta}p} \; (M^2)$$

$$\simeq \frac{1}{(2s_b+1)} \; \frac{\mathrm{Im}}{(2s'+1)} \sum_{r,\lambda_b} 2A_4 \; p_b^\nu \; \bar{v}_\nu(P,r)$$

$$\not{p}_b \; v_{\nu'}(P,r) p_b^{\nu'} \qquad (2.8)$$

where A_4 belongs to the set of 2×5 form factors which describe elastic $\bar{\Delta}p$ scattering. A complete discussion of this formalism is given in Appendix 2.1. For large M^2 we could expect the $\bar{\Delta}p$ total cross section to become independent of M^2, so that we can estimate the M^2-dependence and magnitude of $\mathrm{Im}\, A_4$ by taking $\sigma^{\bar{\Delta}p}_{TOT}(M^2) \sim \text{constant} = \sigma(\bar{\Delta}p)$ and using equation (2.8). Hence (Appendix 2.1) we have

$$\mathrm{Im}\, A_4 = \frac{3m^3}{M^4}\, \sigma(\bar{\Delta}p) \tag{2.9}$$

In obtaining this result we have assumed that the term involving the form factor A_4 gives the dominant contribution to the $\bar{\Delta}p$ total cross section. This assumption will almost certainly over-estimate the size of A_4 and we can expect that $\sigma(\bar{\Delta}p)$ will not correspond to the full (asymptotic) $\bar{\Delta}p$ total cross section.

Now by comparison we have

$$\mathrm{Im}\, W^{\nu\nu'} = \frac{6m^2}{M^4}\, \sigma(\bar{\Delta}p) p_b{}^{\nu}\, \not{p}_b p_b{}^{\nu'}$$

and equation (2.5) becomes

$$H^{\lambda_c}_{\lambda_c} = g^2\, \bar{u}(p_c,\lambda_c) p_{a_\mu} \left[\frac{D^{\mu\nu}}{(u-m^2)}\right]$$

$$\times \left(\frac{6m^2}{M^4}\, \sigma(\bar{\Delta}p)\, p_{b_\nu} \not{p}_b p_{b_{\nu'}}\right) \left[\frac{D^{\nu'\mu'}}{(u-m^2)}\right]^*$$

$$\times\, p_{a_{\mu'}}\, u(p_c,\lambda_c).$$

The Reggeization of this amplitude is carried out by making the standard substitution [32]

$$\frac{1}{u-m^2} \to \frac{\alpha'}{2}\,\Gamma(f(u))\,[1 + i\tau\, e^{-i\pi\alpha(u)}]\quad \left(\frac{s}{M^2}\right)^{\alpha(u)-J}$$

where τ = signature of delta trajectory (= - 1), J = spin = $\frac{3}{2}$, Γ is the Euler gamma function and $f(u) = \frac{3}{2} - \alpha(u)$. This procedure employs the Gell-Man (or nonsense) ghost killing mechanism.

Equation (2.2) has now become

$$\frac{s}{\pi}\,\frac{d\sigma}{dudM^2} = \frac{1}{64\pi^2k^2}\sum_{\lambda_c} H^{\lambda_c}_{\lambda_c}$$

$$= \frac{g^2}{64\pi^2k^2}\,\frac{6m^2}{M^4}\,\sigma(\bar{\Delta}p)\sum_{\lambda_c}\bar{u}(p_c,\lambda_c)\,p_{a_\mu}\,D^{\mu\nu}$$

$$\times\, p_{b_\nu}\,\not{p}_b\,p_{b_{\nu'}}\,D^{\nu'\mu'}\,p_{a_{\mu'}}\,u(p_c,\lambda_c)$$

$$\times\left(\frac{\alpha'}{2}\,\Gamma(\tfrac{3}{2} - \alpha(u))\,[1 - ie^{-i\pi\alpha(u)}]\,\left(\frac{s}{M^2}\right)^{\alpha(u)-\frac{3}{2}}\right)$$

$$\times\left(\frac{\alpha'}{2}\,\Gamma(\tfrac{3}{2} - \alpha(u)\,[1 - ie^{-i\pi\alpha(u)}]^*\,\left(\frac{s}{M^2}\right)^{\alpha(u)-\frac{3}{2}}\right) \tag{2.10}$$

We see that this pole-only Reggeized amplitude will give us the expected s-dependence; the contraction of the structure function with $D^{\mu\nu}$ and vertex currents gives an s^3 factor, we have s^{-1} from the density of states factor and the Reggeized propagators will give $s^{2\alpha(u)-3}$. Hence we have a total $s^{2\alpha(u)-1}$ dependence as expected.

The full expression for equation (2.10) is given in Appendix 2.2, where it can be seen that (as expected) the $g_{\mu\nu}$ terms in the propagators give the dominant contribution.

In accordance with the Carlitz-Kislinger prescription for removing unobserved parity partners, cuts in the complex angular momentum plane are incorporated into the Mueller-Regge model by means of the Gottfried-Jackson-Sopkovich absorption formalism [33]. In this method, the impact parameter amplitudes are modified to take into account absorptive (unitarity) effects due to initial and final state rescatterings. We shall give a brief description of the derivation of this absorption model.

First we write out a general expression for the helicity amplitude (see fig. 2.2)

$$H^{\lambda_{\bar{a}}\lambda_{\bar{b}}\lambda_c}_{\lambda_a\lambda_b\lambda_{\bar{c}}}(p_{\bar{a}}, p_{\bar{b}}, p_c; p_a, p_b, p_{\bar{c}})$$

$$= \sum_{n_X(\lambda,s_X)} \langle p_{\bar{a}}\lambda_{\bar{a}}, p_{\bar{b}}\lambda_{\bar{b}}|T|p_c\lambda_c, n_X(\lambda, s_X)\rangle$$

$$\langle p_{\bar{c}}\lambda_{\bar{c}}, n_X(\lambda,s_X)|T|p_a\lambda_a, p_b\lambda_b\rangle \qquad (2.11)$$

where $n_X(\lambda,s_X)$ denotes an intermediate state with spin s_X and helicity λ. Next, to perform an independent partial wave expansion, we choose the frame with intermediate state along z-axis and only enforce the relaxed condition

$$p_a + p_b - p_{\bar{c}} = p_{\bar{a}} + p_{\bar{b}} - p_c.$$

The resulting analysis [3, 34] gives

$$H^{\lambda_{\bar{a}}\lambda_{\bar{b}}\lambda_c}_{\lambda_a\lambda_b\lambda_{\bar{c}}} = \sum_{\lambda} e^{-i\phi'(\bar{\mu}'-\mu')} \; e^{-i\phi(\bar{\mu}-\mu)}$$

$$\times \sum_{J=J_o}^{\infty} \sum_{J'=J_o'}^{\infty} \frac{2J+1}{4\pi} \frac{2J'+1}{4\pi} \; d^{J'}_{\mu'\bar{\mu}'}(\theta') \; d^{J}_{\mu\bar{\mu}}(\theta)$$

$$\times \; h(J, J'; \lambda, M^2)$$

where

$$h(J, J'; \lambda, M^2) = \sum_{n_X(\lambda,s_X)} \langle\lambda_{\bar{a}},\lambda_{\bar{b}}|T^{J'}(M^2)|\lambda_c,n_X(\lambda,s_X)\rangle$$

$$\times \langle\lambda_{\bar{c}},n_X(\lambda,s_X)|T^{J}(M^2)|\lambda_a,\lambda_b\rangle, \qquad (2.12)$$

d's are the usual rotation functions and $\bar{\mu} = \lambda-\lambda_{\bar{c}}$, $\mu = \lambda_b - \lambda_a$, $\mu' = \lambda - \lambda_c$, $\bar{\mu}' = \lambda_{\bar{b}} - \lambda_{\bar{a}}$, $J_o = \max\{|\mu|,|\bar{\mu}|\}$ $J_o' = \max\{|\mu'|,|\bar{\mu}'|\}$. For physical situations when $h(J, J'; \lambda, M^2)$ does not vary rapidly with J and J', we can replace the sums over angular momentum in equation (2.12) by integrals. Also, for high energy scattering with small values of λ, we can adopt the usual approximation

$$d^{J}_{\mu\mu'}(\theta) = (-1)^{\mu-\mu'} \; J_{|\mu-\mu'|}[2(J+\tfrac{1}{2})\sin\tfrac{\theta}{2}]$$

where $J_\nu[z]$ is a Bessel function of the first kind. So

$$H^{\lambda_{\bar{a}}\lambda_{\bar{b}}\lambda_c}_{\lambda_a\lambda_b\lambda_{\bar{c}}} = \sum_{\lambda} e^{-i\phi'(\bar{\mu}'-\mu')} e^{-i\phi(\bar{\mu}-\mu)}$$

$$\times \frac{1}{4\pi^2} \int_{J_o}^{\infty} dJ \, (J + \tfrac{1}{2}) \int_{J_{o'}}^{\infty} dJ' \, (J' + \tfrac{1}{2})$$

$$\times J_\nu \left[2(J + \tfrac{1}{2}) \sin\tfrac{\theta}{2}\right] J_{\nu'}\left[2(J' + \tfrac{1}{2}) \sin\tfrac{\theta'}{2}\right]$$

$$\times h(J, J'; \lambda, M^2) \qquad (2.13)$$

where $\nu = |\mu - \bar{\mu}|$ and $\nu' = |\mu' - \bar{\mu}'|$.

The impact parameters (b, b') are defined by

$$kb = (J + \tfrac{1}{2})$$

and

$$kb' = (J' + \tfrac{1}{2}).$$

We also introduce the variables τ and τ' with

$$\tau = 2k \sin \frac{\theta}{2} ,$$

$$\tau' = 2k \sin \frac{\theta'}{2}$$

and correspondingly

$$u = u_{min} - \tau^2 \frac{q}{k} ,$$

$$u' = u'_{min} - \tau'^2 \frac{q}{k}$$

where u_{min}, u'_{min} are kinematic limits and q is the final state c.m. three momentum. The variable τ corresponds to the transverse momentum.

Again in the limit of small λ amd large s, we can set b_o $(= \frac{1}{k}(J_o + \frac{1}{2}))$ and b_o' to zero and get

$$H^{\lambda_{\bar{a}}\lambda_{\bar{b}}\lambda_c}_{\lambda_a\lambda_b\lambda_{\bar{c}}} = \sum_{\lambda} e^{-i\phi'(\bar{\mu}' - \mu')}\, e^{-i\phi(\bar{\mu} - \mu)}$$

$$\times \frac{1}{4\pi^2}\int_0^\infty db\; b\; J_\nu(b\tau) \int_0^\infty db'\; b'\; J_{\nu'}(b'\tau')$$

$$\times\; h(b,\, b';\, \lambda,\, M^2). \qquad (2.14)$$

Integrating over ϕ and ϕ' simplifies equation (2.14) to

$$H^{\lambda_{\bar{a}}\lambda_{\bar{b}}\lambda_c}_{\lambda_a\lambda_b\lambda_{\bar{c}}} = \sum_{\lambda} \int_0^\infty db\; b\; J_\nu(b\tau) \int_0^\infty db'\; b'\; J_{\nu'}(b'\tau')$$

$$\times\; h(b,\, b';\, \lambda,\, M^2).$$

We have already seen that the approximations made so far require that λ be small and, since we expect helicity flip into the missing mass state will be negligible in the forward reaction $(\tau = \tau')$, we make the additional simplifying assumption that the sum over λ collapses to $\lambda_b = \lambda = \lambda_{\bar{b}}$. It has been argued [17] that this will be the dominant configuration from consideration of angular momentum and there is an absence of phenomenological evidence to the contrary.

Finally, we can use the orthogonality properties of Bessel functions (see Appendix 2.3), to obtain

$$h(b,\ b';\ M^2) = \int_0^\infty \tau d\tau\ J_\nu(b\tau) \int_0^\infty \tau' d\tau'\ J_{\nu'}(b'\tau')$$

$$\times\ H^{\lambda_{\bar{a}}\lambda_{\bar{b}}\lambda_c}_{\lambda_a\lambda_b\lambda_{\bar{c}}}\ (\tau,\ \tau',\ M^2) \qquad (2.15)$$

where

$$\nu' = |\bar{\mu}' - \mu'| = |\lambda_{\bar{a}} - \lambda_c| = |\lambda_c|$$

and

$$\nu = |\mu - \mu'| = |\lambda_a - \lambda_{\bar{c}}| = |\lambda_{\bar{c}}|,$$

and we are now in a position to introduce absorption in the impact parameter amplitude.

The absorption corrections we consider take into account elastic rescatterings in the external channels. Elastic scattering matrices $S(b)$ are introduced and

$$h_{abs}(b,b';M^2) = S^{\frac{1}{2}}(b')^* h(b,b';M^2) S^{\frac{1}{2}}(b). \qquad (2.16)$$

We take the usual Gaussian form for the elastic scattering matrices,

$$S(b) = 1 - C\ e^{-\lambda b^2}$$

where C is the opacity and $\lambda = R^{-2}$ (R = radius of interaction). Both these parameters can be obtained from elastic scattering data.

$$C = \frac{\sigma_{TOT}}{4\pi R^2}$$

and R is related to the slope of the elastic diffraction peak

$$\frac{(\frac{d\sigma}{dt})}{(\frac{d\sigma}{dt})|_{t=0}} = e^{-\frac{1}{2}R^2|t|}\ .$$

Clearly, it is expected that rescatterings in both ab ($\bar{a}$ $\bar{b}$) and $\bar{c}$ b (c $\bar{b}$) channels will contribute (figs. 2.4(a) and (b)).

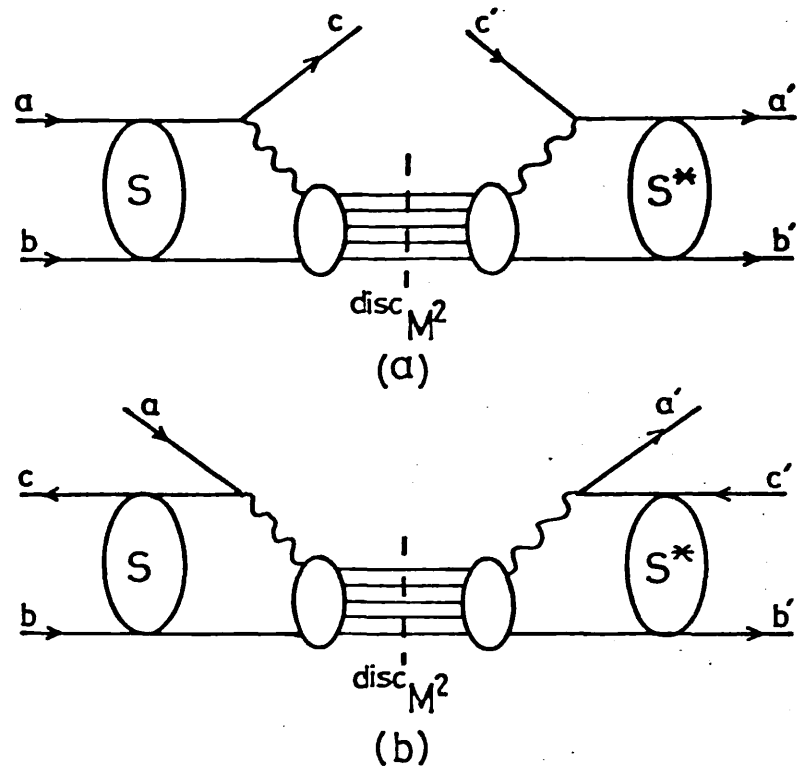

Figure 2.4 Rescatterings in (a) ab and $\bar{a}'\bar{b}'$ channels, (b) $\bar{c}$b and $\bar{b}'$c channels.

However, we make the simplifying assumption that

$$S_{ab}^{\frac{1}{2}} \, S_{\bar{c}b}^{\frac{1}{2}} \simeq \frac{S_{ab} + S_{\bar{c}b}}{2} = S \qquad (2.17)$$

and we fix the parameters of S from the ab channel. Unitarity requires that $C \leq 1$ and for $\pi^- p$ scattering at $p_{lab} = 12$ GeV/c we have $C \sim 0.7$ and $\lambda \sim 0.068$. Now, returning to equation (2.15) we have

$$H_{abs}{}^{\lambda_{\bar{a}}\lambda_{\bar{b}}\lambda_c}_{\lambda_a\lambda_b\lambda_{\bar{c}}}(\tau, \tau', M^2)$$

$$= \int_0^\infty db\ b\ J_\nu(b\tau) \int_0^\infty db'\ b'\ J_{\nu'}(b'\tau')$$

$$S(b)\ S(b') \int_0^\infty d\tau_o\ \tau_o\ J_\nu(b\tau_o) \int_0^\infty d\tau_o'\ \tau_o'\ J_{\nu'}(b'\tau_o')$$

$$H^{\lambda_{\bar{a}}\lambda_{\bar{b}}\lambda_c}_{\lambda_a\lambda_b\lambda_{\bar{c}}}(\tau_o, \tau_o', M^2) \tag{2.18}$$

and performing the integrals over b and b' (see Appendix 2.3),

$$H_{abs}{}^{\lambda_{\bar{a}}\lambda_{\bar{b}}\lambda_c}_{\lambda_a\lambda_b\lambda_{\bar{c}}}(\tau, \tau', M^2)$$

$$= \int_0^\infty d\tau_o\ \tau_o \int_0^\infty d\tau_o'\ \tau_o'\ H^{\lambda_{\bar{a}}\lambda_{\bar{b}}\lambda_c}_{\lambda_a\lambda_b\lambda_{\bar{c}}}(\tau_o, \tau_o', M^2)$$

$$x\left(\frac{1}{\tau_o}\ \delta(\tau - \tau_o) - \frac{C}{2\lambda} \exp\left(-\frac{\tau^2+\tau_o^2}{4\lambda}\right) I_\nu\left(\frac{\tau\tau_o}{2\lambda}\right)\right)$$

$$x\left(\frac{1}{\tau_o'}\ \delta(\tau' - \tau_o') - \frac{C}{2\lambda} \exp\left(-\frac{\tau'^2+\tau_o'^2}{4\lambda}\right) I_{\nu'}\left(\frac{\tau'\tau_o'}{2\lambda}\right)\right) \tag{2.19}$$

where I_ν is the Bessel function of imaginary argument.

Inserting the absorbed Mueller-Regge helicity amplitude of equation (2.19) into equation (2.2), we can obtain the single particle inclusive cross section for this absorption model.

In practice we encounter some difficulties in evaluating the absorbed amplitude. The gamma function which results from the ghost-eliminating scheme of Reggeization, $\Gamma(\frac{3}{2} - \alpha(u))$, is only valid at small u. But the presence of this gamma function in

the integral of equation (2.19) will prevent that integral from converging. So, we make the approximation

$$\Gamma(\tfrac{3}{2} - \alpha(u)) = A_1 \exp(B_1 u) + A_2 \exp(B_2 u) \qquad (2.20)$$

with

$$A_1 = .444798, \quad A_2 = .440391$$

$$B_1 = .813327, \quad B_2 = -.825487$$

where the parameter values are obtained from a least squares fit to the delta trajectory over the range $0 < |u| < 1\ (\mathrm{GeV})^2$ [35].

A more serious problem is associated with extending the helicity amplitude away from the forward direction. There is no difficulty with the τ_o and τ_o' dependence of the Regge exchanges (see fig. 2.5),

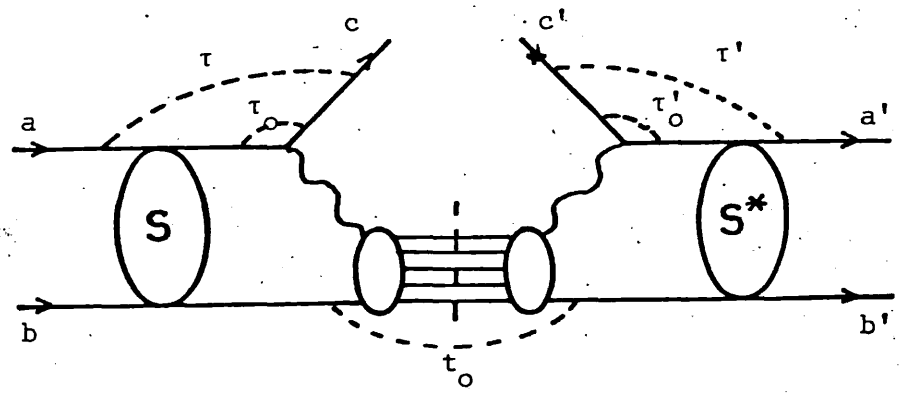

Figure 2.5 Rescattering in ab channels showing the momentum transfer variables.

but for $\tau_o \neq \tau_o'$ we can have non-zero t_o and we would expect some t_o dependence to be introduced. However, since we know that the elastic scattering effects we have introduced will be peaked about $\tau_o = \tau$ and $\tau_o' = \tau'$, we assume that this t_o dependence can be neglected.

A full expression for the absorbed amplitude is given in Appendix 2.3.

APPENDIX 2.1

We consider the forward, elastic, no spin-flip Δp scattering amplitude (see figure).

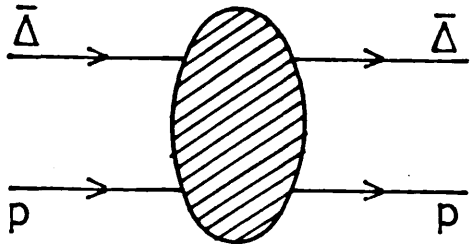

Figure Amplitude for $\bar{\Delta}p$ elastic scattering.

The energy variable for this amplitude is $M^2 = (P + p_b)^2$, $P = p_a - p_c$. We can write [36]

$$T(\bar{\Delta}p) = \sum_{r,\lambda_b} (D_1^{\alpha\alpha'} S_{\alpha\alpha'} + D_2^{\alpha\alpha'} T_{\alpha\alpha'}$$

$$+ D_3^{\alpha\alpha'} A_{\alpha\alpha'} + D_4^{\alpha\alpha'} V_{\alpha\alpha'} + D_5^{\alpha\alpha'} P_{\alpha\alpha'}) \qquad \text{(i)}$$

where $D_i^{\alpha\alpha'} = A_i p_b^{\alpha} p_b^{\alpha'} - B_i\, g^{\alpha\alpha'}$. Since we can make use of the following properties of Rarita-Schwinger wave functions (see Appendix),

$$P^{\alpha} v_{\alpha}(P,r) = 0 \quad \text{and} \quad \gamma^{\alpha} v_{\alpha}(P,r) = 0,$$

we know that equation (i) will be the most general ansatz, with

$$S_{\alpha\alpha'} = \bar{v}_\alpha(P,r)\ v_{\alpha'}(P,r)\ \bar{u}(p_b,\lambda_b)\ u(p_b,\lambda_b),$$

$$T_{\alpha\alpha'} = \tfrac{1}{2}\ \bar{v}_\alpha(P,r)\sigma^{\rho\delta}\ v_{\alpha'}(P,r)\ \bar{u}(p_b,\lambda_b)\sigma_{\rho\delta}\ u(p_b,\lambda_b),$$

$$A_{\alpha\alpha'} = \bar{v}_\alpha(P,r)i\gamma_5\gamma^\rho v_{\alpha'}(P,r)\ \bar{u}(p_b,\lambda_b)i\gamma_5\gamma_\rho u(p_b,\lambda_b),$$

$$V_{\alpha\alpha'} = \bar{v}_\alpha(P,r)\gamma^\rho\ v_{\alpha'}(P,r)\ \bar{u}(p_b,\lambda_b)\gamma_\rho\ u(p_b,\lambda_b)$$

and

$$P_{\alpha\alpha'} = \bar{v}_\alpha(P,r)\gamma_5\ v_{\alpha'}(P,r)\ \bar{u}(p_b,\lambda_b)\gamma_\rho\ u(p_b,\lambda_b).$$

Using the properties of the spin-half wave functions, (see Appendix), only vector $(V_{\alpha\alpha'})$ and scalar $(S_{\alpha\alpha'})$ contributions will remain in the forward direction

$$T(\bar{\Delta}p) = \sum_{r,\lambda_b} \left(A_1 p_b^\alpha p_b^{\alpha'} - B_1 g^{\alpha\alpha'}\right) \bar{v}_\alpha(P,r)v_{\alpha'}(P,r)\bar{u}(p_b,\lambda_b)u(p_b,\lambda_b)$$

$$+ \left(A_4 p_b^\alpha p_b^{\alpha'} - B_4 g^{\alpha\alpha'}\right) \bar{v}_\alpha(P,r)\gamma^\rho v_{\alpha'}(P,r)\bar{u}(p_b,\lambda_b)\gamma_\rho u(p_b,\lambda_b) \qquad \text{(ii)}$$

Now we note the following results, for spin $\frac{1}{2}$:

$$\bar{u}(p_b,\lambda_b)\ u(p_b,\lambda_b')\ = 2m_b\ \delta_{\lambda_b\lambda_b'} \qquad \text{(iii)}$$

$$\bar{u}(p_b,\lambda_b)\gamma^\mu u(p_b,\lambda_b')\ = 2p_b^{\ \mu}\ \delta_{\lambda_b\lambda_b'} \qquad \text{(iv)}$$

for spin $\frac{1}{2}$:

$$\bar{v}_\alpha(P,r)\ v_\alpha(P,r') = 2m\delta_{rr'} \qquad \text{(v)}$$

$$\bar{v}_\alpha(P,r)\gamma^\mu\ v_\alpha(P,r') = -2P^\mu\delta_{rr'} \qquad \text{(vi)}$$

(where m = mass of delta).

Also, for $2P.p_b >> m_b^2, m^2$, we can make the approximation

$$p_b^{\alpha}\bar{v}_{\alpha}(P,r)\gamma^{\mu}\, v_{\beta}(P,r')p_b^{\beta} = \frac{4}{3m^2}\,(p_b.P)^2\, P^{\mu}\delta_{rr'} \qquad \text{(vii)}$$

(we give a proof of the above result at the end of this appendix). Using equations (iii) to (vi) in equation (ii), we obtain

$$T(\bar{\Delta}p) = \sum_{r,\lambda_b} \Big(-4m_b m\, B_1 + 4p_b.P\, B_4$$

$$+ 2m_b\, A_1\, p_b^{\alpha}\bar{v}_{\alpha}(P,r)\, v_{\alpha'}(P,r)p_b^{\alpha'}$$

$$+ 2A_4\, p_b^{\alpha}\bar{v}_{\alpha}(P,r)\, \not{p}_b\, v_{\alpha'}(P,r)p_b^{\alpha'}\Big)$$

Now this scattering process has subenergy M^2 and by the Optical theorem we may write

$$\sigma_{TOT}^{\bar{\Delta}p}(M^2) = \frac{1}{M^2}\,\frac{1}{(2s_b+1)}\,\frac{1}{(2s'+1)}\sum_{r,\lambda_b} \mathrm{Im}\,\langle\lambda_b,r|A(M^2,\ t=0)$$

$$|\lambda_b,r\rangle$$

$$= \frac{1}{M^2}\,\frac{1}{(2s_b+1)}\,\frac{1}{(2s'+1)}\sum_{r,\lambda_b} \mathrm{Im}\Big(-4m_b m\, B_1$$

$$+ 4p_b.P\, B_4 + 2m_b\, A_1\, p_b^{\alpha}\bar{v}_{\alpha}(P,r)v_{\alpha'}(P,r)p_b^{\alpha'}$$

$$+ 2A_4\, p_b^{\alpha}\bar{v}_{\alpha}(P,r)\, \not{p}_b\, v_{\alpha'}(p,r)\, p_b^{\alpha'}\Big).$$

Now, we can expect that $\sigma_{TOT}^{\bar{\Delta}p}(M^2)$ will become independent of M^2 for large M^2. We can also see from equation (2.4) that in the inclusive cross section the term with form factor A_4 will behave like s^3

whereas the remaining terms are suppressed by at least a factor of s. With this in mind, we take

$$\sigma_{TOT}^{\bar{\Delta}p}(M^2) \sim \frac{1}{M^2} \frac{1}{(2s_b+1)} \frac{1}{(2s'+1)} \sum_{r,\lambda_b} 2\,\mathrm{Im}\,(A_4)$$

$$\times\; p_b^{\alpha}\, \bar{v}_{\alpha}(P,r)\not{p}_b\, v_{\alpha'}(P,r) p_b^{\alpha'} \qquad \text{(viii)}$$

and using equation (vii) for the limit $2P.p_b >> m_b^2,\ m^2$,

$$\sigma_{TOT}^{\bar{\Delta}p}(M^2) \sim \frac{1}{M^2}\,\frac{8}{3}\,\frac{(p_b.P)^3}{m^2}\,\mathrm{Im}\,(A_4)$$

$$\simeq \frac{1}{3}\,\frac{M^4}{m^2}\,\mathrm{Im}\,(A_4) \qquad \text{(ix)}$$

and thus

$$\mathrm{Im}\,(A_4) \sim \frac{3m^2}{M^4}\,\sigma_{TOT}^{\bar{\Delta}p}(M^2). \qquad \text{(x)}$$

While we realise that equation (viii) is not the full expression for the $\bar{\Delta}p$ total cross section, we expect that equation (x) will, at worst, give us an order of magnitude estimate for $\mathrm{Im}\,(A_4)$ and a reasonable M^2 - dependence.

<u>Proof of equation (vii)</u>[36]

$$p_b^{\alpha}\bar{v}_{\alpha}(P,r)\gamma^{\mu}v_{\beta}(P,r')p_b^{\beta} = \frac{4}{3m^2}\,(p_b.P)^2\,P^{\mu}\delta_{rr'}$$

Now let

$$A^{\mu} = \frac{4}{3m^2}\,(p_b.P)^2\,P^{\mu}\delta_{rr'}$$

and

$$(\not{P}-m)\,T_{\alpha\beta} = \sum_r \bar{v}_{\alpha}(P,r)\,v_{\beta}(P,r),$$

then equation (vii) implies the following result,

$$p_b{}^{\rho}(\not{P}-m)\ T_{\alpha\rho}\gamma^{\mu}\ (\not{P}-m)\ T_{\beta\delta}p_b{}^{\beta} = A^{\mu}(\not{P}-m)\ T_{\alpha\delta}$$

=>

$$(\not{P}-m)\gamma^{\mu}\ (\not{P}-m)p_b{}^{\rho}T_{\alpha\rho}T_{\beta\delta}p_b{}^{\beta} = A^{\mu}(\not{P}-m)\ T_{\alpha\delta}$$

=>

$$2P^{\mu}(\not{P}-m)p_b{}^{\rho}T_{\alpha\rho}T_{\beta\delta}p_b{}^{\beta} = A^{\mu}(\not{P}-m)\ T_{\alpha\delta}$$

Now inserting the expression for the projection operator (see Appendix),

$$\begin{aligned}
-\frac{2}{9}P^{\mu}\Bigg(&-3p_{b_\alpha}p_{b_\delta} - \frac{p_\alpha p_\delta}{m^4}\left[4(P.p_b)^2 - m_b{}^2m^2\right] \\
&+ \left[(P.p_b)^2 - m_b{}^2m^2\right]\frac{\gamma_\alpha\gamma_\delta}{m^2} + 3(\not{p}_b + \frac{P.p_b}{m})\left[p_{b_\alpha}\gamma_\delta - p_{b_\delta}\gamma_\alpha\right] \\
&+ \frac{3}{m}\left[(\not{p}_b + \frac{2P.p_b}{m})p_{b_\delta}P_\alpha - \not{p}_b p_{b_\alpha}P_\delta\right] \\
&+ \frac{1}{m^3}\left[m_b{}^2m^2 + 2(P.p_b)^2 + 3P.p_b m\not{p}_b\right](\gamma_\alpha P_\delta - \gamma_\delta P_\alpha)\Bigg) \\
&= A^{\mu}(-g_{\alpha\delta} + \frac{2}{3m^2}P_\alpha P_\delta + \frac{1}{3}\gamma_\alpha\gamma_\delta - \frac{1}{3m}(\gamma_\alpha P_\delta - \gamma_\delta P_\alpha))
\end{aligned}$$

and comparing terms for the limit $2P.p_b >> m^2m_b{}^2$, we get

$$A^{\mu} = \frac{4}{3m^2}\ (P.p_b)^2\ P^{\mu}.$$

APPENDIX 2.2

We examine the behaviour of the helicity amplitude including the full propagator.

Consider

$$H = \sum_{\lambda_c} \bar{u}(p_c,\lambda_c)\; p_a{}^{\mu}\Bigg[(\not{P}+m)\;\Bigg(-g_{\mu\nu} + 2\,\frac{P_\mu P_\nu}{3m^2}$$

$$+ \frac{1}{3}\,\gamma_\mu\gamma_\nu + \frac{1}{3m}\;(\gamma_\mu P_\nu - \gamma_\nu P_\mu)\Bigg)$$

$$- \frac{2}{3m^2}\,(P^2-m^2)\;\Big(\gamma_\mu P_\nu - P_\mu\gamma_\nu + (\not{P}+m)\gamma_\mu\gamma_\nu\Big)\Bigg]$$

$$p_b^{\nu}\not{p}_b p_b{}^{\nu'}\Bigg[(\not{P}+m)\;\Bigg(-g_{\nu'\mu'} + 2\frac{p_{\nu'}P_{\mu'}}{3m^2}$$

$$+ \frac{1}{3}\,\gamma_{\nu'}\gamma_{\mu'} + \frac{1}{3m}\,(\gamma_{\nu'}P_{\mu'} - P_{\nu'}\gamma_{\mu'})\Bigg)$$

$$- \frac{2}{3m^2}\,(P^2 - m^2)\;\Big(\gamma_{\nu'}P_{\mu'} - P_{\nu'}\gamma_{\mu'} + (\not{P}+m)\gamma_{\nu'}\gamma_{\mu'}\Big)\Bigg]$$

$$p_a{}^{\mu'}\; u(p_c,\lambda_c)$$

Then using trace theorems and putting

$$C = -\,p_a\cdot p_b + \frac{2}{3m^2}\,p_a\cdot P\;p_b\cdot P$$

we have

$$H = AC^2 + BC + D$$

$$- \frac{2}{3m^2} (P^2 - m^2)E + \frac{4}{9m^4} (P^2 - m^2)^2 F.$$

Expressions for the coefficients are given below. We see easily that the leading contribution (in AC^2) comes from the $g_{\mu\nu}$ terms in the propagators.

$$A = 4(m-m_c)^2 p_b \cdot p_c + 8(m-m_c)m_c p_a \cdot p_b$$
$$+ 4\,[-m_a^2 p_b \cdot p_c + 2p_a \cdot p_b p_a \cdot p_c]$$

$$B = \frac{4}{3}\Big((m-m_c)^2[m_b^2 p_a \cdot p_c - m_b^2 \frac{m_c}{m} p_a \cdot P]$$
$$+ 2m_a^2 m_b^2 m_c (m-m_c) + \frac{2}{m}(m-m_c) p_b \cdot P\; p_a \cdot p_b\; p_a \cdot p_c$$
$$- \frac{2}{m} m_b^2 (m-m_c)\; p_a \cdot P\; p_a \cdot p_c + m_a^2 m_b^2 p_a \cdot p_c$$
$$- m_a^2 m_b^2 \frac{m_c}{m} p_a \cdot P + \frac{2}{m} m_a^2 m_c\; p_b \cdot P\; p_a \cdot p_b$$
$$+ m_b^2 m\,[m_a^2 m_c + (m-m_c)\; p_a \cdot p_c]$$
$$+ m_b^2\; p_a \cdot P\,[p_a \cdot p_c + (m-m_c)m_c]$$
$$- p_b \cdot P\,[-m_a^2\; p_b \cdot p_c + 2p_a \cdot p_b\; p_a \cdot p_c]$$
$$- 2\; p_b \cdot P\; p_a \cdot p_b\; m_c(m-m_c)$$
$$+ [p_a \cdot p_c + (m-m_c)m_c]\;(m_a^2 m_b^2 - 2m_b^2\; p_a \cdot P$$
$$+ 4p_a \cdot p_b\; p_b \cdot P + m_b^2 \frac{m_c}{m} p_a \cdot P - 2\frac{m_c}{m} p_a \cdot p_b\; p_b \cdot P)$$
$$+ [m_a^2 m_c + (m-m_c)\; p_a \cdot p_c]\;(-m_b^2 m_c - \frac{m_b^2}{m} p_a \cdot P)$$
$$- 2\; m_a^2\; p_b \cdot P\; p_b \cdot p_c + 2\frac{m_c^2}{m} p_a \cdot p_b\; p_b \cdot P\; (m-m_c)\Big)$$

$$D = \frac{4}{9} m(m-m_c)\, D_o + \frac{4}{9} (m-m_c)\, D_1$$
$$+ \frac{4}{9} D_2 + \frac{4m}{9} D_3 .$$

$$D_o = -m_a^{\,2}\, m_b^{\,2}\, p_b\cdot p_c + 2m_b^{\,2}\, p_a\cdot p_b\, p_a\cdot p_c$$
$$+ 2\,\frac{m_b^{\,2}}{m^2}\, p_a\cdot P\, p_b\cdot P\, p_a\cdot p_c + \frac{m_a^{\,2}}{m^2}\,(p_b\cdot P)^2\, p_b\cdot p_c$$
$$- \frac{2}{m^2}\, p_a\cdot p_b\, p_a\cdot p_c\,(p_b\cdot P)^2 - \frac{2}{m}\, m_b m_c\, p_a\cdot p_b\, p_a\cdot P$$
$$- \frac{m_b^{\,2}}{m^2}\,(p_a\cdot P)^2\, p_b\cdot p_c$$

$$D_1 = m_a^{\,2} m_b^{\,2} m_c\, p_b\cdot p_c - 2m_b^{\,2} m_c\, p_a\cdot p_b\, p_a\cdot p_c$$
$$+ 2\, m_a^{\,2} m_b^{\,2} m_c\, p_b\cdot P - 2\,\frac{m_b^{\,2}}{m}\, p_a\cdot p_b\, p_a\cdot p_c\, p_a\cdot P$$
$$+ \frac{2}{m}\, m_a^{\,2} m_b^{\,2}\, p_a\cdot p_c\, p_b\cdot P - 2\,\frac{m_a^{\,2}}{m}\, m_b^{\,2} m_c^{\,2}\, p_b\cdot P$$
$$- 4\,\frac{m_b^{\,2}}{m}\, p_a\cdot p_c\, p_a\cdot P\, p_b\cdot P - 2\,\frac{m_a^{\,2}}{m}\,(p_b\cdot P)^2\, p_b\cdot p_c$$
$$+ \frac{4}{m}\,(p_b\cdot P)^2\, p_a\cdot p_b\, p_a\cdot p_c - 2\,\frac{m_a^{\,2}}{m^2}\, m_b^{\,2} m_c\, p_a\cdot P\, p_b\cdot P$$
$$+ \frac{2}{m^2}\, m_b^{\,2}\, p_a\cdot p_c\, p_a\cdot P\, p_b\cdot P m_c + \frac{m_a^{\,2}}{m^2}\, m_c\, p_b\cdot p_c\,(p_b\cdot P)^2$$
$$- 2\,\frac{m_c}{m^2}\,(p_b\cdot P)^2\, p_a\cdot p_b\, p_a\cdot p_c + 2\,\frac{m_b^{\,2}}{m}\, m_c^{\,2}\, p_a\cdot p_b\, p_a\cdot P$$
$$+ 2\,\frac{m_b^{\,2}}{m}\,(p_a\cdot P)^2\, p_b\cdot p_c + 2\,\frac{m_b^{\,2}}{m^2}\, m_c (p_a\cdot P)^2\, p_a\cdot p_b$$
$$- \frac{m_b^{\,2}}{m^2}\, m_c\,(p_a\cdot P)^2\, p_b\cdot p_c$$

$$D_2 = m_a^4 m_b^2\, p_b\cdot p_c - 2m_a^2 m_b^2 m_c^2\, p_a\cdot p_b$$

$$- 2m_a^2 m_b^2\, p_a\cdot P\, p_b\cdot p_c + 2m_a^2 m_b^2\, p_b\cdot P\, p_a\cdot p_c$$

$$- 2\,\frac{m_a^2}{m}\, m_b^2\, p_a\cdot p_b\, p_a\cdot P\, m_c + 2\,\frac{m_a^4}{m}\, m_b^2 m_c\, p_b\cdot P$$

$$- 2\,\frac{m_a^2}{m}\, m_b^2 m_c\, p_b\cdot P\, p_a\cdot p_c - 4\,\frac{m_a^2}{m}\, m_b^2 m_c\, p_a\cdot P\, p_b\cdot P$$

$$+ \frac{4}{m}\, m_a^2 m_c\, p_a\cdot p_b\, (p_b\cdot P)^2 - \frac{2}{m^2}\, m_a^2 m_b^2\, p_a\cdot P\, p_b\cdot P\, p_a\cdot p_c$$

$$+ \frac{m_a^4}{m^2}\, (p_b\cdot P)^2\, p_b\cdot p_c - 2\,\frac{m_a^2}{m^2}\, m_c^2\, p_a\cdot p_b\, (p_b\cdot P)^2$$

$$+ 2\,\frac{m_b^2}{m}\, m_c\, p_a\cdot p_b\, p_a\cdot p_c\, p_a\cdot P - \frac{m_a^2}{m^2}\, m_b^2\, (p_a\cdot P)^2\, p_b\cdot p_c$$

$$+ 2\,\frac{m_b^2}{m^2}\, (p_a\cdot P)^2\, p_a\cdot p_b\, p_a\cdot p_c + 2\,\frac{m_a^2}{m^2}\, m_b^2 m_c^2\, p_a\cdot P\, p_b\cdot P$$

$$D_3 = 2\, m_a^2 m_b^2 m_c\, p_a\cdot p_b + 2\,\frac{m_a^2}{m}\, m_b^2\, p_a\cdot P\, p_b\cdot p_c$$

$$+ 2\,\frac{m_a^2}{m^2}\, m_b^2 m_c\, p_a\cdot P\, p_b\cdot P - 2\,\frac{m_a^2}{m^2}\, (p_b\cdot P)^2\, p_a\cdot p_b\, m_c$$

$$- 2\,\frac{m_b^2}{m}\, p_a\cdot p_b\, p_a\cdot p_c\, p_a\cdot P$$

$$E = 8\Big(E_1(p_a\cdot p_c + (m-m_c)m_c)$$

$$+ E_2(-\, m_a^2\, p_b\cdot p_c + 2\, p_a\cdot p_b\, p_a\cdot p_c)$$

$$+ E_3(m_a^2 m_c + (m-m_c)p_a\cdot p_c) + E_4\Big)$$

$$E_1 = -\, C\, m_b^2\, p_a\cdot P + C m_a^2 m_b^2 + \frac{2}{3}\, m_a^2 m_b^2\, p_b\cdot P$$

$$- \frac{m_a^2 m_b^2}{3m}\, m_c\, p_b\cdot P - \frac{2}{3}\, m_b^2\, p_a\cdot P\, p_a\cdot p_b$$

$$E_2 = C\, p_b\cdot P + \frac{1}{3}(m-m_c)m^2{}_b m - \frac{1}{3} m_b{}^2 m_c (m-m_c)$$

$$+ \frac{1}{3m}(m-m_c)(p_b\cdot P)^2 + \frac{1}{3m} m_b{}^2 m_c\, p_a\cdot P$$

$$E_3 = Cmm_b{}^2 - Cm_b{}^2 m_c - \frac{2}{3m} m_b{}^2\, p_a\cdot P\, p_b\cdot P$$

$$+ \frac{1}{3m} m_a{}^2 m_b{}^2\, p_b\cdot P$$

$$E_4 = \frac{2}{3} m_a{}^2 m_b{}^2 m_c m\, p_a\cdot p_b + \frac{1}{3} m_a{}^4 m_b{}^2\, p_b\cdot p_c$$

$$- \frac{2}{3} m_a m_b{}^2 m_c{}^2\, p_a\cdot p_b + (m-m_c)\frac{m_b{}^2}{3m}(p_a\cdot P)^2\, p_b\cdot p_c$$

$$+ \frac{m_a{}^2 m_b{}^2}{3m} m_c\, p_a\cdot P\, p_b\cdot p_c + (m-m_c)\, Cm_c\, p_b\cdot P\, p_a\cdot p_b$$

$$+ \frac{2m_a{}^2}{3m}(p_b\cdot P)^2\, p_a\cdot p_b\, m_c + \frac{2(m-m_c)}{3m} m_b{}^2 m_c{}^2\, p_a\cdot P\, p_a\cdot p_b$$

$$+ \frac{2}{3m} m_b{}^2 m_c\, (p_a\cdot P)^2\, p_a\cdot p_b - \frac{2}{3} m_a{}^2 m_b{}^2\, p_a\cdot P\, p_b\cdot p_c$$

$$- \frac{2}{3m} p_a\cdot P\, m_a{}^2 m_b{}^2 m_c\, p_a\cdot p_b$$

$$F = 4\Big([- m_a{}^2\, p_b\cdot p_c + 2\, p_a\cdot p_b\, p_a\cdot p_c]\, ((p_b\cdot P)^2 + m_b{}^2 m^2)$$

$$+ 2\, m_a{}^2 m_b{}^2 m_c m\, p_b\cdot P - 2\, m_a{}^2 m_b{}^2 m_c{}^2\, p_b\cdot P$$

$$- m_b{}^2\, (p_a\cdot p_c)^2\, p_b\cdot p_c - 2\, m_b{}^2 m_c m\, p_a\cdot p_b\, p_a\cdot p_c$$

$$+ 2\, m_b{}^2\, (p_a\cdot p_c)^2\, p_a\cdot p_b + 2\, m_a{}^2 m_b{}^2 m_c m\, p_b\cdot p_c$$

$$- m_a{}^2 m_b{}^2 m_c{}^2\, p_b\cdot p_c \Big)$$

APPENDIX 2.3

1. Kinematics

For the evaluation of Mueller amplitudes we work in the centre-of-mass frame. The beam direction is taken along the z-axis and the reaction plane is the x-z plane. The situation is shown in the figure. We have

$$p_a = (E_a, 0, 0, k)$$

$$p_b = (E_b, 0, 0, -k)$$

$$p_c = (E_c, q\sin\theta, 0, q\cos\theta)$$

where k and q are the initial and final state 3-momenta.

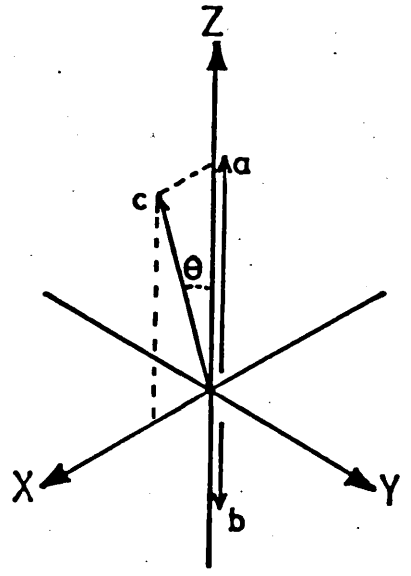

Figure Kinematics for a + b → c + X in centre-of-mass frame.

2. Wave functions

For produced proton,

$$u(p_c, +\tfrac{1}{2}) = \frac{1}{\sqrt{E_c+m_c}} \begin{pmatrix} (E_c+m_c)\cos\frac{\theta}{2} \\ (E_c+m_c)\sin\frac{\theta}{2} \\ q\cos\frac{\theta}{2} \\ q\sin\frac{\theta}{2} \end{pmatrix}$$

$$u(p_c, -\tfrac{1}{2}) = \frac{1}{\sqrt{E_c+m_c}} \begin{pmatrix} -(E_c+m_c)\sin\frac{\theta}{2} \\ (E_c+m_c)\cos\frac{\theta}{2} \\ q\sin\frac{\theta}{2} \\ -q\cos\frac{\theta}{2} \end{pmatrix}$$

3. Pole-only amplitude (c.f. eqn. (2.10))

Define

$$H_{\lambda_c}^{\lambda'_c}(\tau,\tau') = N\left(C' f(\tau) f^*(\tau') + S\, g(\tau) g^*(\tau')\right)$$

with

$$N = g^2 \frac{6m^2}{M^4} (E_aE_b + k^2)^2 \sigma(\bar{\Delta}p),$$

$$C' = 2(E_bE_c - kq)\left[(m-m_c)^2 - m_a{}^2\right]$$

$$+ 4(E_aE_b+k^2)(E_aE_c + kq) + 4(m-m_c)m_c(E_aE_b+k^2)$$

and

$$S = 2(E_bE_c+kq)\ [(m-m_c)^2 - m_a{}^2]$$

$$+ 4(E_aE_b+k^2)(E_aE_c-kq) + 4(m-m_c)m_c(E_aE_b+k^2).$$

We also make the following definitions, where A_j and B_j are associated with the exponential approximation to the gamma function (see equation (2.20)),

$$M_o = \frac{\alpha'}{2}\left(\frac{s}{M^2}\right)^{\alpha_o+\alpha' u_{min}-1.5},$$

$$\phi_j = -\frac{q}{k}\ \left(B_j + \alpha' \ln\left(\frac{s}{M^2}\right)\right),$$

$$\xi_o = -\ i\ \exp(-i\pi\alpha_o - i\pi\alpha' u_{min}),$$

$$\beta_o = i\ \pi\alpha'\ \frac{q}{k},$$

$$a_j = A_j\ \exp(B_j\ u_{min})$$

and

$$\psi_j = \phi_j + \beta_o.$$

Then we have

$$f(\tau) = M_o \sum_j a_j \left(\exp(\phi_j\tau^2) + \xi_o\exp(\psi_j\tau^2)\right)\sqrt{1 - \frac{\tau^2}{4k^2}}$$

and

$$g(\tau) = M_o \sum_j a_j \left(\exp(\phi_j\tau^2) + \xi_o\exp(\psi_j\tau^2)\right)\ \frac{\tau}{2k}\ .$$

4. Absorbed amplitude (c.f. eqn. (2.19))

$$H_{\mathrm{abs}}^{\lambda_c'}{}_{\lambda_c}(\tau,\tau')$$

$$= N\Big(C'(f(\tau) - f_{\mathrm{abs}}(\tau))(f(\tau') - f_{\mathrm{abs}}(\tau'))^*$$

$$+ S(g(\tau) - g_{\mathrm{abs}}(\tau))(g(\tau') - g_{\mathrm{abs}}(\tau'))^*\Big)$$

where

$$f_{\mathrm{abs}}(\tau) = \frac{C}{2\lambda}\exp(-\frac{\tau^2}{4\lambda})\, M_o \sum_j a_j \Big(F(\phi_j,\tau) + \xi_o F(\psi_j,\tau)\Big)$$

and

$$g_{\mathrm{abs}}(\tau) = \frac{C}{2\lambda}\exp(-\frac{\tau^2}{4\lambda})\, M_o \sum_j a_j \Big(G(\phi_j,\tau) + \xi_o G(\psi_j,\tau)\Big).$$

The functions $F(\alpha_j,\tau)$ and $G(\alpha_j,\tau)$ represent the following integrals:

$$F(\alpha_j,\tau) = \int_o^\infty d\tau_1\, \tau_1\sqrt{1 - \frac{\tau_1^2}{4k^2}}\, \exp(\alpha_j\tau_1^2 - \frac{\tau_1^2}{4\lambda})\quad I_{\frac{1}{2}}(\frac{\tau\tau_1}{2\lambda})$$

$$G(\alpha_j,\tau) = \int_o^\infty d\tau_1\, \frac{\tau_1^2}{2k}\exp(\alpha_j\tau_1^2 - \frac{\tau_1^2}{4\lambda})\, I_{\frac{1}{2}}(\frac{\tau\tau_1}{2\lambda}) .$$

Using the integrals and other mathematical relations given in the following section, we obtain

$$F(\alpha_j,\tau) = \frac{1}{4}(\frac{\tau}{\lambda})^{\frac{1}{2}}\ \frac{\Gamma(1.25)}{\Gamma(1.5)}\,(-E_j)^{-1.25}$$

$$\times \sum_{n=0}^{\infty} B(n)\,(\frac{1}{4k^2E_j})^n\ \Phi(n+\frac{5}{4},\ \frac{3}{2};\ z)$$

where

$$B(n) = \binom{\frac{1}{2}}{n} (n-1 + \tfrac{5}{4})(n-2 + \tfrac{5}{4})\ldots(\tfrac{5}{4}), \quad B(o) = 1,$$

$$E_j = \alpha_j - \frac{1}{4\lambda}$$

and

$$z = - \frac{\tau^2}{16\lambda^2 E_j} \quad .$$

Similarly,

$$G(\alpha_j,\tau) = \frac{1}{8k} \left(\frac{\tau}{\lambda}\right)^{\frac{1}{2}} \frac{\Gamma(1.75)}{\Gamma(1.5)} (- E_j)^{1.75} \quad \Phi(\tfrac{7}{4}, \tfrac{3}{2}; z) \ .$$

Φ in the above equations is the degenerate hypergeometric function (see below).

5. The Degenerate Hypergeometric function $\Phi(\alpha,\gamma;z)$

is given by the following series:

$$\Phi(\alpha,\gamma;z) = 1 + \frac{\alpha}{\gamma}\frac{z}{1!} + \frac{\alpha}{\gamma}\frac{(\alpha+1)}{(\gamma+1)}\frac{z^2}{2!} + \frac{\alpha}{\gamma}\frac{(\alpha+1)}{(\gamma+1)}\frac{(\alpha+2)}{(\gamma+2)}\frac{z^3}{3!} + \ldots.$$

and obeys the functional relations,

$$\Phi(\alpha,\gamma;z) = e^z \ \Phi(\gamma-\alpha, \gamma; - z)$$

and

$$\alpha\Phi(\alpha+1, \gamma; z) = (z + 2\alpha - \gamma)\Phi(\alpha, \gamma; z) + (\gamma - \alpha)\Phi(\alpha - 1, \gamma; z)$$

6. Bessel functions

J_ν is a Bessel function of the first kind.

Fourier-Bessel transform:- $(\nu > - 1)$

$$F(b) = \int_o^\infty J_\nu(bt)Q(t)t \, dt$$

with inverse transform

$$Q(t) = \int_0^\infty J_\nu(bt)\, F(b)\, bdb.$$

Orthogonality conditions:-

$$\int_0^\infty J_\nu(bt)\, J_\nu(b't)\, tdt = \frac{1}{b}\, \delta(b'-b)$$

and

$$\int_0^\infty J_\nu(bt)\, J_\nu(bt')bdb = \frac{1}{t}\, \delta(t'-t)\ .$$

Useful integrals:-

$$\int_0^\infty db\, b\, J_\nu(b\tau)J_\nu(b\tau')\, \exp(-\lambda b^2)$$

$$= \frac{1}{2\lambda}\, \exp\left(-\frac{\tau^2+\tau'^2}{4\lambda}\right)\, I_\nu\left(\frac{\tau\tau'}{2\lambda}\right)$$

where I_ν is the Bessel function of imaginary argument which is related to J_ν through

$$I_\nu(z) = e^{-i\frac{1}{2}\pi\nu}\, J_\nu(iz)$$

for $-\pi < \arg z \leq \frac{\pi}{2}$.

$$\int_0^\infty dx\, x^\mu\, e^{-\alpha x^2}\, J_\nu(\beta x)$$

$$= \frac{\beta^\nu\, \Gamma\left(\frac{\mu+\nu+1}{2}\right)}{2^{\nu+1}\alpha^{\frac{1}{2}(\mu+\nu+1)}\Gamma(\nu+1)}\, \Phi\left(\frac{\nu+\mu+1}{2},\ \nu+1;\ \frac{-\beta^2}{4\alpha}\right)$$

for $\mathrm{Re}\ \alpha > 0$ and $\mathrm{Re}(\mu+\nu) > -1$.

7. Gamma functions

Γ is the Euler gamma function and obeys the relation

$$\Gamma(1 + x) = x\Gamma(x).$$

8. Binomial coefficient

$$\binom{p}{n} = \frac{p(p-1)\ldots(p-n+1)}{1.2\ldots n}, \quad \binom{p}{0} = 1 .$$

CHAPTER III

The data with which we compare our model for the process $\pi^- + p \to p + X$ comes from experiments in the Omega spectrometer at CERN. A fast forward proton is detected in the laboratory with a negative pion beam at 12 GeV/c incident on a target proton. A total of 300,000 events were recorded over a range of $0.8\ \mathrm{GeV}^2 < M^2 < 8.0\ \mathrm{GeV}^2$ and $-u < 1.8\ \mathrm{GeV}^2$. The first reports [37] concluded that a triple-Regge model did not account for the experimental distributions. The simple triple-Regge model used (fig. 3.1) is given by [38]

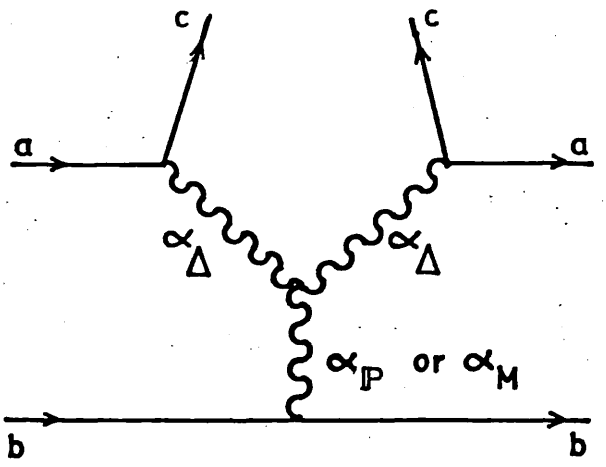

Figure 3.1 Triple-Regge model with Pomeron or meson exchange at lower vertex.

$$f(ab\to c) = f(M^2,u,s)$$

$$= G(u)\left(\frac{M^2}{s}\right)^{\alpha_E(0)-2\alpha_{eff}(u)} s^{\alpha_E(0)-1} \qquad (3.1)$$

where α_E is introduced as a simplification to account for the sum over Pomeron and meson "third leg" exchanges and α_{eff} is the effective baryon trajectory. The main conclusion reached was that the slope of the baryon Δ_δ trajectory obtained (~ 0.5) was too low compared with the spectroscopic value (~ 0.9), but the M^2-dependence was also found to be stronger than that predicted by the model.

The experimental group have communicated their numerical results to us [39]; the bin sizes are $0.05\ \mathrm{GeV}^2$ in u and $0.2\ \mathrm{GeV}^2$ in M^2. The errors on the data are surprisingly small; we shall show statistical errors on our plots and there is an additional 9% systematic error. The normalization is obtained from the calculated luminosity and we understand that there may be some uncertainty [39]. It is also important to note that there is some evidence [38] that the data is contaminated by $N\bar{N}$ pairs and $N^*\Delta$ resonances produced with the forward proton.

Since our model is valid in the region of small u and finite M^2, we consider that a reduced set of data should be used for comparison. We make the additional restrictions $0.0\ \mathrm{GeV}^2 < -u \leq 1.025\ \mathrm{GeV}^2$ and $M^2 \geq 4.2\ \mathrm{GeV}^2$. The previous attempts to compare the data with triple-Regge models (see equation (3.1))

allowed the full range in M^2 and u and this may account for the difficulties encountered. The assumption in the triple-Regge limit is $M^2 \to \infty$ and this cannot be presumed to refer to $M^2 \sim 0.8\ \mathrm{GeV}^2$.

There is some ambiguity concerning the normalization of our model. The $\pi - p - \Delta$ coupling constant which appears at the particle-particle-Reggeon vertex has traditionally been a problem. A parameter-free model for $d\sigma/du$ in $\pi^- + p \to p + \pi^-$ [11] extrapolates to too low a value for the Δ width. But this has been mitigated, it has been shown that the extrapolation of an asymptotic cross section cannot uniquely determine the coupling constant [40]. Also, as we described in Chapter II, we cannot expect $\sigma(\bar{\Delta}p)$, which arises in equation (2.9) and is taken as a constant, to correspond to the full asymptotic $\bar{\Delta}p$ total cross section. We can to some extent justify taking this parameter as a constant since, although we might have expected resonance effects in this M^2 range, the data is overall fairly smooth. With these points in mind, we introduce a normalization constant N and absorb $\sigma(\bar{\Delta}p)$ into the overall normalization $N' = N\sigma(\bar{\Delta}p)$.

The differential cross sections are calculated by incorporating new subroutines into an existing computer program [41] designed to facilitate the visual display of results and accordingly the graphs are computer plotted [42]. A minimization is carried out over 277 data points for the chisquare function of the absorbed prediction [43]. The free parameters are the overall normalization N' and the trajectory

parameters α_o and α'. All other parameters are fixed. The minimum occurs with $N' = 0.46$, $\alpha_o = 0.0085$ and $\alpha' = 0.97$. The solid lines in fig. 3.1 and fig. 3.2 show the absorbed calculation for these minimized parameters for fixed u and fixed M^2/s respectively. The dashed lines correspond to a pole-only model which is calculated with the same normalization but with conventional trajectory parameters ($\alpha_o = 0.05$, $\alpha' = 0.9$).

Both predictions show qualitatively good fits to the data, although the absorbed model shows more structure and seems to indicate that more M^2-dependence is needed in that model. The value obtained for the overall normalization is reasonable, although lower than naive estimates would predict. If we take a reduction ~ 0.25 for the coupling constant (in analogy with two-body results, although essentially this is unknown as we have discussed) and $\sigma(\bar{\Delta}p) \sim 20$ mb from the typical values obtained by R. Tegen when [36] considering the process $\gamma_V + p \to p + X$, then we expect $N' \sim 5$, a factor of 10 larger than the result obtained. Undoubtedly, we could have increased the value of N' by allowing the absorption parameters C and λ to vary. The trajectory parameter values obtained after chisquare minimization correspond very closely to the values expected from hadron spectroscopy.

We are satisfied that the nature of this fit allows us to conclude that the model with Δ_δ exchange is acceptable, contrary to the previous results.

There is no data for the other observables, the polarization of the produced proton and the target asymmetry. Traditionally, of course, polarization measurements provide stringent tests of cut models [44]. For our model for this process, which has $t_o \equiv 0$ and is factorizable and has essentially only one flip amplitude (see fig. 2.5), identically zero polarization is predicted.

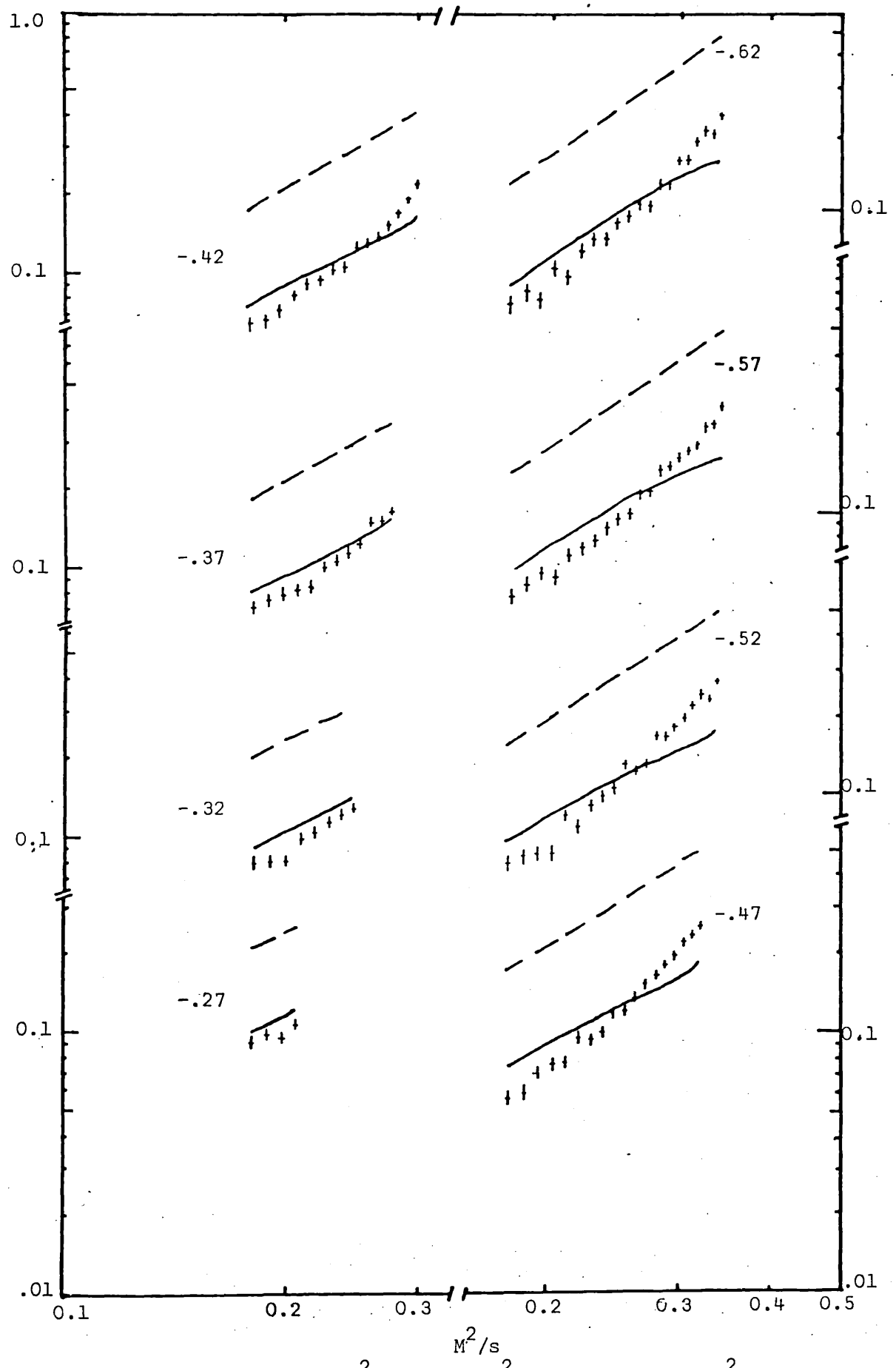

Figure 3.1 $(s/\pi)(d\sigma/dudM^2)$ in mb/GeV^2 plotted against M^2/s for fixed values of u.

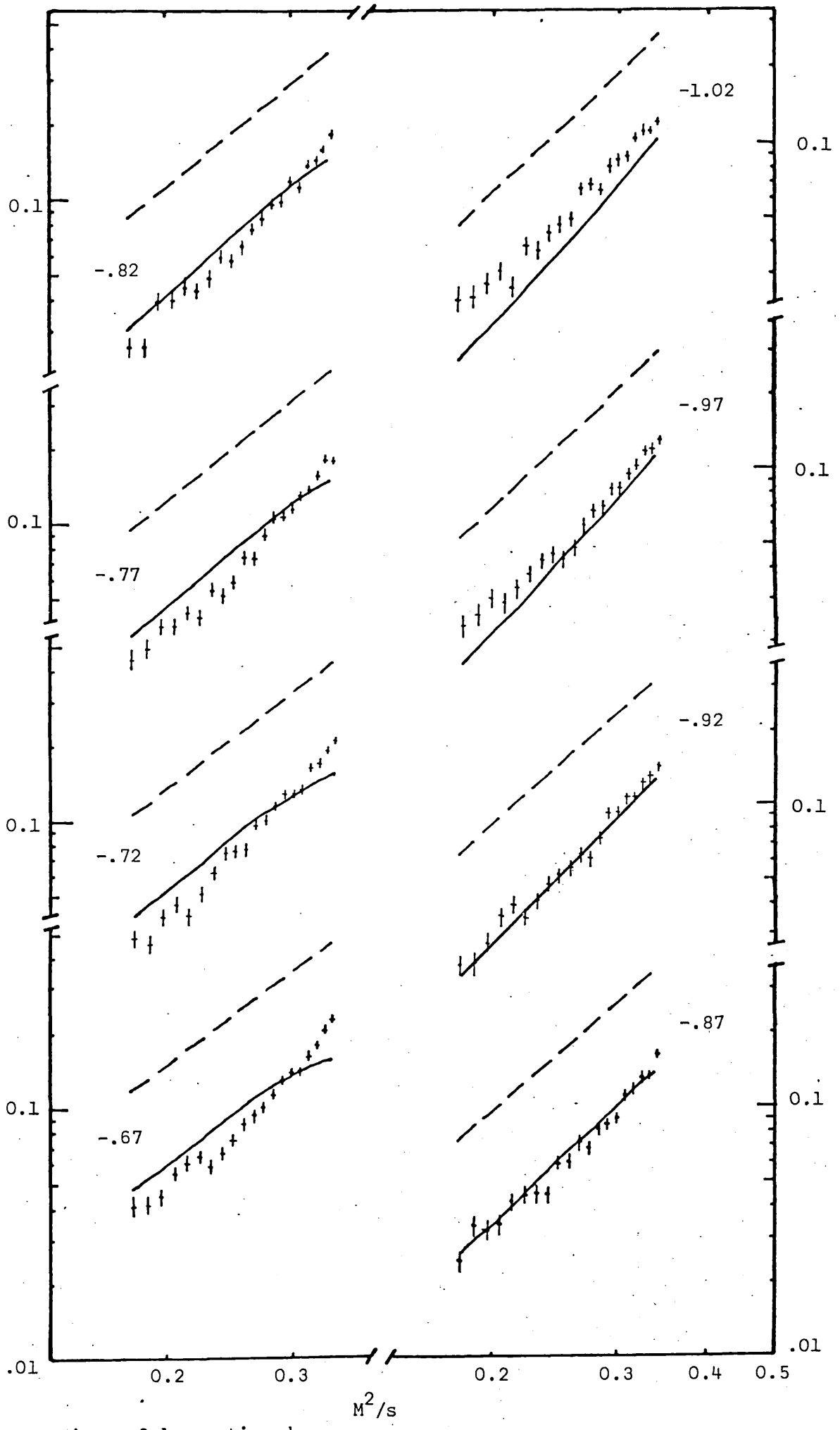

Figure 3.1 continued.

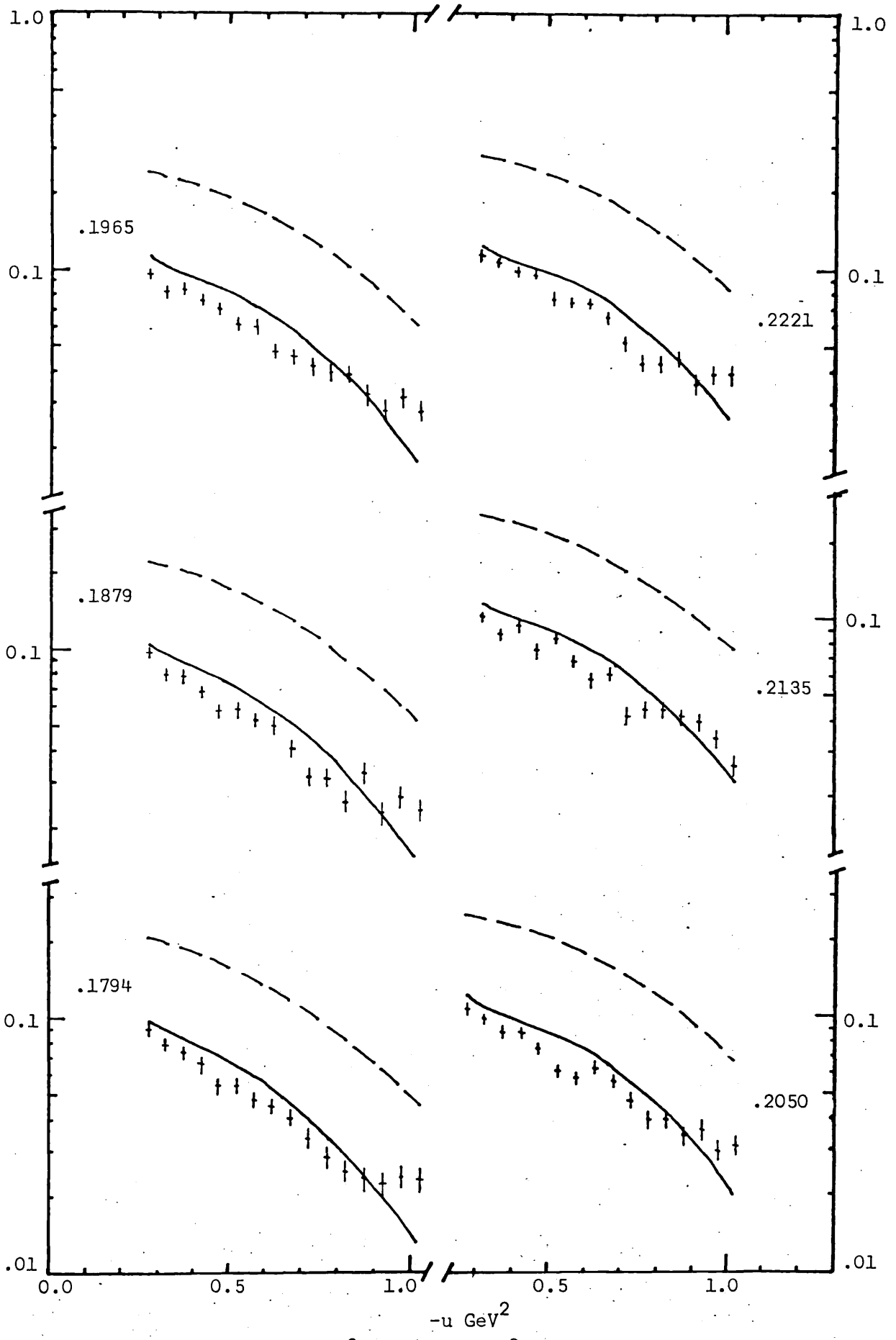

Figure 3.2 $(s/\pi)(d\sigma/dudM^2)$ in mb/GeV^2 plotted against -u for fixed values of M^2/s.

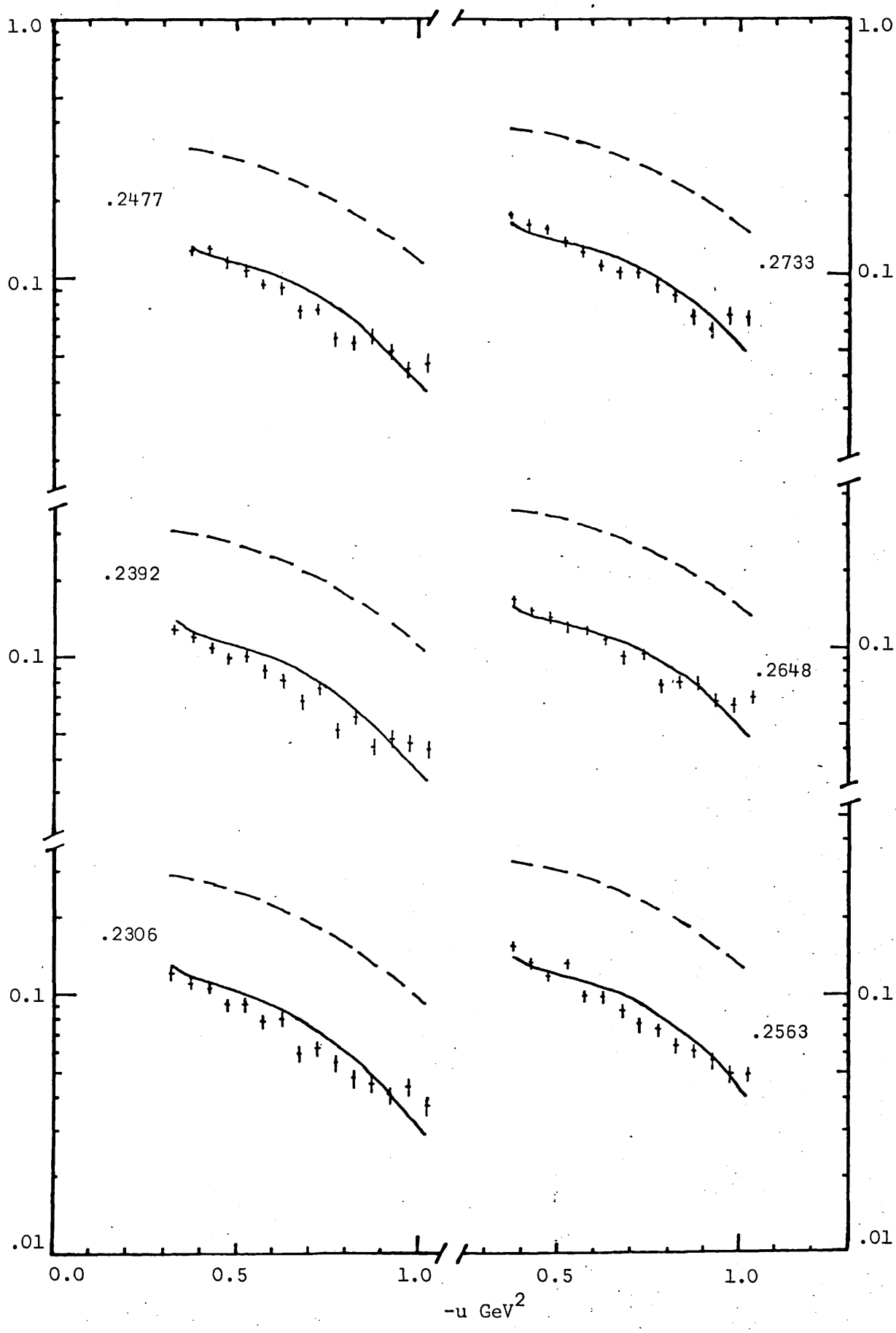

Figure 3.2 continued.

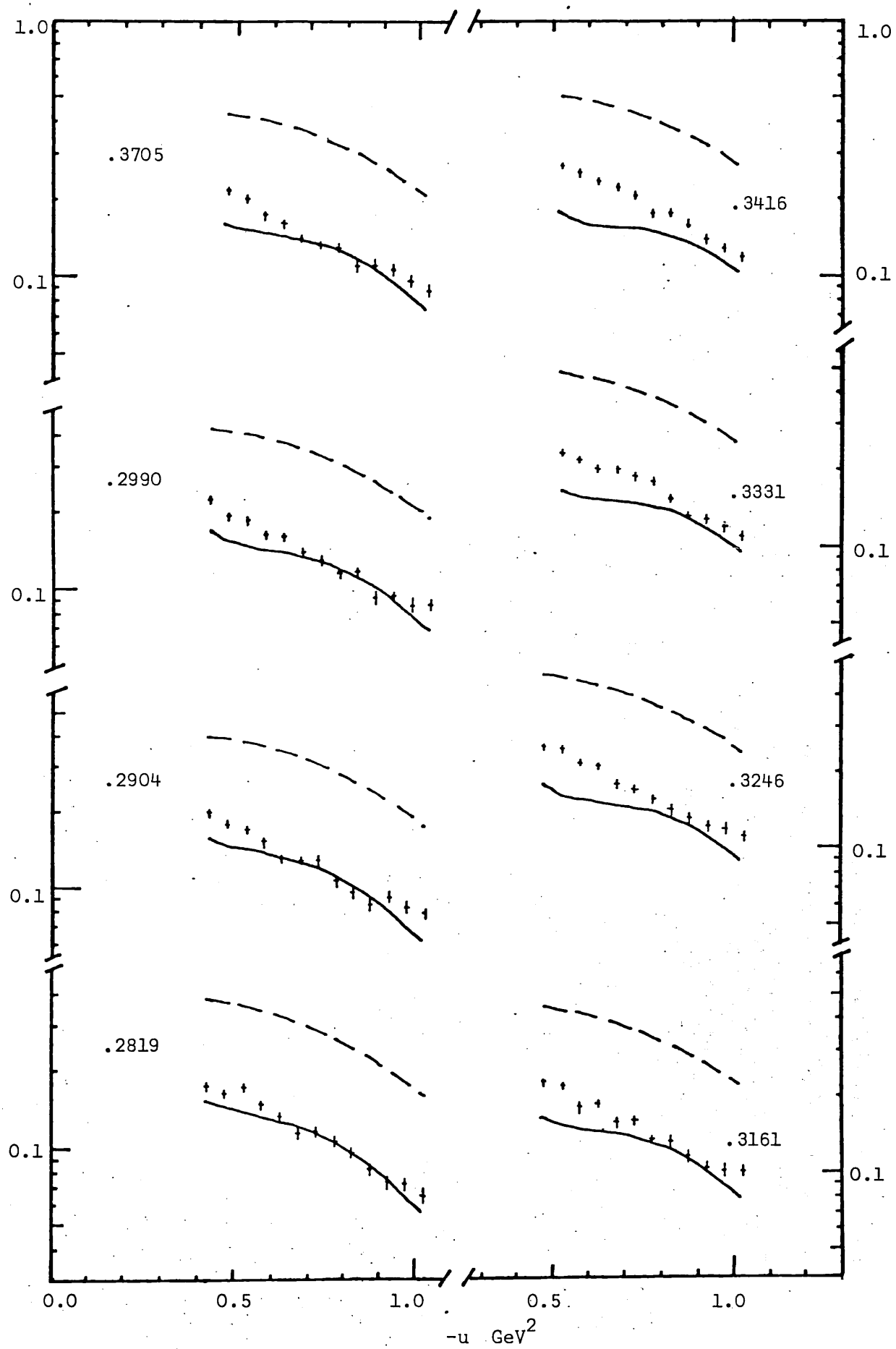

Figure 3.2 continued.

0024: UTS.OYOSHIDA 06/06/78 18:42

0024: UTS.OYOSHIDA 06/06/78 18:42

0024: UTS.OYOSHIDA 06/06/78 18:42

0024: UTS.OYOSHIDA 06/06/78 18:42

0024: UTS.OYOSHIDA 06/06/78 18:42

0024: UTS.OYOSHIDA 06/06/78 18:42

0024: UTS.OYOSHIDA 06/06/78 18:42

0024: UTS.OYOSHIDA 06/06/78 18:42

0024: UTS.OYOSHIDA 06/06/78 18:42

0024: UTS.OYOSHIDA 06/06/78 18:42

0024: UTS.OYOSHIDA 06/06/78 18:42

0024: UTS.OYOSHIDA 06/06/78 18:42

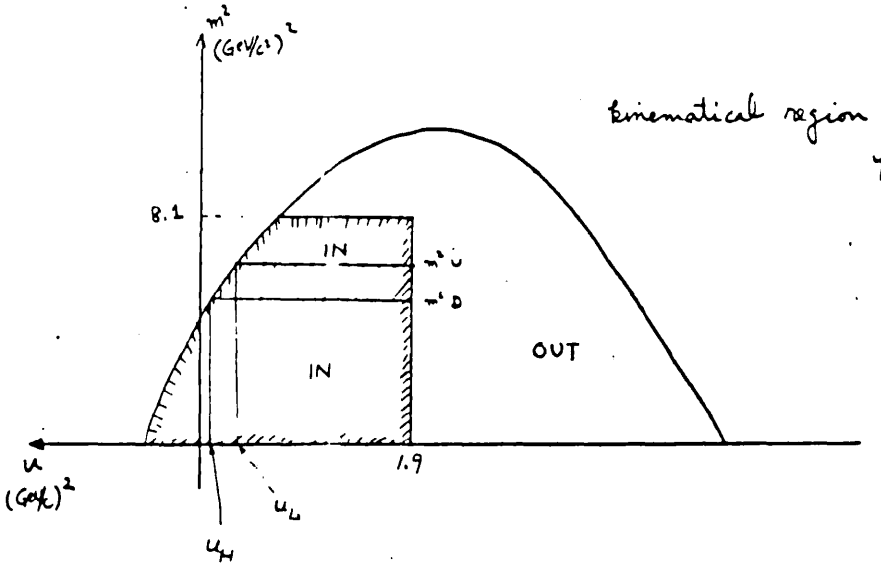

Kinematical region explored in the present experiment

DR K.J.M.MORIARTY
ROYAL HOLLOWAY COLLEGE
UNIVERSITY OF LONDON
DEPARTMENT OF MATHEMATICS
EGHAM HILL EGHAM
SURREY TW20 0EX

HAJIME YOSHIDA
Faculty [redacted] OF ENGINEERING
FUKUI UNIVERSITY
BUNKYO 3-9-1,FUKUI-SHI
FUKUI,JAPAN , 910

6 JUNE 1978,FUKUI

DEAR DR K.J.M.MORIARTY,

THE TABLE OF INVARIANT DIFFERENTIAL CROSS SECTIONS FOR THE REACTION PI- + P = FAST PROTON + ANYTHING AT 12 GEV/C HAS BEEN JUST OBTAINED, AS IS SEEN IN THE FOLLOWING PAGES,AS FOR THESE DATA , I SHOULD ADD SOME COMMENTS :

1) THE TABLE IS GIVEN IN FUNCTION OF U FOR FIXED VALUE OF MISSING MASS SQUARED.
THE CENTRE VALUE OF MOMENTUM TRANSFER FROM PI MINUS TO THE FAST PROTON IS USED .

2) THE LEFT HALF OF THE TABLE CONTAINS THE DCS DATA WITH ERROR , THE RIGHT HALF THE U VALUE CORRESPONDING TO THEM

3) THE VALUES OF CROSS SECTION ARE NOT UNFOLDED AS FUNCTION OF U AND M**2 ,BECAUSE
THE EXPERIMENTAL RESOLUTIONS IN M**2 AND U ARE GOOD ENOUGH NOT TO GIVE SEIZABLE
EFFECTS TO THE NUMERICAL ANALYSIS(TRIPLE REGGE ETC).
BUT CARE SHOULD BE TAKEN NEAR THE KINEMATICAL BOUNDARY WHERE U DEPENDENCE IS IMPORTANT.
IT IS , THEREFORE,ADVISED TO DISCARD TWO DATA POINTS NEAREST TO THE BOUNDARY WHICH
ARE INDICATED IN THE BRAKETS.THE EXPERIMENTAL RESOLUTION IN U IS LESS THAN .05 GEV**2

4) ERRORS IN THE TABLE ARE ONLY STATISTICAL ONESISYSTEMATICAL ERROR OF ABOUT 9 % MUST
BE TAKEN INTO ACCOUNT IN THE ANALYSYS COMPARING WITH ANOTHER EXPERIMENTAL DATA.

5) THE ABOVE DATA CORRESPOND TO THE FIGURE 15 OF MY THESE D'ETAT , AND THE FIGURES 14 AND 20A
CAN BE OBTAINED FROM THIS TABLE .

I WISH YOUR SUCCESS IN THE WORK , AND I WOULD LIKE TO KNOW THE RESULTS WHEN COMPLETED.

YOURS SINCERELY
HAJIME YOSHIDA

PI- + P = FAST PROTON + X AT 12 GEV/C
INVARIANT CROSS SECTIONS F(S,M**2,U) IN UNIT OF MICROBARN/GEV**2 $\frac{s}{\pi}\frac{d^2\sigma}{dm^2\,du}$ ($\mu b/GeV^2$)
ARE TABULATED IN FUNCTION OF U AT FIXED M**2 VALUES
U STEP IS 0.05 GEV**2 , M**2 STEP IS 0.2 GEV**2

OUT OF K.B. = NO DATA BECAUSE (M**2 , U) IS OUT OF KINEMATICAL BOUNDARY

!! NOTICE , TWO DATA POINTS NEAREST TO THE KINEMATICAL BOUNDARY SHOULD NOT BE USED,
TAKING INTO ACCOUNT THE EXPERIMENTAL RESOLUTION OF U (LESS THAN .05GEV**2)

------MASS**2 FROM .1 (m^2_D) GEV**2 TO .3 (m^2_U) GEV**2 CORRESPONDING TO MAXIMAL U = .029 (U_H) AND .021 (U_L) | CENTRE VALUE OF U

OUT OF K.B.	(13.630 +-1.790)	(27.967 +-2.564)	20.964 +-2.220	18.299 +-2.074	.075 .025 -.025 -.075 -.125
17.453 +-2.025	11.980 +-1.678	10.250 +-1.550	10.117 +-1.542	8.310 +-1.397	-.175 -.225 -.275 -.325 -.375
3.459 +-.902	4.963 +-1.080	5.842 +-1.172	2.966 +-.835	4.077 +-.979	-.425 -.475 -.525 -.575 -.625
2.780 +-.808	1.231 +-.538	1.448 +-.583	1.887 +-.666	.731 +-.414	-.675 -.725 -.775 -.825 -.875
.940 +-.470	.956 +-.474	2.115 +-.705	.705 +-.407	.707 +-.408	-.925 -.975-1.025-1.075-1.125
.733 +-.415	.470 +-.332	1.880 +-.665	.235 +-.235	.256 +-.245	-1.175-1.225-1.275-1.325-1.375
.235 +-.235	.000 +-.000	.268 +-.251	.296 +-.264	.000 +-.000	-1.425-1.475-1.525-1.575-1.625
.557 +-.362	1.452 +-.584	.000 +-.000	.000 +-.000	1.358 +-.565	-1.675-1.725-1.775-1.825-1.875

------MASS**2 FROM .3 GEV**2 TO .5 GEV**2 CORRESPONDING TO MAXIMAL U = .021 AND .014 | CENTRE VALUE OF U

OUT OF K.B.	(17.625 +-2.035)	(37.367 +-2.963)	26.125 +-2.478	22.236 +-2.286	.075 .025 -.025 -.075 -.125
18.478 +-2.084	17.757 +-2.043	13.625 +-1.789	7.440 +-1.322	8.636 +-1.425	-.175 -.225 -.275 -.325 -.375
7.457 +-1.324	6.564 +-1.242	6.239 +-1.211	3.619 +-.922	3.906 +-.958	-.425 -.475 -.525 -.575 -.625
2.115 +-.705	1.469 +-.588	1.887 +-.666	1.410 +-.576	2.359 +-.745	-.675 -.725 -.775 -.825 -.875
1.283 +-.549	2.249 +-.727	1.410 +-.576	1.730 +-.638	1.410 +-.576	-.925 -.975-1.025-1.075-1.125
1.222 +-.536	1.187 +-.528	.489 +-.339	.242 +-.238	.726 +-.413	-1.175-1.225-1.275-1.325-1.375
1.008 +-.487	.000 +-.000	.000 +-.000	1.018 +-.489	.968 +-.477	-1.425-1.475-1.525-1.575-1.625
.000 +-.000	.498 +-.342	1.126 +-.514	.545 +-.358	.472 +-.333	-1.675-1.725-1.775-1.825-1.875

------MASS**2 FROM .5 GEV**2 TO .7 GEV**2 CORRESPONDING TO MAXIMAL U = .014 AND .006 | CENTRE VALUE OF U

OUT OF K.B.	(10.575 +-1.576)	(39.952 +-3.064)	34.893 +-2.864	30.541 +-2.679	.075 .025 -.025 -.075 -.125
23.239 +-2.337	18.006 +-2.057	14.852 +-1.868	9.033 +-1.457	11.447 +-1.640	-.175 -.225 -.275 -.325 -.375
7.727 +-1.348	4.973 +-1.081	4.559 +-1.035	5.809 +-1.168	4.787 +-1.061	-.425 -.475 -.525 -.575 -.625
3.595 +-.919	4.004 +-.970	3.661 +-.928	2.150 +-.711	2.155 +-.712	-.675 -.725 -.775 -.825 -.875
2.895 +-.825	1.882 +-.665	1.730 +-.638	1.814 +-.653	.000 +-.000	-.925 -.975-1.025-1.075-1.125
1.175 +-.525	.940 +-.470	.705 +-.407	.714 +-.410	.980 +-.480	-1.175-1.225-1.275-1.325-1.375
1.292 +-.551	.759 +-.422	1.445 +-.583	.254 +-.244	.815 +-.438	-1.425-1.475-1.525-1.575-1.625
.275 +-.254	.966 +-.476	.823 +-.440	.000 +-.000	.627 +-.384	-1.675-1.725-1.775-1.825-1.875

------MASS**2 FROM .7 GEV**2 TO .9 GEV**2 CORRESPONDING TO MAXIMAL U = .006 AND -.002 | CENTRE VALUE OF U

OUT OF K.B.	(1.645 +-.622)	(49.117 +-3.397)	33.184 +-2.793	26.680 +-2.504	.075 .025 -.025 -.075 -.125
24.536 +-2.401	21.888 +-2.268	15.874 +-1.931	11.172 +-1.620	8.507 +-1.414	-.175 -.225 -.275 -.325 -.375
9.475 +-1.492	6.317 +-1.218	6.695 +-1.254	4.352 +-1.011	4.275 +-1.002	-.425 -.475 -.525 -.575 -.625
4.322 +-1.008	2.355 +-.744	3.154 +-.861	3.525 +-.910	1.422 +-.578	-.675 -.725 -.775 -.825 -.875
2.139 +-.709	2.115 +-.705	1.650 +-.623	2.115 +-.705	1.880 +-.665	-.925 -.975-1.025-1.075-1.125
1.880 +-.665	.470 +-.332	.785 +-.429	1.758 +-.643	.484 +-.337	-1.175-1.225-1.275-1.325-1.375
1.079 +-.503	.573 +-.367	.902 +-.461	.801 +-.434	.385 +-.301	-1.425-1.475-1.525-1.575-1.625
.555 +-.361	.425 +-.316	.912 +-.463	.000 +-.000	.522 +-.350	-1.675-1.725-1.775-1.825-1.875

------MASS**2 FROM.9 GEV**2 TO 1.1 GEV**2 CORRESPONDING TO MAXIMAL U = -.002 AND-.010 I CENTRE VALUE OF U

OUT OF K.B.	OUT OF K.B.	(40.890 +-3.100)	(37.633 +-2.974)	33.187 +-2.793	I	.075 .025 -.025 -.075 -.125
29.178 +-2.619	23.244 +-2.337	19.533 +-2.142	15.461 +-1.906	14.187 +-1.826	I	-.175 -.225 -.275 -.325 -.375
11.614 +-1.652	7.771 +-1.351	9.311 +-1.479	8.185 +-1.387	6.260 +-1.213	I	-.425 -.475 -.525 -.575 -.625
3.344 +-.886	5.464 +-1.133	4.162 +-.989	3.861 +-.953	2.686 +-.794	I	-.675 -.725 -.775 -.825 -.875
2.512 +-.768	2.691 +-.795	3.668 +-.928	1.483 +-.590	2.141 +-.709	I	-.925 -.975-1.025-1.075-1.125
.940 +-.470	2.115 +-.705	.705 +-.407	2.651 +-.789	1.201 +-.531	I	-1.175-1.225-1.275-1.325-1.375
.508 +-.345	.505 +-.345	.564 +-.364	1.332 +-.560	.268 +-.251	I	-1.425-1.475-1.525-1.575-1.625
.392 +-.304	.374 +-.296	.555 +-.361	.000 +-.000	.000 +-.000	I	-1.675-1.725-1.775-1.825-1.875

------MASS**2 FROM1.1 GEV**2 TO 1.3 GEV**2 CORRESPONDING TO MAXIMAL U = -.010 AND-.018 I CENTRE VALUE OF U

OUT OF K.B.	OUT OF K.B.	(35.722 +-2.897)	(48.535 +-3.377)	35.184 +-2.875	I	.075 .025 -.025 -.075 -.125
37.036 +-2.950	25.655 +-2.455	24.210 +-2.385	17.249 +-2.013	17.547 +-2.031	I	-.175 -.225 -.275 -.325 -.375
14.149 +-1.823	8.676 +-1.428	8.646 +-1.425	9.337 +-1.481	6.166 +-1.204	I	-.425 -.475 -.525 -.575 -.625
9.567 +-1.499	7.729 +-1.348	4.559 +-1.035	5.041 +-1.088	4.028 +-.973	I	-.675 -.725 -.775 -.825 -.875
3.619 +-.922	3.109 +-.855	4.056 +-.976	2.115 +-.705	4.108 +-.983	I	-.925 -.975-1.025-1.075-1.125
.989 +-.482	3.135 +-.858	1.410 +-.576	1.683 +-.629	1.462 +-.586	I	-1.175-1.225-1.275-1.325-1.375
1.732 +-.638	2.131 +-.708	.839 +-.444	1.819 +-.654	1.088 +-.506	I	-1.425-1.475-1.525-1.575-1.625
1.208 +-.533	.334 +-.280	1.356 +-.564	.985 +-.481	.689 +-.402	I	-1.675-1.725-1.775-1.825-1.875

------MASS**2 FROM1.3 GEV**2 TO 1.5 GEV**2 CORRESPONDING TO MAXIMAL U = -.018 AND-.027 I CENTRE VALUE OF U

OUT OF K.B.	OUT OF K.B.	(29.845 +-2.648)	(48.979 +-3.393)	37.732 +-2.978	I	.075 .025 -.025 -.075 -.125
41.823 +-3.135	32.402 +-2.759	33.344 +-2.799	23.484 +-2.349	21.298 +-2.237	I	-.175 -.225 -.275 -.325 -.375
17.237 +-2.013	13.830 +-1.803	16.079 +-1.944	12.352 +-1.704	10.490 +-1.570	I	-.425 -.475 -.525 -.575 -.625
11.040 +-1.611	7.586 +-1.335	6.378 +-1.224	7.966 +-1.368	5.962 +-1.184	I	-.675 -.725 -.775 -.825 -.875
5.309 +-1.117	3.814 +-.947	4.315 +-1.007	3.368 +-.890	3.302 +-.881	I	-.925 -.975-1.025-1.075-1.125
4.472 +-1.025	3.424 +-.897	1.410 +-.576	2.860 +-.820	2.538 +-.772	I	-1.175-1.225-1.275-1.325-1.375
2.211 +-.721	3.111 +-.855	1.328 +-.559	1.485 +-.591	1.948 +-.677	I	-1.425-1.475-1.525-1.575-1.625
1.391 +-.572	1.250 +-.542	1.046 +-.496	1.292 +-.551	.000 +-.000	I	-1.675-1.725-1.775-1.825-1.875

------MASS**2 FROM1.5 GEV**2 TO 1.7 GEV**2 CORRESPONDING TO MAXIMAL U = -.027 AND-.035 I CENTRE VALUE OF U

OUT OF K.B.	OUT OF K.B.	(19.505 +-2.141)	(42.831 +-3.173)	40.674 +-3.092	I	.075 .025 -.025 -.075 -.125
42.140 +-3.147	31.058 +-2.702	31.182 +-2.707	27.765 +-2.554	27.408 +-2.538	I	-.175 -.225 -.275 -.325 -.375
21.599 +-2.253	9.228 +-1.473	14.058 +-1.818	13.336 +-1.770	12.890 +-1.740	I	-.425 -.475 -.525 -.575 -.625
6.841 +-1.268	11.167 +-1.620	8.103 +-1.380	7.746 +-1.349	4.954 +-1.079	I	-.675 -.725 -.775 -.825 -.875
5.983 +-1.186	4.470 +-1.025	6.716 +-1.256	3.889 +-.956	2.825 +-.815	I	-.925 -.975-1.025-1.075-1.125
4.148 +-.987	1.180 +-.527	4.073 +-.978	2.169 +-.714	3.544 +-.913	I	-1.175-1.225-1.275-1.325-1.375
1.854 +-.660	2.348 +-.743	1.741 +-.640	.956 +-.474	1.476 +-.589	I	-1.425-1.475-1.525-1.575-1.625
2.637 +-.787	.616 +-.380	1.614 +-.616	1.027 +-.491	1.342 +-.562	I	-1.675-1.725-1.775-1.825-1.875

------MASS**2 FROM1.7 GEV**2 TO 1.9 GEV**2 CORRESPONDING TO MAXIMAL U = -.035 AND-.044 I CENTRE VALUE OF U

OUT OF K.B.	OUT OF K.B.	(11.750 +-1.662)	(54.814 +-3.589)	41.144 +-3.109	I	.075 .025 -.025 -.075 -.125
44.377 +-3.229	34.037 +-2.828	36.824 +-2.942	32.938 +-2.782	24.814 +-2.415	I	-.175 -.225 -.275 -.325 -.375
27.866 +-2.559	20.913 +-2.217	12.283 +-1.699	10.810 +-1.594	13.113 +-1.755	I	-.425 -.475 -.525 -.575 -.625
10.655 +-1.582	11.844 +-1.668	7.992 +-1.370	6.599 +-1.245	7.160 +-1.297	I	-.675 -.725 -.775 -.825 -.875
5.896 +-1.177	5.299 +-1.116	3.290 +-.879	4.489 +-1.027	5.259 +-1.112	I	-.925 -.975-1.025-1.075-1.125
3.184 +-.865	4.801 +-1.062	4.021 +-.972	3.118 +-.856	2.460 +-.760	I	-1.175-1.225-1.275-1.325-1.375
1.278 +-.548	1.311 +-.555	.994 +-.483	1.368 +-.567	1.208 +-.533	I	-1.425-1.475-1.525-1.575-1.625
2.254 +-.728	1.039 +-.494	1.560 +-.606	1.126 +-.514	1.391 +-.572	I	[illegible]

------MASS**2 FROM1.9 GEV**2 TO 2.1 GEV**2 CORRESPONDING TO MAXIMAL U = -.044 AND-.053 I CENTRE VALUE OF U

OUT OF K.B.	OUT OF K.B.	(2.585 +-.779)	(51.987 +-3.495)	47.338 +-3.335	I .075 .025 -.025 -.075 -.125
41.494 +-3.123	45.724 +-3.278	36.914 +-2.945	29.711 +-2.642	23.693 +-2.360	I -.175 -.225 -.275 -.325 -.375
23.333 +-2.342	18.878 +-2.106	23.009 +-2.325	13.919 +-1.809	10.923 +-1.602	I -.425 -.475 -.525 -.575 -.625
9.508 +-1.495	9.224 +-1.472	10.201 +-1.548	7.905 +-1.363	7.520 +-1.329	I -.675 -.725 -.775 -.825 -.875
7.623 +-1.338	7.318 +-1.311	5.656 +-1.153	5.950 +-1.182	3.570 +-.916	I -.925 -.975-1.025-1.075-1.125
3.772 +-.941	1.685 +-.629	2.350 +-.743	4.159 +-.989	2.289 +-.733	I-1.175-1.225-1.275-1.325-1.375
1.962 +-.479	3.029 +-.844	2.507 +-.768	2.693 +-.796	2.171 +-.714	I-1.425-1.475-1.525-1.575-1.625
1.307 +-.554	1.358 +-.565	.804 +-.435	2.077 +-.699	.512 +-.347	I-1.675-1.725-1.775-1.825-1.875

------MASS**2 FROM2.1 GEV**2 TO 2.3 GEV**2 CORRESPONDING TO MAXIMAL U = -.053 AND-.062 I CENTRE VALUE OF U

OUT OF K.B.	OUT OF K.B.	OUT OF K.B.	(51.004 +-3.462)	(50.845 +-3.457)	I .075 .025 -.025 -.075 -.125
49.108 +-3.397	38.596 +-3.012	43.017 +-3.179	26.910 +-2.515	28.933 +-2.608	I -.175 -.225 -.275 -.325 -.375
22.090 +-2.278	23.930 +-2.371	20.017 +-2.169	17.916 +-2.052	12.615 +-1.722	I -.425 -.475 -.525 -.575 -.625
12.558 +-1.718	10.932 +-1.603	10.218 +-1.550	7.271 +-1.307	11.602 +-1.651	I -.675 -.725 -.775 -.825 -.875
6.178 +-1.205	5.372 +-1.124	4.507 +-1.029	6.712 +-1.256	6.223 +-1.209	I -.925 -.975-1.025-1.075-1.125
3.760 +-.940	4.498 +-1.028	5.078 +-1.092	3.964 +-.965	3.074 +-.850	I-1.175-1.225-1.275-1.325-1.375
2.902 +-.826	3.631 +-.924	2.406 +-.752	3.753 +-.939	2.787 +-.809	I-1.425-1.475-1.525-1.575-1.625
2.014 +-.688	1.370 +-.567	1.323 +-.558	4.773 +-1.059	1.173 +-.525	I-1.675-1.725-1.775-1.825-1.875

------MASS**2 FROM2.3 GEV**2 TO 2.5 GEV**2 CORRESPONDING TO MAXIMAL U = -.062 AND-.072 I CENTRE VALUE OF U

OUT OF K.B.	OUT OF K.B.	OUT OF K.B.	(44.189 +-3.222)	(53.528 +-3.547)	I .075 .025 -.025 -.075 -.125
53.129 +-3.533	50.024 +-3.429	41.590 +-3.126	34.345 +-2.841	31.596 +-2.725	I -.175 -.225 -.275 -.325 -.375
25.845 +-2.464	24.167 +-2.383	17.153 +-2.008	21.387 +-2.242	15.310 +-1.897	I -.425 -.475 -.525 -.575 -.625
14.269 +-1.831	12.739 +-1.730	13.031 +-1.750	10.803 +-1.593	8.023 +-1.373	I -.675 -.725 -.775 -.825 -.875
8.420 +-1.407	10.025 +-1.535	6.897 +-1.273	7.593 +-1.336	6.305 +-1.217	I -.925 -.975-1.025-1.075-1.125
5.887 +-1.176	6.639 +-1.249	5.675 +-1.155	4.810 +-1.063	4.141 +-.986	I-1.175-1.225-1.275-1.325-1.375
2.808 +-.812	4.301 +-1.005	1.676 +-.627	2.498 +-.766	4.087 +-.980	I-1.425-1.475-1.525-1.575-1.625
1.614 +-.616	1.424 +-.579	1.361 +-.565	3.321 +-.883	2.221 +-.722	I-1.675-1.725-1.775-1.825-1.875

------MASS**2 FROM2.5 GEV**2 TO 2.7 GEV**2 CORRESPONDING TO MAXIMAL U = -.072 AND-.081 I CENTRE VALUE OF U

OUT OF K.B.	OUT OF K.B.	OUT OF K.B.	(33.154 +-2.791)	(59.095 +-3.727)	I .075 .025 -.025 -.075 -.125
64.916 +-3.906	50.541 +-3.446	49.021 +-3.394	44.283 +-3.226	36.211 +-2.917	I -.175 -.225 -.275 -.325 -.375
29.335 +-2.626	27.641 +-2.549	28.329 +-2.580	22.205 +-2.284	21.246 +-2.234	I -.425 -.475 -.525 -.575 -.625
15.729 +-1.923	14.030 +-1.816	13.536 +-1.784	10.230 +-1.550	9.767 +-1.515	I -.675 -.725 -.775 -.825 -.875
9.999 +-1.533	10.714 +-1.587	6.940 +-1.277	7.755 +-1.350	7.153 +-1.297	I -.925 -.975-1.025-1.075-1.125
7.673 +-1.343	5.781 +-1.166	7.410 +-1.320	5.177 +-1.103	3.854 +-.952	I-1.175-1.225-1.275-1.325-1.375
4.550 +-1.034	3.624 +-.923	4.019 +-.972	3.593 +-.919	4.667 +-1.047	I-1.425-1.475-1.525-1.575-1.625
1.591 +-.611	1.711 +-.634	4.503 +-1.029	3.492 +-.906	4.035 +-.974	I-1.675-1.725-1.775-1.825-1.875

------MASS**2 FROM2.7 GEV**2 TO 2.9 GEV**2 CORRESPONDING TO MAXIMAL U = -.081 AND-.091 I CENTRE VALUE OF U

OUT OF K.B.	OUT OF K.B.	OUT OF K.B.	(17.860 +-2.049)	(67.729 +-3.990)	I .075 .025 -.025 -.075 -.125
64.571 +-3.895	59.810 +-3.749	50.783 +-3.455	42.309 +-3.153	40.956 +-3.102	I -.175 -.225 -.275 -.325 -.375
39.781 +-3.058	35.121 +-2.873	30.947 +-2.697	26.865 +-2.513	20.736 +-2.207	I -.425 -.475 -.525 -.575 -.625
20.386 +-2.189	12.880 +-1.740	15.806 +-1.927	11.879 +-1.671	13.050 +-1.751	I -.675 -.725 -.775 -.825 -.875
11.066 +-1.615	10.918 +-1.602	9.271 +-1.476	7.560 +-1.333	9.574 +-1.500	I -.925 -.975-1.025-1.075-1.125
4.766 +-1.058	6.204 +-1.207	6.674 +-1.252	8.671 +-1.428	5.546 +-1.142	I-1.175-1.225-1.275-1.325-1.375
5.725 +-1.160	5.476 +-1.134	3.990 +-.968	3.565 +-.915	2.994 +-.839	I-1.425-1.475-1.525-1.575-1.625
5.149 +-1.100	2.087 +-.838	2.599 +-.782	2.470 +-.762	3.438 +-.899	I-1.675-1.725-1.775-1.825-1.875

------MASS**2 FROM2.9 GEV**2 TO 3.1 GEV**2 CORRESPONDING TO MAXIMAL U = -.091 AND-.101 I CENTRE VALUE OF U

OUT OF K.B.	OUT OF K.B.	OUT OF K.B.	(5.405 +-1.127)	(66.063 +-3.940)	I	.075	.025	-.025	-.075 -.125
68.575 +-4.014	57.991 +-3.692	50.377 +-3.441	47.028 +-3.324	45.343 +-3.264	I	-.175	-.225	-.275	-.325 -.375
35.234 +-2.877	35.161 +-2.875	26.069 +-2.475	28.830 +-2.603	22.121 +-2.280	I	-.425	-.475	-.525	-.575 -.625
26.445 +-2.493	19.044 +-2.116	14.927 +-1.873	15.475 +-1.907	16.622 +-1.976	I	-.675	-.725	-.775	-.825 -.875
12.518 +-1.715	9.428 +-1.488	9.776 +-1.516	10.246 +-1.552	10.688 +-1.585	I	-.925	-.975	-1.025	-1.075 -1.125
9.259 +-1.475	8.977 +-1.452	7.231 +-1.304	6.061 +-1.193	5.269 +-1.113	I	-1.175	-1.225	-1.275	-1.325 -1.375
6.994 +-1.282	6.949 +-1.241	4.959 +-1.079	3.344 +-.886	3.567 +-.916	I	-1.425	-1.475	-1.525	-1.575 -1.625
4.867 +-1.049	2.303 +-.736	2.522 +-.770	3.024 +-.843	6.227 +-1.210	I	-1.675	-1.725	-1.775	-1.825 -1.875

------MASS**2 FROM3.1 GEV**2 TO 3.3 GEV**2 CORRESPONDING TO MAXIMAL U = -.101 AND-.111 I CENTRE VALUE OF U

OUT OF K.B.	OUT OF K.B.	OUT OF K.B.	OUT OF K.B.	(67.826 +-3.992)	I	.075	.025	-.025	-.075 -.125
(63.586 +-3.966)	65.440 +-5.922	55.312 +-3.605	50.729 +-3.453	46.873 +-3.319	I	-.175	-.225	-.275	-.325 -.375
37.776 +-2.979	42.559 +-3.162	39.684 +-3.054	31.441 +-2.718	28.388 +-2.583	I	-.425	-.475	-.525	-.575 -.625
23.326 +-2.341	18.878 +-2.106	18.375 +-2.078	18.593 +-2.090	14.495 +-1.846	I	-.675	-.725	-.775	-.825 -.875
14.648 +-1.855	13.296 +-1.768	7.901 +-1.363	10.587 +-1.577	8.803 +-1.438	I	-.925	-.975	-1.025	-1.075 -1.125
10.013 +-1.534	7.388 +-1.318	6.683 +-1.253	6.982 +-1.281	7.541 +-1.331	I	-1.175	-1.225	-1.275	-1.325 -1.375
7.727 +-1.348	3.751 +-.939	4.726 +-1.054	2.778 +-.808	5.123 +-1.097	I	-1.425	-1.475	-1.525	-1.575 -1.625
5.203 +-1.106	3.055 +-.847	2.423 +-.755	2.858 +-.819	4.033 +-.973	I	-1.675	-1.725	-1.775	-1.825 -1.875

------MASS**2 FROM3.3 GEV**2 TO 3.5 GEV**2 CORRESPONDING TO MAXIMAL U = -.111 AND-.122 I CENTRE VALUE OF U

OUT OF K.B.	OUT OF K.B.	OUT OF K.B.	OUT OF K.B.	(54.781 +-3.588)	I	.075	.025	-.025	-.075 -.125
(71.127 +-4.088)	63.382 +-3.859	60.719 +-3.777	57.368 +-3.672	52.492 +-3.512	I	-.175	-.225	-.275	-.325 -.375
48.335 +-3.370	41.125 +-3.109	38.004 +-2.988	34.218 +-2.836	28.094 +-2.569	I	-.425	-.475	-.525	-.575 -.625
23.977 +-2.374	26.285 +-2.485	24.104 +-2.380	21.267 +-2.236	19.216 +-2.125	I	-.675	-.725	-.775	-.825 -.875
17.190 +-2.010	16.208 +-1.952	15.917 +-1.934	14.542 +-1.849	10.321 +-1.557	I	-.925	-.975	-1.025	-1.075 -1.125
10.279 +-1.554	8.037 +-1.374	6.782 +-1.262	7.818 +-1.355	12.251 +-1.697	I	-1.175	-1.225	-1.275	-1.325 -1.375
6.519 +-1.238	7.043 +-1.287	3.981 +-.967	5.135 +-1.098	5.231 +-1.109	I	-1.425	-1.475	-1.525	-1.575 -1.625
6.848 +-1.269	8.380 +-1.403	4.225 +-.996	5.257 +-1.111	1.671 +-.627	I	-1.675	-1.725	-1.775	-1.825 -1.875

------MASS**2 FROM3.5 GEV**2 TO 3.7 GEV**2 CORRESPONDING TO MAXIMAL U = -.122 AND-.132 I CENTRE VALUE OF U

OUT OF K.B.	OUT OF K.B.	OUT OF K.B.	OUT OF K.B.	(34.853 +-2.862)	I	.075	.025	-.025	-.075 -.125
(83.310 +-4.425)	72.136 +-4.117	66.387 +-3.950	58.936 +-3.722	55.364 +-3.607	I	-.175	-.225	-.275	-.325 -.375
48.485 +-3.376	47.548 +-3.343	39.736 +-3.056	38.232 +-2.997	27.634 +-2.548	I	-.425	-.475	-.525	-.575 -.625
23.244 +-2.337	22.781 +-2.314	17.787 +-2.044	24.233 +-2.386	20.494 +-2.195	I	-.675	-.725	-.775	-.825 -.875
18.746 +-2.099	15.327 +-1.898	15.686 +-1.920	14.937 +-1.874	11.332 +-1.632	I	-.925	-.975	-1.025	-1.075 -1.125
15.693 +-1.920	8.707 +-1.430	11.562 +-1.648	10.986 +-1.607	8.540 +-1.417	I	-1.175	-1.225	-1.275	-1.325 -1.375
8.667 +-1.427	5.906 +-1.178	6.836 +-1.267	3.619 +-.922	5.125 +-1.097	I	-1.425	-1.475	-1.525	-1.575 -1.625
5.950 +-1.182	4.049 +-.975	3.466 +-.903	4.881 +-1.071	4.519 +-1.031	I	-1.675	-1.725	-1.775	-1.825 -1.875

------MASS**2 FROM3.7 GEV**2 TO 3.9 GEV**2 CORRESPONDING TO MAXIMAL U = -.132 AND-.143 I CENTRE VALUE OF U

OUT OF K.B.	OUT OF K.B.	OUT OF K.B.	OUT OF K.B.	(23.058 +-2.328)	I	.075	.025	-.025	-.075 -.125
(81.094 +-4.365)	70.298 +-4.079	73.778 +-4.164	61.746 +-3.809	62.249 +-3.825	I	-.175	-.225	-.275	-.325 -.375
57.533 +-3.677	49.808 +-3.421	45.233 +-3.260	47.143 +-3.328	43.844 +-3.210	I	-.425	-.475	-.525	-.575 -.625
32.348 +-2.757	29.457 +-2.631	28.729 +-2.598	24.858 +-2.417	23.009 +-2.325	I	-.675	-.725	-.775	-.825 -.875
19.272 +-2.128	15.743 +-1.923	13.950 +-1.811	17.186 +-2.010	15.729 +-1.923	I	-.925	-.975	-1.025	-1.075 -1.125
14.072 +-1.818	13.162 +-1.759	13.411 +-1.775	10.591 +-1.578	10.183 +-1.547	I	-1.175	-1.225	-1.275	-1.325 -1.375
11.346 +-1.633	5.995 +-1.187	8.359 +-1.402	10.481 +-1.569	8.042 +-1.375	I	-1.425	-1.475	-1.525	-1.575 -1.625
7.292 +-1.309	4.129 +-.985	6.047 +-1.192	7.045 +-1.287	4.258 +-1.000	I	-1.675	-1.725	-1.775	-1.825 -1.875

------MASS**2 FROM3.9 GEV**2 TO 4.1 GEV**2 CORRESPONDING TO MAXIMAL U = -.143 AND-.154 I CENTRE VALUE OF U

OUT OF K.B.	OUT OF K.B.	OUT OF K.B.	OUT OF K.B.	(4.935 +-1.077)	I .075 .025 -.025 -.075 -.125
(96.804 +-4.770)	87.921 +-4.545	71.539 +-4.100	73.116 +-4.145	62.623 +-3.836	I -.175 -.225 -.275 -.325 -.375
60.755 +-3.779	54.755 +-3.587	49.717 +-3.418	46.243 +-3.297	39.807 +-3.059	I -.425 -.475 -.525 -.575 -.625
38.521 +-3.009	27.782 +-2.555	24.186 +-2.384	26.877 +-2.513	26.348 +-2.488	I -.675 -.725 -.775 -.825 -.875
18.657 +-2.094	21.390 +-2.242	20.060 +-2.171	17.895 +-2.051	17.087 +-2.004	I -.925 -.975-1.025-1.075-1.125
14.779 +-1.864	12.671 +-1.726	10.927 +-1.602	9.405 +-1.487	9.391 +-1.486	I-1.175-1.225-1.275-1.325-1.375
9.713 +-1.511	7.713 +-1.346	9.898 +-1.525	9.438 +-1.489	7.043 +-1.287	I-1.425-1.475-1.525-1.575-1.625
6.648 +-1.250	7.459 +-1.324	7.360 +-1.315	2.778 +-.808	4.947 +-1.078	I-1.675-1.725-1.775-1.825-1.875

------MASS**2 FROM4.1 GEV**2 TO 4.3 GEV**2 CORRESPONDING TO MAXIMAL U = -.154 AND-.166 I CENTRE VALUE OF U

OUT OF K.B.	OUT OF K.B.	OUT OF K.B.	OUT OF K.B.	OUT OF K.B.	I .075 .025 -.025 -.075 -.125
(81.505 +-4.376)	(104.681 +-4.960)	90.717 +-4.617	79.569 +-4.324	73.994 +-4.170	I -.175 -.225 -.275 -.325 -.375
66.764 +-3.961	55.056 +-3.597	55.317 +-3.605	48.250 +-3.367	45.484 +-3.269	I -.425 -.475 -.525 -.575 -.625
40.921 +-3.101	34.033 +-2.828	28.583 +-2.592	25.223 +-2.435	23.726 +-2.361	I -.675 -.725 -.775 -.825 -.875
22.661 +-2.308	24.024 +-2.376	23.542 +-2.352	21.054 +-2.224	17.183 +-2.009	I -.925 -.975-1.025-1.075-1.125
19.430 +-2.137	15.202 +-1.890	13.564 +-1.785	14.109 +-1.821	12.361 +-1.704	I-1.175-1.225-1.275-1.325-1.375
8.664 +-1.477	12.048 +-1.683	7.196 +-1.300	10.284 +-1.555	6.829 +-1.267	I-1.425-1.475-1.525-1.575-1.625
7.945 +-1.366	6.850 +-1.269	4.681 +-1.049	6.481 +-1.234	3.513 +-.909	I-1.675-1.725-1.775-1.825-1.875

------MASS**2 FROM4.3 GEV**2 TO 4.5 GEV**2 CORRESPONDING TO MAXIMAL U = -.166 AND-.178 I CENTRE VALUE OF U

OUT OF K.B.	OUT OF K.B.	OUT OF K.B.	OUT OF K.B.	OUT OF K.B.	I .075 .025 -.025 -.075 -.125
(53.721 +-3.553)	(93.741 +-4.694)	97.234 +-4.780	80.572 +-4.351	78.925 +-4.307	I -.175 -.225 -.275 -.325 -.375
68.477 +-4.011	57.883 +-3.688	58.630 +-3.712	53.538 +-3.547	50.957 +-3.460	I -.425 -.475 -.525 -.575 -.625
41.416 +-3.120	32.171 +-2.750	31.704 +-2.730	25.465 +-2.446	33.314 +-2.798	I -.675 -.725 -.775 -.825 -.875
23.089 +-2.329	26.658 +-2.503	24.196 +-2.385	22.569 +-2.303	18.690 +-2.096	I -.925 -.975-1.025-1.075-1.125
15.750 +-1.924	17.150 +-2.008	14.138 +-1.823	15.559 +-1.912	10.450 +-1.567	I-1.175-1.225-1.275-1.325-1.375
11.327 +-1.632	10.913 +-1.601	13.745 +-1.797	8.072 +-1.377	8.859 +-1.443	I-1.425-1.475-1.525-1.575-1.625
7.116 +-1.293	6.970 +-1.280	5.769 +-1.164	7.116 +-1.293	7.012 +-1.284	I-1.675-1.725-1.775-1.825-1.875

------MASS**2 FROM4.5 GEV**2 TO 4.7 GEV**2 CORRESPONDING TO MAXIMAL U = -.178 AND-.190 I CENTRE VALUE OF U

OUT OF K.B.	OUT OF K.B.	OUT OF K.B.	OUT OF K.B.	OUT OF K.B.	I .075 .025 -.025 -.075 -.125
(34.912 +-2.864)	(114.856 +-5.195)	94.348 +-4.709	81.007 +-4.363	82.802 +-4.411	I -.175 -.225 -.275 -.325 -.375
74.873 +-4.195	69.170 +-4.032	60.421 +-3.768	58.990 +-3.723	47.190 +-3.330	I -.425 -.475 -.525 -.575 -.625
44.911 +-3.249	41.456 +-3.121	39.104 +-3.031	38.719 +-3.016	32.301 +-2.755	I -.675 -.725 -.775 -.825 -.875
27.829 +-2.557	31.032 +-2.700	27.424 +-2.539	21.267 +-2.236	21.933 +-2.270	I -.925 -.975-1.025-1.075-1.125
19.207 +-2.125	22.346 +-2.292	19.427 +-2.137	16.389 +-1.962	15.263 +-1.894	I-1.175-1.225-1.275-1.325-1.375
14.885 +-1.870	13.611 +-1.788	12.979 +-1.746	9.026 +-1.456	11.259 +-1.627	I-1.425-1.475-1.525-1.575-1.625
8.622 +-1.423	9.153 +-1.467	8.892 +-1.446	7.496 +-1.327	6.752 +-1.260	I-1.675-1.725-1.775-1.825-1.875

------MASS**2 FROM4.7 GEV**2 TO 4.9 GEV**2 CORRESPONDING TO MAXIMAL U = -.190 AND-.202 I CENTRE VALUE OF U

OUT OF K.B.	OUT OF K.B.	OUT OF K.B.	OUT OF K.B.	OUT OF K.B.	I .075 .025 -.025 -.075 -.125
(10.772 +-1.591)	(116.059 +-5.222)	106.810 +-5.010	97.450 +-4.785	86.393 +-4.506	I -.175 -.225 -.275 -.325 -.375
85.799 +-4.490	74.432 +-4.182	60.212 +-3.762	56.764 +-3.652	62.461 +-3.831	I -.425 -.475 -.525 -.575 -.625
55.589 +-3.614	46.457 +-3.304	39.254 +-3.037	39.391 +-3.043	33.833 +-2.820	I -.675 -.725 -.775 -.825 -.875
35.812 +-2.901	29.525 +-2.634	30.797 +-2.690	24.012 +-2.375	27.394 +-2.537	I -.925 -.975-1.025-1.075-1.125
21.425 +-2.244	24.896 +-2.419	18.769 +-2.100	15.054 +-1.881	17.084 +-2.004	I-1.175-1.225-1.275-1.325-1.375
17.717 +-2.040	14.507 +-1.846	17.296 +-2.016	14.196 +-1.827	10.260 +-1.553	I-1.425-1.475-1.525-1.575-1.625
15.435 +-1.905	12.401 +-1.707	8.850 +-1.442	9.454 +-1.491	4.926 +-1.076	I-1.675-1.725-1.775-1.825-1.875

------MASS**2 FROM4.9 GEV**2 TO 5.1 GEV**2 CORRESPONDING TO MAXIMAL U = -.202 AND-.215 I CENTRE VALUE OF U

					I .075 .025 -.025 -.075 -.125
OUT OF K.B.	OUT OF K.B.	OUT OF K.B.	OUT OF K.B.	OUT OF K.B.	
OUT OF K.B.	(96.919 +-4.772)	(110.513 +-5.096)	103.052 +-4.921	88.179 +-4.552	I -.175 -.225 -.275 -.325 -.375
94.414 +-4.710	75.795 +-4.220	84.520 +-4.457	69.076 +-4.029	57.895 +-3.689	I -.425 -.475 -.525 -.575 -.625
60.898 +-3.783	41.809 +-3.134	44.305 +-3.227	44.025 +-3.216	41.680 +-3.130	I -.675 -.725 -.775 -.825 -.875
39.666 +-3.053	33.882 +-2.822	26.522 +-2.497	29.539 +-2.635	26.273 +-2.485	I -.925 -.975-1.025-1.075-1.125
28.426 +-2.585	20.236 +-2.181	23.834 +-2.367	20.680 +-2.204	20.259 +-2.182	I-1.175-1.225-1.275-1.325-1.375
17.505 +-2.028	17.416 +-2.023	15.663 +-1.919	16.438 +-1.965	9.901 +-1.525	I-1.425-1.475-1.525-1.575-1.625
13.346 +-1.771	12.037 +-1.682	9.125 +-1.464	10.620 +-1.580	8.932 +-1.449	I-1.675-1.725-1.775-1.825-1.875

------MASS**2 FROM5.1 GEV**2 TO 5.3 GEV**2 CORRESPONDING TO MAXIMAL U = -.215 AND-.228 I CENTRE VALUE OF U

					I .075 .025 -.025 -.075 -.125
OUT OF K.B.	OUT OF K.B.	OUT OF K.B.	OUT OF K.B.	OUT OF K.B.	
OUT OF K.B.	(74.716 +-4.190)	(120.875 +-5.330)	112.708 +-5.146	105.405 +-4.977	I -.175 -.225 -.275 -.325 -.375
97.292 +-4.782	94.390 +-4.710	76.575 +-4.242	73.346 +-4.152	72.810 +-4.136	I -.425 -.475 -.525 -.575 -.625
64.813 +-3.903	51.289 +-3.472	42.427 +-3.158	42.685 +-3.167	44.431 +-3.231	I -.675 -.725 -.775 -.825 -.875
35.323 +-2.881	38.667 +-3.014	38.841 +-3.021	35.332 +-2.882	31.744 +-2.731	I -.925 -.975-1.025-1.075-1.125
31.518 +-2.722	30.024 +-2.656	26.017 +-2.473	22.579 +-2.303	24.501 +-2.400	I-1.175-1.225-1.275-1.325-1.375
16.344 +-1.960	17.197 +-2.010	17.806 +-2.046	14.121 +-1.822	14.746 +-1.862	I-1.425-1.475-1.525-1.575-1.625
14.438 +-1.842	11.640 +-1.654	14.286 +-1.832	13.755 +-1.798	8.563 +-1.419	I-1.675-1.725-1.775-1.825-1.875

------MASS**2 FROM5.3 GEV**2 TO 5.5 GEV**2 CORRESPONDING TO MAXIMAL U = -.228 AND-.241 I CENTRE VALUE OF U

					I .075 .025 -.025 -.075 -.125
OUT OF K.B.	OUT OF K.B.	OUT OF K.B.	OUT OF K.B.	OUT OF K.B.	
OUT OF K.B.	(49.254 +-3.402)	(123.706 +-5.392)	120.595 +-5.324	110.951 +-5.106	I -.175 -.225 -.275 -.325 -.375
106.142 +-4.994	92.327 +-4.658	92.010 +-4.650	78.913 +-4.306	80.737 +-4.356	I -.425 -.475 -.525 -.575 -.625
59.255 +-3.732	62.472 +-3.832	54.372 +-3.575	47.583 +-3.344	45.021 +-3.253	I -.675 -.725 -.775 -.825 -.875
41.097 +-3.108	43.769 +-3.207	37.121 +-2.954	38.874 +-3.022	34.909 +-2.864	I -.925 -.975-1.025-1.075-1.125
32.743 +-2.774	35.849 +-2.903	27.963 +-2.563	25.622 +-2.454	24.362 +-2.393	I-1.175-1.225-1.275-1.325-1.375
26.915 +-2.515	19.594 +-2.146	20.151 +-2.176	19.681 +-2.151	22.600 +-2.305	I-1.425-1.475-1.525-1.575-1.625
18.177 +-2.067	11.470 +-1.642	13.421 +-1.776	13.127 +-1.756	13.026 +-1.750	I-1.675-1.725-1.775-1.825-1.875

------MASS**2 FROM5.5 GEV**2 TO 5.7 GEV**2 CORRESPONDING TO MAXIMAL U = -.241 AND-.254 I CENTRE VALUE OF U

					I .075 .025 -.025 -.075 -.125
OUT OF K.B.	OUT OF K.B.	OUT OF K.B.	OUT OF K.B.	OUT OF K.B.	
OUT OF K.B.	(9.753 +-1.514)	(130.547 +-5.539)	127.441 +-5.473	118.870 +-5.285	I -.175 -.225 -.275 -.325 -.375
108.236 +-5.043	98.721 +-4.817	99.880 +-4.845	87.855 +-4.544	80.958 +-4.362	I -.425 -.475 -.525 -.575 -.625
66.655 +-3.958	74.751 +-4.191	51.383 +-3.475	57.984 +-3.691	44.370 +-3.229	I -.675 -.725 -.775 -.825 -.875
47.949 +-3.357	46.006 +-3.288	43.513 +-3.198	41.792 +-3.134	30.033 +-2.657	I -.925 -.975-1.025-1.075-1.125
34.874 +-2.863	31.553 +-2.723	29.116 +-2.616	26.618 +-2.501	31.180 +-2.707	I-1.175-1.225-1.275-1.325-1.375
21.846 +-2.266	23.754 +-2.363	24.503 +-2.400	21.528 +-2.249	21.319 +-2.238	I-1.425-1.475-1.525-1.575-1.625
22.889 +-2.319	15.343 +-1.899	16.020 +-1.940	12.925 +-1.743	17.322 +-2.018	I-1.675-1.725-1.775-1.825-1.875

------MASS**2 FROM5.7 GEV**2 TO 5.9 GEV**2 CORRESPONDING TO MAXIMAL U = -.254 AND-.269 I CENTRE VALUE OF U

					I .075 .025 -.025 -.075 -.125
OUT OF K.B.	OUT OF K.B.	OUT OF K.B.	OUT OF K.B.	OUT OF K.B.	
OUT OF K.B.	OUT OF K.B.	(117.512 +-5.255)	(147.636 +-5.890)	127.187 +-5.467	I -.175 -.225 -.275 -.325 -.375
129.100 +-5.508	116.236 +-5.226	107.219 +-5.020	94.989 +-4.725	92.787 +-4.670	I -.425 -.475 -.525 -.575 -.625
74.822 +-4.193	75.940 +-4.224	58.301 +-3.701	56.102 +-3.631	59.544 +-3.741	I -.675 -.725 -.775 -.825 -.875
52.161 +-3.501	44.307 +-3.227	46.678 +-3.312	39.344 +-3.041	41.861 +-3.136	I -.925 -.975-1.025-1.075-1.125
41.851 +-3.136	36.775 +-2.940	38.054 +-2.990	30.628 +-2.683	29.119 +-2.616	I-1.175-1.225-1.275-1.325-1.375
31.922 +-2.739	24.962 +-2.422	26.806 +-2.510	20.107 +-2.174	19.221 +-2.125	I-1.425-1.475-1.525-1.575-1.625
23.620 +-2.356	21.103 +-2.227	17.366 +-2.020	14.109 +-1.821	11.186 +-1.621	I-1.675-1.725-1.775-1.825-1.875

------MASS**2 FROM5.9 GEV**2 TO 6.1 GEV**2 CORRESPONDING TO MAXIMAL U = -.269 AND-.283 I CENTRE VALUE OF U

OUT OF K.B.	OUT OF K.B.	OUT OF K.B.	OUT OF K.B.	OUT OF K.B.	I	.075	.025	-.025	-.075	-.125
OUT OF K.B.	OUT OF K.B.	(81.197 +-4.368)	(166.942 +-6.263)	154.303 +-6.022	I	-.175	-.225	-.275	-.325	-.375
134.284 +-5.618	117.951 +-5.265	131.426 +-5.557	99.139 +-4.827	98.293 +-4.806	I	-.425	-.475	-.525	-.575	-.625
86.626 +-4.512	77.181 +-4.259	73.372 +-4.152	63.831 +-3.873	60.261 +-3.763	I	-.675	-.725	-.775	-.825	-.875
55.451 +-3.610	49.308 +-3.404	49.091 +-3.397	49.009 +-3.394	45.541 +-3.271	I	-.925	-.975	-1.025	-1.075	-1.125
45.362 +-3.265	42.039 +-3.143	39.856 +-3.060	35.635 +-2.894	29.516 +-2.634	I	-1.175	-1.225	-1.275	-1.325	-1.375
28.940 +-2.608	31.382 +-2.716	28.954 +-2.608	29.504 +-2.633	26.379 +-2.490	I	-1.425	-1.475	-1.525	-1.575	-1.625
25.667 +-2.456	17.028 +-2.000	18.346 +-2.076	20.252 +-2.182	20.753 +-2.208	I	-1.675	-1.725	-1.775	-1.825	-1.875

------MASS**2 FROM6.1 GEV**2 TO 6.3 GEV**2 CORRESPONDING TO MAXIMAL U = -.283 AND-.298 I CENTRE VALUE OF U

OUT OF K.B.	OUT OF K.B.	OUT OF K.B.	OUT OF K.B.	OUT OF K.B.	I	.075	.025	-.025	-.075	-.125
OUT OF K.B.	OUT OF K.B.	(30.541 +-2.679)	(167.785 +-6.279)	156.268 +-6.060	I	-.175	-.225	-.275	-.325	-.375
141.249 +-5.761	132.568 +-5.582	124.000 +-5.398	118.633 +-5.280	109.611 +-5.075	I	-.425	-.475	-.525	-.575	-.625
93.521 +-4.688	95.988 +-4.749	72.460 +-4.127	74.349 +-4.180	72.843 +-4.137	I	-.675	-.725	-.775	-.825	-.875
62.867 +-3.844	60.505 +-3.771	65.119 +-3.912	48.010 +-3.359	51.444 +-3.477	I	-.925	-.975	-1.025	-1.075	-1.125
44.356 +-3.229	43.118 +-3.183	44.051 +-3.217	34.395 +-2.843	34.806 +-2.860	I	-1.175	-1.225	-1.275	-1.325	-1.375
34.406 +-2.843	31.800 +-2.734	27.234 +-2.530	29.100 +-2.615	26.080 +-2.476	I	-1.425	-1.475	-1.525	-1.575	-1.625
21.632 +-2.255	29.502 +-2.633	19.228 +-2.126	25.805 +-2.463	19.883 +-2.162	I	-1.675	-1.725	-1.775	-1.825	-1.875

------MASS**2 FROM6.3 GEV**2 TO 6.5 GEV**2 CORRESPONDING TO MAXIMAL U = -.298 AND-.313 I CENTRE VALUE OF U

OUT OF K.B.	OUT OF K.B.	OUT OF K.B.	OUT OF K.B.	OUT OF K.B.	I	.075	.025	-.025	-.075	-.125
OUT OF K.B.	OUT OF K.B.	(.503 +-.344)	(161.071 +-6.152)	168.429 +-6.291	I	-.175	-.225	-.275	-.325	-.375
155.286 +-6.041	148.257 +-5.903	133.786 +-5.607	120.771 +-5.327	107.693 +-5.031	I	-.425	-.475	-.525	-.575	-.625
100.796 +-4.867	100.831 +-4.868	90.400 +-4.609	82.509 +-4.403	68.674 +-4.017	I	-.675	-.725	-.775	-.825	-.875
60.611 +-3.774	68.890 +-4.024	67.551 +-3.984	62.035 +-3.818	48.330 +-3.370	I	-.925	-.975	-1.025	-1.075	-1.125
58.527 +-3.709	43.571 +-3.200	47.183 +-3.330	45.966 +-3.287	42.723 +-3.169	I	-1.175	-1.225	-1.275	-1.325	-1.375
37.569 +-2.971	30.964 +-2.697	27.836 +-2.558	32.000 +-2.742	32.966 +-2.783	I	-1.425	-1.475	-1.525	-1.575	-1.625
30.834 +-2.692	26.040 +-2.474	28.129 +-2.571	26.287 +-2.485	23.869 +-2.368	I	-1.675	-1.725	-1.775	-1.825	-1.875

------MASS**2 FROM6.5 GEV**2 TO 6.7 GEV**2 CORRESPONDING TO MAXIMAL U = -.313 AND-.329 I CENTRE VALUE OF U

OUT OF K.B.	OUT OF K.B.	OUT OF K.B.	OUT OF K.B.	OUT OF K.B.	I	.075	.025	-.025	-.075	-.125
OUT OF K.B.	OUT OF K.B.	OUT OF K.B.	(111.395 +-5.116)	(186.677 +-6.623)	I	-.175	-.225	-.275	-.325	-.375
171.989 +-6.357	161.342 +-6.158	170.147 +-6.323	145.611 +-5.850	130.693 +-5.542	I	-.425	-.475	-.525	-.575	-.625
113.042 +-5.154	114.316 +-5.183	105.214 +-4.972	94.320 +-4.708	81.437 +-4.375	I	-.675	-.725	-.775	-.825	-.875
73.029 +-4.143	71.579 +-4.101	64.157 +-3.883	64.529 +-3.894	60.045 +-3.756	I	-.925	-.975	-1.025	-1.075	-1.125
59.603 +-3.743	55.963 +-3.626	53.289 +-3.539	43.623 +-3.202	49.181 +-3.400	I	-1.175	-1.225	-1.275	-1.325	-1.375
45.334 +-3.264	37.224 +-2.958	32.884 +-2.780	35.384 +-2.884	32.099 +-2.746	I	-1.425	-1.475	-1.525	-1.575	-1.625
35.262 +-2.879	32.127 +-2.748	30.541 +-2.679	33.220 +-2.794	22.447 +-2.297	I	-1.675	-1.725	-1.775	-1.825	-1.875

------MASS**2 FROM6.7 GEV**2 TO 6.9 GEV**2 CORRESPONDING TO MAXIMAL U = -.329 AND-.345 I CENTRE VALUE OF U

OUT OF K.B.	OUT OF K.B.	OUT OF K.B.	OUT OF K.B.	OUT OF K.B.	I	.075	.025	-.025	-.075	-.125
OUT OF K.B.	OUT OF K.B.	OUT OF K.B.	(47.935 +-3.356)	(200.474 +-6.864)	I	-.175	-.225	-.275	-.325	-.375
195.125 +-6.772	177.037 +-6.450	168.448 +-6.292	150.915 +-5.955	129.920 +-5.525	I	-.425	-.475	-.525	-.575	-.625
127.948 +-5.483	128.289 +-5.491	106.873 +-5.012	96.465 +-4.761	85.761 +-4.489	I	-.675	-.725	-.775	-.825	-.875
92.214 +-4.655	83.947 +-4.442	79.884 +-4.333	64.470 +-3.892	67.682 +-3.988	I	-.925	-.975	-1.025	-1.075	-1.125
62.562 +-3.834	54.701 +-3.585	51.340 +-3.473	53.977 +-3.562	52.964 +-3.528	I	-1.175	-1.225	-1.275	-1.325	-1.375
50.591 +-3.448	50.652 +-3.450	41.959 +-3.140	44.149 +-3.221	48.344 +-3.371	I	-1.425	-1.475	-1.525	-1.575	-1.625
34.982 +-2.867	36.681 +-2.936	38.347 +-3.002	27.612 +-2.547	26.682 +-2.504	I	-1.675	[illegible]	[illegible]	[illegible]	[illegible]

------MASS**2 FROM6.9 GEV**2 TO 7.1 GEV**2 CORRESPONDING TO MAXIMAL U = -.345 AND-.362 | CENTRE VALUE OF U

OUT OF K.B.	OUT OF K.B.	OUT OF K.B.	OUT OF K.B.	OUT OF K.B.	.075 .025 -.025 -.075 -.125
OUT OF K.B.	OUT OF K.B.	OUT OF K.B.	(5.511 +-1.138)	(211.824 +-7.055)	-.175 -.225 -.275 -.325 -.375
221.950 +-7.222	191.459 +-6.708	183.422 +-6.565	162.263 +-6.175	159.401 +-6.120	-.425 -.475 -.525 -.575 -.625
138.354 +-5.702	127.849 +-5.481	114.393 +-5.185	115.679 +-5.214	90.696 +-4.617	-.675 -.725 -.775 -.825 -.875
92.360 +-4.659	84.656 +-4.460	85.058 +-4.471	85.016 +-4.470	73.489 +-4.156	-.925 -.975-1.025-1.075-1.125
73.400 +-4.153	64.503 +-3.893	58.640 +-3.712	56.628 +-3.648	55.857 +-3.623	-1.175-1.225-1.275-1.325-1.375
55.138 +-3.600	51.592 +-3.482	49.576 +-3.413	51.122 +-3.466	44.018 +-3.216	-1.425-1.475-1.525-1.575-1.625
40.636 +-3.090	36.472 +-2.928	32.522 +-2.765	30.792 +-2.690	42.190 +-3.149	-1.675-1.725-1.775-1.825-1.875

------MASS**2 FROM7.1 GEV**2 TO 7.3 GEV**2 CORRESPONDING TO MAXIMAL U = -.362 AND-.379 | CENTRE VALUE OF U

OUT OF K.B.	OUT OF K.B.	OUT OF K.B.	OUT OF K.B.	OUT OF K.B.	.075 .025 -.025 -.075 -.125
OUT OF K.B.	OUT OF K.B.	OUT OF K.B.	OUT OF K.B.	(145.056 +-5.839)	-.175 -.225 -.275 -.325 -.375
(240.678 +-7.520)	215.009 +-7.108	197.781 +-6.818	173.139 +-6.379	161.001 +-6.151	-.425 -.475 -.525 -.575 -.625
139.682 +-5.729	132.364 +-5.577	128.926 +-5.504	110.335 +-5.092	111.282 +-5.114	-.675 -.725 -.775 -.825 -.875
106.434 +-5.001	96.249 +-4.756	87.892 +-4.545	88.207 +-4.553	77.689 +-4.273	-.925 -.975-1.025-1.075-1.125
82.774 +-4.410	64.550 +-3.895	67.769 +-3.991	68.973 +-4.026	63.173 +-3.853	-1.175-1.225-1.275-1.325-1.375
66.246 +-3.946	47.938 +-3.356	54.367 +-3.574	56.508 +-3.644	47.249 +-3.332	-1.425-1.475-1.525-1.575-1.625
45.755 +-3.279	37.022 +-2.950	40.916 +-3.101	42.605 +-3.164	37.339 +-2.962	-1.675-1.725-1.775-1.825-1.875

------MASS**2 FROM7.3 GEV**2 TO 7.5 GEV**2 CORRESPONDING TO MAXIMAL U = -.379 AND-.396 | CENTRE VALUE OF U

OUT OF K.B.	OUT OF K.B.	OUT OF K.B.	OUT OF K.B.	OUT OF K.B.	.075 .025 -.025 -.075 -.125
OUT OF K.B.	OUT OF K.B.	OUT OF K.B.	OUT OF K.B.	(78.450 +-4.294)	-.175 -.225 -.275 -.325 -.375
(254.944 +-7.740)	229.409 +-7.342	221.166 +-7.209	183.079 +-6.559	188.498 +-6.656	-.425 -.475 -.525 -.575 -.625
160.261 +-6.137	162.998 +-6.189	136.446 +-5.663	134.505 +-5.622	118.271 +-5.272	-.675 -.725 -.775 -.825 -.875
106.822 +-5.010	104.138 +-4.947	103.699 +-4.937	95.833 +-4.746	91.511 +-4.637	-.925 -.975-1.025-1.075-1.125
81.648 +-4.380	79.418 +-4.320	59.991 +-3.753	67.551 +-3.984	67.948 +-3.996	-1.175-1.225-1.275-1.325-1.375
56.999 +-3.660	58.698 +-3.714	62.237 +-3.824	53.272 +-3.538	46.502 +-3.306	-1.425-1.475-1.525-1.575-1.625
48.511 +-3.376	52.985 +-3.529	51.406 +-3.476	38.587 +-3.011	42.401 +-3.157	-1.675-1.725-1.775-1.825-1.875

------MASS**2 FROM7.5 GEV**2 TO 7.7 GEV**2 CORRESPONDING TO MAXIMAL U = -.396 AND-.415 | CENTRE VALUE OF U

OUT OF K.B.	OUT OF K.B.	OUT OF K.B.	OUT OF K.B.	OUT OF K.B.	.075 .025 -.025 -.075 -.125
OUT OF K.B.	OUT OF K.B.	OUT OF K.B.	OUT OF K.B.	(4.747 +-1.056)	-.175 -.225 -.275 -.325 -.375
(248.959 +-7.649)	248.762 +-7.646	243.288 +-7.561	214.156 +-7.094	207.820 +-6.988	-.425 -.475 -.525 -.575 -.625
177.618 +-6.461	168.913 +-6.300	155.521 +-6.045	140.840 +-5.753	131.447 +-5.558	-.675 -.725 -.775 -.825 -.875
122.085 +-5.356	118.706 +-5.282	111.108 +-5.110	101.833 +-4.892	90.195 +-4.604	-.925 -.975-1.025-1.075-1.125
94.679 +-4.717	92.541 +-4.663	77.964 +-4.280	71.875 +-4.110	69.687 +-4.047	-1.175-1.225-1.275-1.325-1.375
70.441 +-4.069	61.626 +-3.806	64.127 +-3.882	62.289 +-3.826	65.455 +-3.922	-1.425-1.475-1.525-1.575-1.625
61.182 +-3.792	50.356 +-3.440	49.117 +-3.397	46.939 +-3.321	53.291 +-3.539	-1.675-1.725-1.775-1.825-1.875

------MASS**2 FROM7.7 GEV**2 TO 7.9 GEV**2 CORRESPONDING TO MAXIMAL U = -.415 AND-.433 | CENTRE VALUE OF U

OUT OF K.B.	OUT OF K.B.	OUT OF K.B.	OUT OF K.B.	OUT OF K.B.	.075 .025 -.025 -.075 -.125
OUT OF K.B.	OUT OF K.B.	OUT OF K.B.	OUT OF K.B.	OUT OF K.B.	-.175 -.225 -.275 -.325 -.375
(155.568 +-6.046)	(268.532 +-7.944)	234.758 +-7.428	219.758 +-7.186	202.349 +-6.896	-.425 -.475 -.525 -.575 -.625
203.844 +-6.921	190.663 +-6.694	180.710 +-6.517	155.845 +-6.052	133.504 +-5.601	-.675 -.725 -.775 -.825 -.875
129.297 +-5.512	121.476 +-5.343	110.704 +-5.101	113.474 +-5.164	102.307 +-4.903	-.925 -.975-1.025-1.075-1.125
103.548 +-4.933	101.666 +-4.888	86.903 +-4.519	79.096 +-4.311	70.314 +-4.065	-1.175-1.225-1.275-1.325-1.375
80.802 +-4.358	79.465 +-4.321	70.662 +-4.075	70.813 +-4.079	74.476 +-4.184	-1.425-1.475-1.525-1.575-1.625
68.190 +-4.003	68.467 +-4.011	63.161 +-3.853	50.499 +-3.445	57.161 +-3.665	-1.675-1.725-1.775-1.825-1.875

```
------MASS**2 FROM7.7   GEV**2 TO 7.9  GEV**2 CORRESPONDING TO MAXIMAL U = -.415 AND-.433        I      CENTRE VALUE  OF U

 OUT OF K.B.          OUT OF K.B.          OUT OF K.B.          OUT OF K.B.          OUT OF K.B.       I  .075  .025 -.025 -.075 -.125
 OUT OF K.B.          OUT OF K.B.          OUT OF K.B.          OUT OF K.B.          OUT OF K.B.       I -.175 -.225 -.275 -.325 -.375
(155.568 +-6.046)    (268.532 +-7.944)    234.758 +-7.428      219.758 +-7.186      202.349 +-6.896   I -.425 -.475 -.525 -.575 -.625
 203.844 +-6.921      190.663 +-6.694      180.710 +-6.517      155.845 +-6.052      133.504 +-5.601   I -.675 -.725 -.775 -.825 -.875
 129.297 +-5.512      121.476 +-5.343      110.704 +-5.101      113.474 +-5.164      102.307 +-4.903   I -.925 -.975-1.025-1.075-1.125
 103.548 +-4.933      101.666 +-4.888      86.903 +-4.519       79.096 +-4.311       70.314 +-4.065    I-1.175-1.225-1.275-1.325-1.375
 80.802 +-4.358       79.465 +-4.321       70.662 +-4.075       70.813 +-4.079       74.476 +-4.184    I-1.425-1.475-1.525-1.575-1.625
 68.190 +-4.003       68.467 +-4.011       63.161 +-3.853       50.499 +-3.445       57.161 +-3.665    I-1.675-1.725-1.775-1.825-1.875

------MASS**2 FROM7.9   GEV**2 TO 8.1  GEV**2 CORRESPONDING TO MAXIMAL U = -.433 AND-.453        I      CENTRE VALUE  OF U

 OUT OF K.B.          OUT OF K.B.          OUT OF K.B.          OUT OF K.B.          OUT OF K.B.       I  .075  .025 -.025 -.075 -.125
 OUT OF K.B.          OUT OF K.B.          OUT OF K.B.          OUT OF K.B.          OUT OF K.B.       I -.175 -.225 -.275 -.325 -.375
(54.532 +-3.580)     (272.449 +-8.002)    273.683 +-8.020      256.192 +-7.759      236.918 +-7.462   I -.425 -.475 -.525 -.575 -.625
 225.739 +-7.283      208.581 +-7.001      178.642 +-6.479      179.267 +-6.491      161.201 +-6.155   I -.675 -.725 -.775 -.825 -.875
 141.028 +-5.757      130.754 +-5.543      120.884 +-5.330      116.344 +-5.229      105.047 +-4.969   I -.925 -.975-1.025-1.075-1.125
 112.826 +-5.149      95.565 +-4.739       95.001 +-4.725       92.421 +-4.660       83.745 +-4.436    I-1.175-1.225-1.275-1.325-1.375
 76.483 +-4.240       84.915 +-4.467       74.157 +-4.175       77.726 +-4.274       73.501 +-4.156    I-1.425-1.475-1.525-1.575-1.625
 63.483 +-3.862       69.567 +-4.043       66.211 +-3.945       58.118 +-3.696       66.315 +-3.948    I-1.675-1.725-1.775-1.825-1.875
0024:   UTS,OYOSHIDA    06/06/78    18:42

0024:   UTS,OYOSHIDA    06/06/78    18:42

0024:   UTS,OYOSHIDA    06/06/78    18:42

0024:   UTS,OYOSHIDA    06/06/78    18:42

0024:   UTS,OYOSHIDA    06/06/78    18:42

0024:   UTS,OYOSHIDA    06/06/78    18:42

0024:   UTS,OYOSHIDA    06/06/78    18:42

0024:   UTS,OYOSHIDA    06/06/78    18:42

0024:   UTS,OYOSHIDA    06/06/78    18:42

0024:   UTS,OYOSHIDA    06/06/78    18:42

0024:   UTS,OYOSHIDA    06/06/78    18:42

0024:   UTS,OYOSHIDA    06/06/78    18:42

0024:   UTS,OYOSHIDA    06/06/78    18:42

0024:   UTS,OYOSHIDA    06/06/78    18:42
```

REFERENCES

1. P.D.B. Collins and E.J. Squires, "Regge-Poles in Particle Physics", Springer-Verlag (1968), Tract No. 45.
2. P.D.B. Collins, Phys. Reports 1C (1970) 103.
3. P.D.B. Collins, "An Introduction to Regge Theory and High Energy Physics", C.U.P. (1977).
4. M.L. Perl, "High Energy Hadron Physics", Wiley (1974).
5. A.C. Irving and R.P. Worden, Phys. Reports 34C (1977) 117.
6. V.D. Barger and D.B. Cline, "Phenomenological Theories of High Energy Scattering", Benjamin (1969).
7. G.L. Shaw and D.Y. Wong (eds), "Pion-Nucleon Scattering", Wiley (1969).
8. S. MacDowell, Phys. Rev. 116 (1959) 774.
9. R. Carlitz and M. Kislinger, Phys. Rev. Lett. 24 (1970) 186.
10. E.L. Berger and G.C. Fox, Nucl. Phys. B26 (1971) 1.
11. Tin Maung Aye and K.J.M. Moriarty, Acta Physica Austriaca 44 (1976) 279.
12. A.H. Mueller, Phys. Rev. D2 (1970) 2963.
13. H.D.I. Abarbanel, J. Bartels, J.M. Bronzan and D. Sidhu, Phys. Rev. D12 (1975) 2459.

    I. Halliday and C.T. Sachrajda, Phys. Rev. D8 (1973) 3589.
14. H.D.I. Abarbanel and D.J. Gross, Phys. Rev. Lett. 26 (1971) 732.

    G.R. Goldstein and J.F. Owens, Nucl. Phys. B103 (1976) 145.

    K. Ahmed, J.G. Körner, G. Kramer and N.S. Craigie, Nucl. Phys. B106 (1976) 275.

15. N.S. Craigie and G. Kramer, Nucl. Phys. B75 (1974) 509.

16. F.E. Paige and D.P. Sidhu, Phys. Rev. D14 (1976) 2307.

17. J. Pumplin, Phys. Rev. D13 (1976) 1249 and 1261.

18. See for example,

K.J.M. Moriarty, J.H. Tabor and A. Ungkitchanukit, Phys. Rev. D16 (1977) 130.

K.J.M. Moriarty and J.H. Tabor, J. Phys. G4 (1978) 1215.

N.S. Craigie, K.J.M. Moriarty and J.H. Tabor, Phys. Rev. D18 (1978) 590.

K.J.M. Moriarty, J.P. Rad, J.H. Tabor and A. Ungkitchanukit, Nuovo Cim. Lett. 17 (1976) 366.

K.J.M. Moriarty, J.H. Tabor and H.N. Thompson, Phys. Rev. D18 (1978).

19. D. Horn and F. Zachariasen, "Hadron Physics at Very High Energies", Benjamin (1973).

20. I. Halliday, D.I.C. Lecture Notes, (1975-76).

21. K.J.M. Moriarty and J.H. Tabor, Nuovo Cim. Lett. 15 (1976) 17.

22. C.I. Tan, Phys. Rev. D4, (1972) 2412.

K.E. Cahill and H.P. Stapp, Phys. Rev. D6 (1972) 1007.

K.E. Cahill and H.P. Stapp, Phys. Rev. D8 (1973) 2714.

J.C. Polkinghorne, Nuovo Cim. 7A (1972) 555.

23. H.D.I. Abarbanel and D.J. Gross, Phys. Rev. Lett. 26 (1971) 732.

G.A. Ringland, R.J.N. Phillips and R. Worden, Phys. Lett. 40B (1972) 239.

24. J.P. Ader, C. Meyers and Ph. Salin, Nucl. Phys. B47 (1972) 397.

J.P. Ader, C. Meyers and Ph. Salin, Nucl. Phys. B82 (1974) 237.

J. Randa and A. Donnachie, Nucl. Phys. B109 (1976) 495.

25. M. Jacob and G.C. Wick, Ann. Phys. 7 (1959) 404.

26. M. Jacob and G.F. Chew, "Strong Interaction Physics", Benjamin (1964)

27. D. Amati, S. Fubini and A. Stranghellini, Nuovo Cim. 26 (1962) 896.

28. R.P. Feynman, Phys. Rev. Lett. 23 (1969) 1415.

29. M.D. Scadron, Phys. Rev. 165 (1968) 1640.

30. M.M. Nagels et al., Nucl. Phys. B109 (1976) 1.

31. K.J.M. Moriarty, J.P. Rad, J.H. Tabor and A. Ungkitchanukit, Acta Physica Austriaca 46 (1977) 105.

32. S.A. Adjei, P.A. Collins, B.J. Hartley, K.J.M. Moriarty and R.W. Moore, Ann. of Phys. (N.Y.) 75 (1973) 405.
P.A. Collins, B.J. Hartley, R.W. Moore and K.J.M. Moriarty, Journal of Phys. A6 (1973) 506.

33. J.D. Jackson, Rev. Mod. Phys. 37 (1965) 484.

34. J.H. Tabor, Thesis, London University (1978).

35. R.W.B. Ardill, private communication.

36. R. Tegen, "Inklusive Photo-und Elektroproduktion von Protonen im Triple-Reggebereich", Thesis, Hamburg (1976).
(We are grateful to Professor G. Kramer for communicating this work to us).

37. J. Six, Rapporteurs Talk, XIII Rencontre de Moriond, (1978

38. H. Yoshida, "Production de protons rapides vers l'avant par un faisceau de π^- à 12 GeV/c dans le spectromètre à chambres à étincelles Oméga", Thesis, Orsay (1977).

39. H. Yoshida, Private communication.

40. D.P. Roy, R.G. Roberts, R.J.N. Phillips and H.J. Miettinen, Phys. Rev. D6 (1972) 1317.

41. K.J.M. Moriarty and J.H. Tabor, Comput. Phys. Commun. 12 (1976) 277.

42. J. Anderson, K.J.M. Moriarty and R.C. Beckwith, Comput. Phys. Commun. 9 (1975) 85.

43. F. James and M. Roos, Comput. Phys. Commun. 10 (1975) 343.

44. J.P. Rad, Thesis, London University (1977)
A.V. Turbiner, JETP Lett. 22 (1975), 182.

APPENDIX

Notations and Conventions [A1]

Metric:

$$g_{\mu\nu}: g_{oo} = -g_{11} = -g_{22} = -g_{33} = 1,$$

$$g_{\mu\nu} = 0 \quad \text{otherwise.}$$

Four-vector:

$$p_\mu = (E, \underline{p}) \quad \text{with scalar product} \quad p_\mu p^\mu = E^2 - \underline{p}^2.$$

Pauli matrices:

$$\sigma_1 = \begin{pmatrix} 0 & 1 \\ 1 & 0 \end{pmatrix}, \quad \sigma_2 = \begin{pmatrix} 0 & -i \\ i & 0 \end{pmatrix}, \quad \sigma_3 = \begin{pmatrix} 1 & 0 \\ 0 & -1 \end{pmatrix}.$$

Dirac matrices:

$$\gamma_\mu = (\gamma_o, \underline{\gamma})$$

satisfying anticommutation relations

$$\gamma^\mu \gamma^\nu + \gamma^\nu \gamma^\mu = 2g^{\mu\nu},$$

in the familiar representation

$$\gamma_o = \begin{pmatrix} 1 & 0 \\ 0 & -1 \end{pmatrix}, \qquad \underline{\gamma} = \begin{pmatrix} 0 & \underline{\sigma} \\ -\underline{\sigma} & 0 \end{pmatrix},$$

$$\gamma_5 = i\gamma^0\gamma^1\gamma^2\gamma^3, \qquad \sigma^{\mu\nu} = \frac{i}{2}[\gamma^\mu, \gamma^\nu].$$

The inner product $\gamma_\mu a^\mu = \not{a}$.

Wave Functions

The helicity basis is adopted for the wave functions.

i) Spinor wave functions:

$$\bar{u}(p, \lambda)u(p, \lambda') = 2m\, \delta_{\lambda\lambda'}$$

where λ and λ' are helicity labels and $\bar{u} = u^{\dagger}\gamma^{o}$.

$$\bar{v}(p,\lambda)v(p,\lambda') = -2m\delta_{\lambda\lambda'} \ .$$

Equations of motion,

$$(\not{p}-m)u(p,\lambda) = 0 \qquad (\not{p}+m)v(p,\lambda) = 0$$

$$\bar{u}(p,\lambda)(\not{p}-m) = 0 \qquad \bar{v}(p,\lambda)(\not{p}+m) = 0.$$

Projection operators,

$$\sum_{\lambda} u(p,\lambda)\bar{u}(p,\lambda) = (\not{p}+m)$$

$$\sum_{\lambda} v(p,\lambda)\bar{v}(p,\lambda) = (\not{p}-m) \ .$$

It follows that

$$\bar{u}(p,\lambda)\ \gamma^{\mu}u(p,\lambda) = 2p^{\mu}\ \delta_{\lambda\lambda'}$$

$$\bar{v}(p,\lambda)\ \gamma^{\mu}v(p,\lambda) = 2p^{\mu}\ \delta_{\lambda\lambda'} \ .$$

ii) Spin 3/2 wave functions: [A2, A3, A4, A5, A6]

$$\bar{u}_\alpha(p,\lambda)u_\alpha(p,\lambda') = -2m\ \delta_{\lambda\lambda'}$$

$$\bar{v}_\alpha(p,\lambda)v_\alpha(p,\lambda') = 2m\ \delta_{\lambda\lambda'}$$

Rarita-Schwinger equations of motion, for all α

$$(\not{p}-m)u_\alpha(p,\lambda) = 0 \qquad (\not{p}+m)v_\alpha(p,\lambda) = 0$$

$$\gamma^\mu\ u_\mu(p,\lambda) = 0 \qquad \gamma^\mu\ v_\mu(p,\lambda) = 0\ .$$

Divergenceless subsidiary conditions follow,

$$p^\mu\ u_\mu(p,\lambda) = 0 \qquad p^\mu\ v_\mu(p,\lambda) = 0\ .$$

Projection operators,

$$\sum_\lambda\ u_\mu(p,\lambda)\bar{u}_\nu(p,\lambda) = (\not{p}+m)\Big(-g_{\mu\nu}$$

$$+\frac{1}{3}\gamma_\mu\gamma_\nu + \frac{2}{3m^2}p_\mu p_\nu + \frac{1}{3m}(\gamma_\mu p_\nu - p_\mu\gamma_\nu)\Big)$$

$$\sum_\lambda\ v_\mu(p,\lambda)\bar{v}_\nu(p,\lambda) = (\not{p}-m)\ \Big(-g_{\mu\nu}$$

$$+\frac{1}{3}\gamma_\mu\gamma_\nu + \frac{2}{3m^2}p_\mu p_\nu - \frac{1}{3m}(\gamma_\mu p_\nu - p_\mu\gamma_\nu)\Big).$$

It follows that

$$\bar{u}_\nu(p,\lambda)\gamma^\mu u_\nu(p,\lambda') = 2p^\mu\ \delta_{\lambda\lambda'}$$

$$\bar{v}_\nu(p,\lambda)\gamma^\mu v_\nu(p,\lambda') = -2p^\mu\ \delta_{\lambda\lambda'}$$

Trace Theorems [A1, A4]

i) $\mathrm{Tr}\,(1) = 4$

ii) $\mathrm{Tr}\,(\not{a}_1\not{a}_2\ldots\not{a}_n) = 0$ for n odd.

iii) $\mathrm{Tr}\,(\not{a}_1\not{a}_2\ldots\not{a}_n) = a_1\cdot a_2\ \mathrm{Tr}\,(\not{a}_3\ldots\not{a}_n)$

$$- a_1\cdot a_3\ \mathrm{Tr}(\not{a}_2\not{a}_4\ldots\not{a}_n)+\ldots+a_1\cdot a_n\ \mathrm{Tr}\,(\not{a}_2\ldots\not{a}_{n-1}).$$

Feynman Rules [A1]

Differential cross section: ($a + b \to n$ particles)

$$d\sigma = \frac{1}{4[(p_a\cdot p_b)^2-m_a{}^2m_b{}^2]^{\frac{1}{2}}}\ |T|^2\ \frac{d^3p_1}{2E_1(2\pi)^3}\cdots\frac{d^3p_n}{2E_n(2\pi)^3}$$

$$\times\ (2\pi)^4\ \delta^4(p_a+p_b - \sum_{i=1}^{n} p_i)\ S,$$

where

- a and b are initial state particles,
- T is the invariant amplitude,
- $S = \prod_i \frac{1}{n_i!}$ is the statistical factor if there are n_i identical particles of type i in the final state.

Polarizations are summed over final and averaged over initial states.

Rules for invariant amplitudes:

1. For each external fermion line entering $u(p,\lambda)$ or $v(p,\lambda)$.

   For each external fermion line leaving $\bar{u}(p,\lambda)$ or $\bar{v}(p,\lambda)$.

2. For each external photon line a factor ε_μ.

3. Spin zero meson propagator

$$\frac{1}{p^2 - m^2} .$$

4. Spin $\frac{1}{2}$ fermion propagator

$$\frac{(\not{p} + m)}{p^2 - m^2} .$$

5. Photon propagator

$$\frac{- g_{\mu\nu}}{q^2} .$$

6. Spin 3/2 propagator [A3, A4, A5, A6]

$$(p^2-m^2)^{-1} \Bigg((\not{p}+m) \Big[-g_{\mu\nu} + \frac{2}{3m^2} p_\mu p_\nu + \frac{1}{3} \gamma_\mu \gamma_\nu + \frac{1}{3m} (\gamma_\mu p_\nu - p_\mu \gamma_\nu) \Big] - \frac{2}{3m^2} (p^2-m^2) \Big[\gamma_\mu p_\nu - p_\mu \gamma_\nu + (\not{p}+m) \gamma_\mu \gamma_\nu \Big] \Bigg)$$

7. Polarization sums for photons [A1, A7]

$$\sum_{\lambda=\pm} \varepsilon_\nu(q,\lambda)\varepsilon_\mu(q,\lambda)$$

$$= - g_{\nu\mu} - \frac{q_\nu q_\mu}{(q.\eta)^2-q^2} + (q.\eta) \frac{(q_\nu \eta_\mu + \eta_\nu q_\mu)}{(q.\eta)^2 - q^2} - \frac{q^2 \eta_\nu \eta_\mu}{(q.\eta)^2-q^2}$$

with $\eta = (1, 0, 0, 0)$.

References for Appendix

A1. J.D. Bjorken and S.D. Drell, "Relativistic Quantum Mechanics", McGraw-Hill (1964).
J.D. Bjorken and S.D. Drell, "Relativistic Quantum Fields", McGraw-Hill (1965).

A2. S. Gasiorowicz, "Elementary Particle Physics", Wiley (1966).

A3. Suh Urk Chung, "Spin Formalisms", CERN 71-8.

A4. D. Lurié, Particles and Fields", Wiley (1968).

A5. H. Umezawa, "Quantum Field Theory", North-Holland (1956)

A6. Y. Frishman and E. Gotsman, Phys. Rev. 140 (1965) 1151..

A7. J.M. Jauch and F. Rohrlich, "Theory of Photons and Electrons", Addison-Wesley (1955).